POLYCATENAR AMPHIPHILIC LIQUID CRYSTALS

by

Adrian Gainar

Submitted in conformity with the requirements for the degree of

MSc in Chemistry by Research

The University of York

Department of Chemistry

February 2012

Abstract

In order to study the effect on mesophase organisation of incorporating groups (hydrocarbon and fluorocarbon) that normally phase separate into the same liquid-crystalline molecules, a series of tri- and tetra-catenar mesogens has been prepared containing various combinations of hydrocarbon (C_nH_{2n+1}–: n = 12 or 14) and semiperfluorocarbon ($C_mF_{2m+1}(CH_2)_4$–; m = 8 or 10) chains. In addition, many of the intermediate compounds prepared *en route* were studied for their liquid crystal properties. The semiperfluorocarbon chains were added using Williamson ether chemistry with $C_mF_{2m+1}(CH_2)_4Br$, itself prepared *via* a radical addition of $C_mF_{2m+1}I$ to 3-buten-1-ol to give a secondary iodide which was deiodinated in a radical process. Conversion of the alcohol to the bromide used HBr under phase-transfer conditions. The properties of the new compounds were elucidated using optical microscopy, differential scanning calorimetry and low-angle X-ray diffraction.

The all-hydrocarbon compounds had been prepared previously and their mesomorphism was qualitatively identical to that of the all-semiperfluorocarbon analogues. However, when both hydrocarbon and semiperfluorocarbon chains were mixed in the same molecule, there was a significant change in behaviour as the mesogens organised themselves in order to maximise hydrocarbon-hydrocarbon and fluorocarbon-fluorocarbon interactions while minimising hydrocarbon-fluorocarbon interactions. For example, with tricatenar mesogens with a fluorocarbon chain at one end, this manifested itself as a doubling of the lamellar periodicity, while in unsymmetric tetracatenar mesogens, a reduction in phase symmetry from hexagonal (*p*6*mm*) to rectangular (*p*2*gg*) was seen along with a massive increase in lattice parameter.

Table of contents

Acknowledgements

I would like to thank my supervisor Professor Duncan W. Bruce, for the patience and dedication he proved to have along this complex project and for being a wonderful advisor even in delicate situations.

I am grateful to my project colleague Mei-Chun Tzeng, who shared her knowledge and skills throughout the project determining me to work harder.

My acknowledgments should also be directed towards Graeme McAllister who made extraordinary efforts to do the Elemental Analysis as quickly as possible and towards Bertrand Donnio/Benoît Heinrich from University of Strasbourg who have done an excellent expertise on low-angle X-ray diffraction.

My personal financial support throughout a major part part of the MSc by Research programme was ensured by the 'Dinu Patriciu' Romanian Foundation whom I would like to thank for their massive generosity and tolerance they proved.

I also need to mention that I am thankful to my research group colleague Navpreet K. Sethi who was not only an excellent mentor but also sustained me morally with valuable pieces of her knowledge. Also, my gratefulness goes to Javier Torroba, Álvaro Díez, Antonina Smirnova, Linda McAllister, Martin Walker and Steve Wainwright for their support and friendship.

I want to thank Isabel Saez, Stephen Cowling, Heather Fish and Emily Bevis for support and advice whenever I had new questions.

Not lastly, I would like to thank my parents for their patience and mental pieces of advice who inspired me and made me feel motivated.

Author's Declaration

I hereby declare that this is my own work and effort and that it has not been submitted anywhere for any award. Where other sources of information have been used, they have been acknowledged.

In the Results and Discussion – Synthesis sub-section, compounds in **Scheme 2.2**, compound **24**, compounds in **Scheme 2.9** have been synthesized by Mei-Chun Tzeng and compound **51** by Dr. Richard Date to whom I address my acknowledgements.

Signature: .....

Date: .....

CHAPTER 1

INTRODUCTION

1.1. Liquid Crystals: a Brief History

The forms of existence of the matter are usually solid, liquid and gas. There is another state of matter which has both characteristics of solid and liquid with properties typical of both liquid (fluid) and solid (which is spatially ordered). The name of this particular state of matter is *liquid crystal* and holds two behaviours depending on the presence or absence of a solvent. Therefore, when the compound passes through a solid, liquid and liquid crystal state without being in the presence of a solvent while the temperature is changed, it is known as a *thermotropic* liquid crystal. When the concentration of the liquid crystal in a solvent determines the phase behaviour, then one is discussing *lyotropic* liquid crystals.

In 1888, it was discovered that certain cholesteryl esters presented two successive melting points (**Figure 1.1**) [1]. After this major event, the discovery of the cyanobiphenyl liquid crystals by Gray in the 1970s brought a significant development of technology based on liquid crystal displays. The areas covered by the study of liquid crystalline materials are chemistry, physics, mathematics, biology, electronics *etc*.

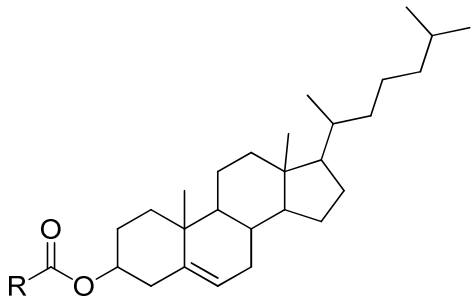

Figure 1.1. Cholesteryl esters discovered by Reinitzer.

Concerning the terminology used, a compound which is liquid crystalline is also called a *mesogen* and its behaviour denotes is known as *mesomorphism*. The

important difference is that a compound with properties similar to liquid crystals is *mesogenic* but not necessarily *mesomorphic*. The liquid state is conventionally termed as *isotropic*. The *melting point* represents the temperature when a solid goes into a mesophase, whereas the *clearing point* is the temperature at which the mesophase becomes an isotropic liquid.

1.2. Low Molar Mass Thermotropic Liquid Crystals

Based on the mesophases they form, they can be classified as *rod-like* (*calamitic)*, and *disc-like (discotic)*. Describing the shape characteristics of the rod-like molecules, their length is much greater than the breadth; thus, it presents one long axis along the molecule, unlike disc-like mesogens which are flatter and have a unique short axis (**Figure 1.2**).

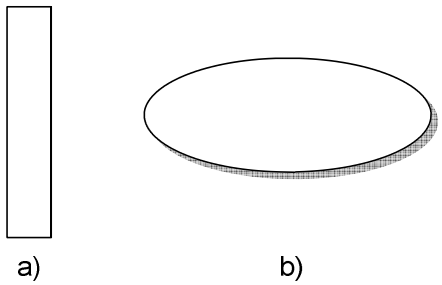

Figure 1.2. (a) Calamitic (rod-like), and (b) discotic (disc-like) mesogens.

1.3. Calamitic Mesogens

An indicative molecular structure for such compounds is depicted in **Figure 1.3**, which is an anisotropic molecule composed of aromatic rings connected in a manner in which the total anisotropy is maintained. In general, the minimum number of rings is three although linking group B preserves the system conjugation (this can be: −CH=CH−, −C≡C−, −N=N− *etc.*). The terminal groups A and C may be identical or

may differ; in general, one will be an alkyl or alkoxy chain with the purpose of both increasing the anisotropy and lowering the melting point. The lateral grafted group D such as lateral fluoro substituents is present in certain cases with the aim of having favourable consequences [1].

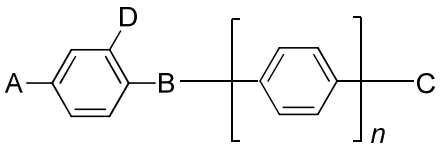

Figure 1.3. A general molecular formula of calamitics.

1.4. Mesophases of Calamitic Mesogens

The phases a calamitic compound may show are broadly nematic and smectic. Beside these true mesophases, there exist some rather crystal smectic phases but they are less mentioned [1].

1.4.1. The Nematic Phase

Compounds exhibiting a nematic phase have the least order and orientation of all the other existing mesophases. As a consequence, the fluidity is high. The terminology is connected to the Greek-derived word, *nematos*, which is translated as thread-like, shape confirmed by the optical texture of the phase. The main aspect of the phase organisation conveys the one-dimensional non-polar orientational order of molecules and the absence of a translational order (**Figure 1.4**) [1].

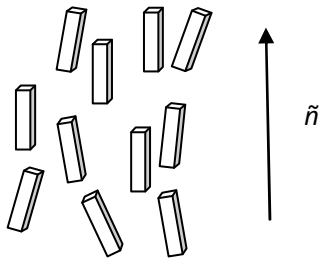

Figure 1.4. Molecular orientational order characteristic to a nematic mesophase, where *ñ* represents the director which describes the average molecular spatial orientation.

1.4.2. The True Smectic Phases

Compared to nematic phases, smectic phases present a higher order state and the molecules are organised into layers exhibiting partial translational ordering. The simplest smectic organisation is the smectic A mesophase (as depicted in **Figure 1.5**). The axes of the molecules have mainly the same orientation; what is distinguishable from nematics is the arrangement in layers of molecules where the orientational direction forms a 90° angle with the layer normal.

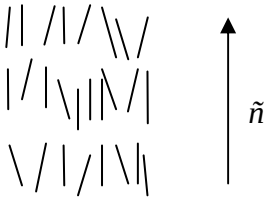

Figure 1.5. On-side view of smectic A phase (*ñ* gives the direction of the average molecular orientation).

The smectic C is a phase resembling the smectic A. The molecules are tilted but still organised loosely into layers. If a hexagonal symmetry defines the structural organisation into layers and the molecules sit at points which form a hexagon, a new smectic phase arises: smectic B (**Figure 1.6**) [1].

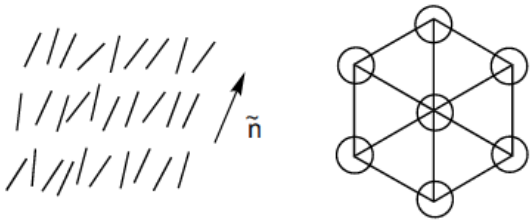

Figure 1.6. Representation of smectic C (left-hand side) and from-above view of smectic B phase (right-hand side).

Two more smectic phases derive from the hexagonal smectic described above: in the smectic I phase, molecules forming the hexagon are tilted along a vertex, whereas in a smectic F phase the molecules tilt towards the edge of the hexagon (**Figure 1.7**).

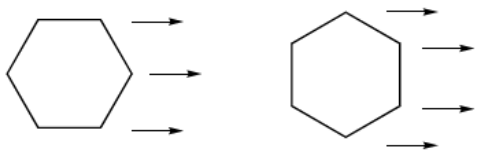

Figure 1.7. Representations of smectic I (left-hand side) and smectic F phase (right-hand side), respectively which show directions of tilting.

The five phases are considered as true smectic phases where one adds the nematic phase. The expected phase series is shown in **Figure 1.8**; as the temperature is lowered, the system becomes more ordered.

$$I \rightarrow N \rightarrow SmA \rightarrow SmC \rightarrow SmI \rightarrow SmF \rightarrow SmB$$

Figure 1.8. The expected phase sequence as temperature is lowered, hence order is enhanced (where I represents isotropic, N – nematic, SmA – smectic A, SmC – smectic C, SmI – smectic I, SmF – smectic F, SmB – smectic B).

1.5. Discotic Mesogens

Sadashiva, Chandrasekhar, and Suresh discovered in the 1970s this type of liquid crystals able to assemble into columnar phases. Presented in **Figure 1.9,** is a benzene hexaalkanoate which was studied by these illustrious researchers.

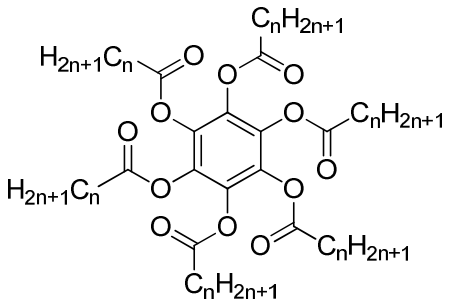

Figure 1.9. Benzene hexaalkanoates.

1.6. Mesophases of Disc-like Mesogens

Rarely encountered, the simplest phase formed is the nematic phase in which there is only orientational order as illustrated in **Figure 1.10a**. More common are the columnar mesophases further classified by the symmetry of the columns in terms of array organisation. **Figure 1.10b** presents a lateral image of a columnar hexagonal phase where the molecules form a symmetrical hexagonal arrangement. **Figure 1.11** depicts the common lattices of the columnar mesophases – hexagonal, oblique, rectangular imagined as geometrical projections of columns on the plane. Thus, the circles denote a maximum projection of the discs which are parallel to the projection plane, while the ellipses are discs tilted with respect to the plane [1].

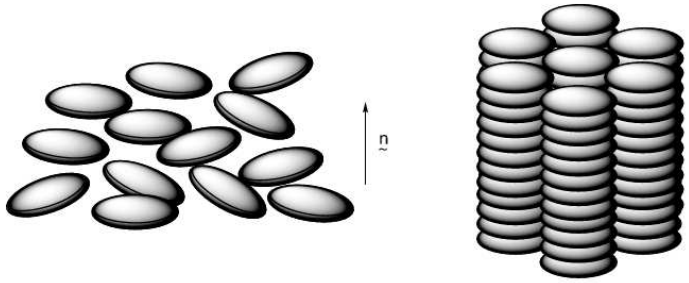

(a) (b)

Figure 1.10. Representation of (a) discotic nematic phase and (b) columnar hexagonal phase

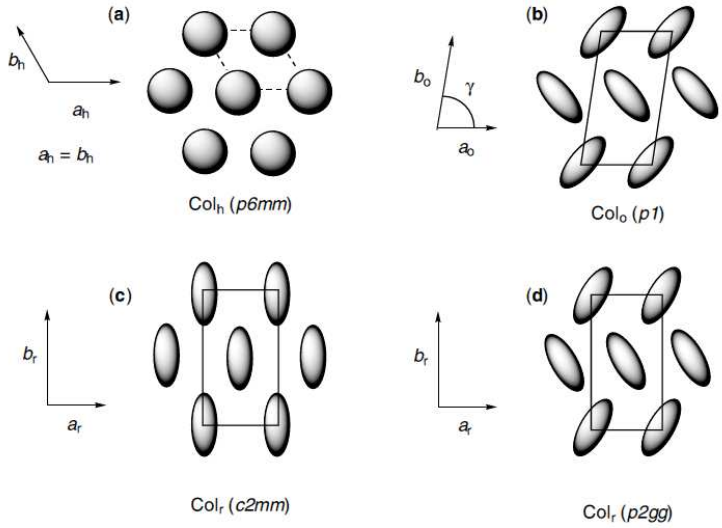

Figure 1.11. Projections of columns on the planes: hexagonal (a), oblique (b) and rectangular lattice (c and d).

1.7. Lyotropic Liquid Crystals

The critical micelle concentration is the typical concentration at which molecules of surfactants dissolved in water will organise and form micelles (**Figure 1.12**). In solutions of surfactants, hydrophobic chains are not molten, but are surrounded by layers of water.

After the micelle is formed, the chains become molten. The surfactants can be cationic, anionic or non-ionic while solvents can be other than water as well.

Figure 1.12. Micelle design of a cylindrical micelle, a rod-like micelle and a plate-like micelle, respectively (from left to right).

In the case where the concentration of surfactant increases over the critical micelle concentration, micelles will form ordered levels of organisations representing lyotropic mesophases. To be precise, micelles in shape of spheres form cubic phases. Rod-like micelles induce hexagonal mesophases since disc-like micelles will lead to a lamellar phase.

Except for surfactant-type of compounds, there are two other categories of molecules exhibiting lyotropic phases: rigid-rod polymers in either aqueous or non-aqueous solvents (for example DNA, a very common genetic material encountered in living organisms), and planar and largely aromatic compounds capable of stacking up one above the other in discotic lyotropic phases named chromonic phases. Thus, the stacks formed may organize into either a nematic or hexagonal phase.

1.8. Physical Properties of Liquid Crystals

The anisotropism may constitute probably one of the important physical properties of a liquid crystalline material due to their fluidity aspect. As an example the refractive indices with a nematic phase are depicted in **Figure 1.13** [2].

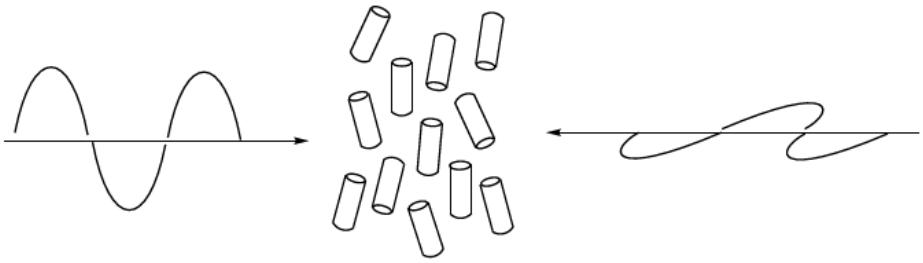

Figure 1.13. Interactions of the polarised light with a nematic phase of a liquid crystal.

Molecules have an enhanced characteristic of being more polarisable along their long axis rather than along their short ones. This argument explains the reason why the electric component of light wave (**Figure 1.13** on left hand side) coincident with the direction of the largest molecular polarisability induces a belatedness of the light, while in the case when the electric vector is coincident to the smallest molecular polarisability, light is the least retarded. Consequently, there are two refractive indices characterizing the liquid crystal.

Now it is right time to define birefringence as the difference between the refractive index of the case when electric vector is coincident with the largest polarisability and the refractive index of the other presented case. Defined as a difference, birefringence may be positive or negative.

Except for the birefringence, there are other physical properties characterizing liquid crystals such as anisotropy in linear birefringence, diamagnetism, dielectric permittivity.

These properties are in direct correlation with their molecular characteristics as presented in **Figure 1.14** which exemplifies the variation of birefringence (Δn) and dielectric permittivity ($\Delta\varepsilon$) as the polarisability of materials decreases in the series of two-ring molecules [2].

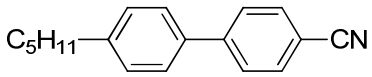

(a)

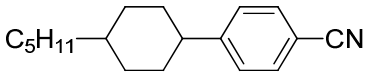

(b)

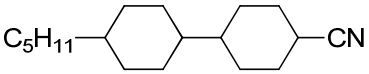

(c)

Figure 1.14. Birefringence and dielectric permittivity decrease in the system as anisotropy decreases from compounds (a) to (c).

After the synthesis of compounds, the phases exhibited need to be analyzed. With this scope, polarized optical microscopy and differential scanning calorimetry are primarily used for establishing the type of mesophases and temperature transitions. X-ray diffraction gives additional information on a more detailed insight of mesophase characteristics when scanning calorimetry and microscopy do not suffice.

1.9. Polarized Optical Microscopy

Polarized optical microscopy usually represents the first useful technique after the material has been purified. Plane-polarized light collides with the sample after it has been loaded on the cover slips (the usual quantity is around 1 mg, spread in a thin layer film). The heating stage of the microscope will be able to heat up/cool down the compound at the desired established temperature. The light meets afterwards an analyzer which is set at 90° with respect to the first polarizer; the outcome is possibility of compound to be viewed through the microscope. **Figure 1.15** details the light path of a polarizing optical microscope.

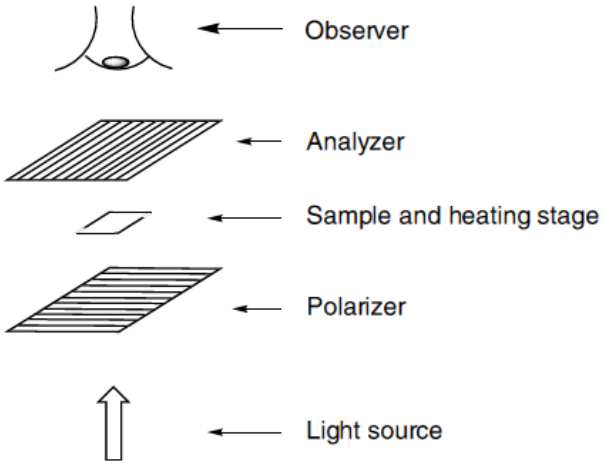

Figure 1.15. Simple illustration of a polarizing optical microscope representation.

When the compound analyzed under the microscope is viewed as black, the molecule displays its isotropic liquid phase while the light is not affected by the first polarizer and is absorbed by the analyzer. However, in liquid crystal phases, plane polarization is lost due to birefringence which induces an elliptical polarization allowing the mesophase texture to be observed. The isotropic phase shall not be confused with homeotropic state (**Figure 1.16**) as the plane-polarized light is black as well with the single difference that there is only one refractive index (the molecules assemble in a way the optic axis is parallel to the sample viewing in phases such as nematic or smectic A) [2].

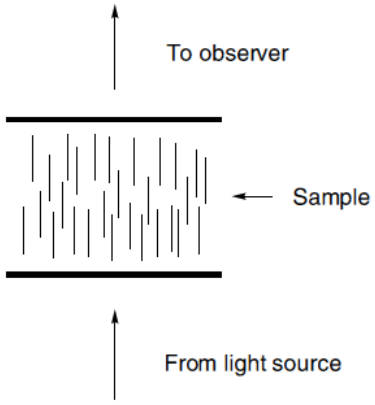

Figure 1.16. Homeotropic arrangement of nematic phase.

Miscibility is yet another property possibly to be exploited in combination with optical microscopy. The preparation of a mixture between the sample and another compound whose mesomorphism is known will facilitate establishing the phase type if they are co-miscible and show the same mesophase at a certain fixed temperature on the microscope. On the contrary, if both compounds are immiscible, one cannot identify the mesophase type (for example, isotropic liquids water and dichloromethane).

1.10. Differential Scanning Calorimetry

The thermodynamic processes accompanying transformations from a mesophase to another mesophase, from a solid state to a mesophase or from a mesophase to the isotropic liquid state can be first- or second-order. Transitions between phases of the same symmetry are always first order and while all liquid crystal transitions are usually first order, the SmC-SmA and SmA-N transitions are often second order.

Equation $\frac{\partial G}{\partial T} = -S$ signifies the change in free energy *G* with respect to temperature and shows the behaviour of entropy *S* in a phase transition. The transition is first-order if the function has a discontinuity in the transformation. $\Delta G = 0$ when transition occurs and the enthalpy ΔH can be calculated as follows: $\Delta H = T\Delta S$.

In a transition, it is possible there is no change in entropy so it is needed to introduce the second derivative of the free energy *G* with respect to temperature $\frac{\partial^2 G}{\partial T^2} = -\frac{C_P}{T}$, in the case of a second-order transition.

Taking into account the approximate value of transitions between phases or between a phase and an isotropic state, this would be of 1 kJ mol^{-1}. Larger values are met in crystal to liquid crystal phase transitions which are first order and comprised in the range 30-50 kJ mol^{-1}. It is interesting to note the transitions smectic C to smectic A and smectic A to nematic can be in majority of cases second order.

Differential scanning calorimetry complements polarized optical microscopy considering that microscope at times cannot diagnose a phase change if transitions occurred are close one to another. Also, sometimes changes in textures during heating/cooling cannot imply transitions if differential calorimetry does not show any transition.

1.11. Small-angle X-ray Diffraction

The path difference between neighbouring planes is an integer multiple of the wavelength of X-rays used according to Bragg law: $n\lambda = 2d\sin\theta$, where n is an integer, λ is the wavelength of the incident wave, d is the spacing between the planes in the atomic lattice, and θ is the angle between the incident ray and the scattering planes. The purpose of using X-ray diffraction is in general to find distances between planes and orientational order of planes (to exemplify, there are determined intercolumnar distances in columnar mesophases or layer thickness in smectic phases).

When specially run for liquid crystals but not for single crystals, X-ray diffraction becomes quite difficult due to the small number of reflections, temperature control and sample alignment. A magnetic field may help induce the sample alignment with the purpose of conducting the X-ray experiments. In the nematic phase, molecules can be oriented similarly in the same sample owing to the diamagnetic anisotropy. The magnetic field will keep them aligned while cooling down the sample thus orientation being maintained in the obtained smectic phases. Gaining the results for columnar mesophases may be more challenging because of a more pronounced viscosity in comparison to the smectic or nematic phases.

The X-ray diffraction technique involves as an experimental system a source of X-ray, a monochromator, a sample chamber and a detector (**Figure 1.17**) [2].

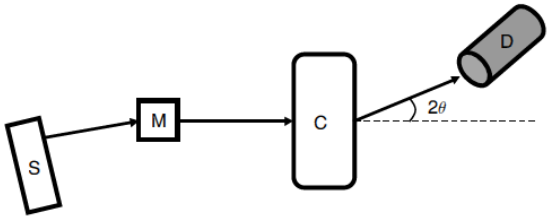

Figure 1.17. Scheme illustrating the X-ray technique concept; abbreviations are: S-source of X-rays, M-monochromator, C-sample chamber where the temperature can be controlled, D-detector and θ represents the diffraction angle.

The source of X-rays is a generator with a sealed tube. The monochromator has the role of choosing only one certain wavelength from the variety of wavelengths emitted by the source. In the chamber there is a magnetic field serving to sample alignment; also, temperature can be controlled here. Detectors may vary depending on the results wished to be exploited: they can be two-dimensional or photographic films to obtain characteristic diffraction patterns but a scintillation counter or a linear position-sensitive detector is absolutely necessary for quantitative details.

Calamitic molecules orient themselves parallel to the magnetic field and therefore a broad signal which corresponds to the molecular length, shows up in the small-angle region that is the central zone of the pattern (**Figure 1.18**). In the wide-angle region, a diffuse peak is created owing to intermolecular distances which is the lateral part of pattern. For a smectic A mesophase diffuse peaks noticed at small angles condense into sharp Bragg spots; at wide angles, the diffuse peaks will appear to be similar as in the nematic phase – the explanation lies in the bidimensionality of the smectic layers. The difference in the case of smectic C is now consisting in the tilt of molecules with respect to the layer and the consequence is that at small angles, reflections are doubled so there will appear two pairs of reflections. If one measures the angle formed between these pairs, this shows up to be double than the tilt angle. When mesophase is columnar, the special technique involves heating a small drop of sample on a cleaned glass plate until it reaches the isotropic liquid state. The immediate process run on the sample drop is cooling down slowly to the temperature the investigation is being made. Thus, mono-domains with a certain alignment are obtained due to the surface interaction. The X-ray beam is parallel to the plate and the two-dimensional detector collects the intensity (an example of a hexagonal

columnar phase pattern is presented in **Figure 1.18**) [1]. If the molecular alignment is not possible to be induced, the spots which would normally appear if the molecules are aligned become rings; such situation does not offer details about tilt angles.

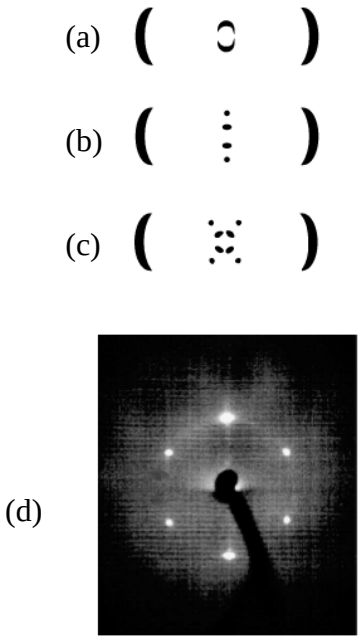

Figure 1.18. X-ray diffraction patterns typical to a nematic (a), smectic A (b), smectic C (c) and hexagonal columnar phase (d), respectively.

1.12. Polycatenar Liquid Crystals

Columnar mesophases are usually formed by discotic molecules but there are exceptional situations where, due to their particular shape, certain compounds are able to show both features of disc-like and rod-like phases. This rather ‘quirky’ type of molecules are known as polycatenar mesogens and present a calamitic unit, a central expanded core, which ends in three or more alkoxy chains (**Figure 1.19**) [1].

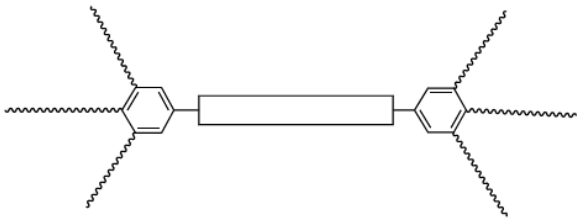

Figure 1.19. Schematic representation of a polycatenar system.

By counting the terminal chains, compounds with three chains are named tricatenars, the ones presenting four external chains are called tetracatenars, the molecules having five chains are pentacatenars and the ones having six rings are named hexacatenars. In a tetracatenar mesogen, one terminal ring may contain only one aliphatic chain and the other three aliphatic chains or the aliphatic chains can be equally distributed two by two at each molecule ring side. A now obvious consequence is that there arise many possibilities in terms of isomery, hence a tetracatenar system may possess terminal chains either in the 3- and 4- positions of the side aromatic ring or in the 3- and 5-positions. If one takes into account the substitution with external chains of the two tetracatenar compound side rings with respect to the molecular centre, these terminal chains may be situated unsymmetrically 3,4- at one side and 3,5- at the other. Here can be included the symmetrical substitution 3,4- at both sides, or 3,5- for each terminal ring. The category of tetracatenars showing a great importance are the symmetric 3,4-substituted compounds (**Figure 1.20**) [2], [3].

In a study where mesomorphic properties are investigated over series of tricatenar, tetracatenar, pentacatenar and hexacatenar mesogens [4], there has been revealed as a general molecular characteristic that increasing the number of chains grafted on the ending benzene rings requires enhancing the length of the core with the scope of the mesomorphism to be preserved. For that reason, in a tetracatenar compound, the minimum number of rings needs to be four to obtain mesomorphic results. The situation is analogous for penta- and hexacatenars where the number of rings is at least five [4].

In the literature, there is also encountered the term of ‘phasmids’ tightly connected to polycatenars. They constitute a junction between rod-like and disc-like compounds

by having the characteristics of the same molecule to exhibit a variety of mesophases (lamellar, nematic, columnar *etc*.). The terminology arrives from the word *'phasma'* which denotes a six-legged insect thus resembling to the hexacatenar systems bearing three alkoxy chains at each end of molecule seeming to be first ever discovered compounds showing both rod-like and disc-like mesophases [4], [5].

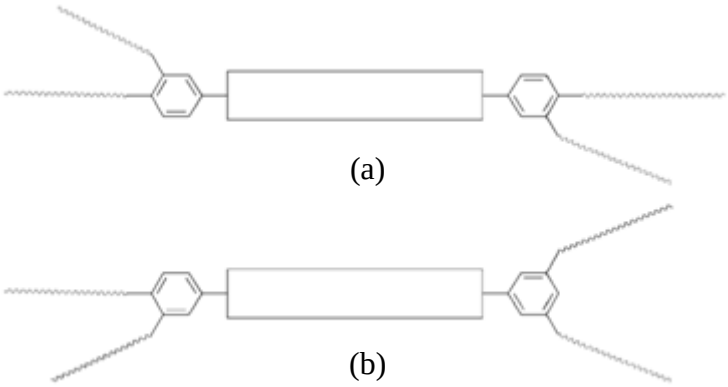

Figure 1.20. Representation of tetracatenars that display a symmetrical substitution (a) and an unsymmetrical one (b), respectively.

The minimum number of rings to be forming the core of the polycatenar is four, these being linked by ester or imine groups [2].

Tetracatenar mesogens which possess two aliphatic chains at each lateral ring are also called biforked mesogens. The particular importance they have connects to the aspect of showing varied mesomorphisms: nematic, lamellar, cubic, columnar *etc*. [6], [7], [8], [9], [10].

It has been proved that the polymorphic behaviour of a polycatenar compound depends on the molecular parameters; therefore, mesomorphic behaviour may be annihilated if an oxymethylene group ($-CH_2O-$) is inserted into the core centre, unlike two methylene groups ($-CH_2-CH_2-$) which when introduced at the last connection between the rings enhances the possibility of the compound to show mesomorphism [10], [11].

A laterally grafted group on one of the rings of the rigid core will induce absence of columnar phases, although smectic and/or nematic mesophases will suggest the fact

that van der Waals forces rigid core – rigid core dictates the assembly of molecules [12].

The mesophase type can be somehow predicted by the ratio between the number n_c of carbon atoms of the paraffinic part and the number n_φ of phenyl rings which form the core. For the observation of a columnar phase, this ratio should be larger than 9 [13].

In a symmetrically substituted tetracatenar system, when the chain is short in length, the observed phases are nematic and smectic C phases. The main arguments supporting these facts are:

- keeping it like with like, the aromatic cores will tend to stay close together as alkyl chains will prefer the same – this characteristic represents the driving force which forms the lamellar mesophase
- the core cross-sectional area seems to be different from the chains at the interface; thus, the dissimilitude between them two is not very ample in a calamitic mesogen, hence the cores and chains will have free access to arrange themselves in either orthogonal or tilted smectic mesophases. What is observed is that the cross-sectional area of the core is greater than that of the rigid core, consequently causing the core to be tilted at a certain angle – the only smectic phase that such symmetrical tetracatenars may exhibit was proved to be smectic C (as depicted in **Figure 1.21**) [2], [5]. Experimentally proven, the tilting angle of the cores has an approximate value of 50°, while the one of the external chains is close to 20° [3]

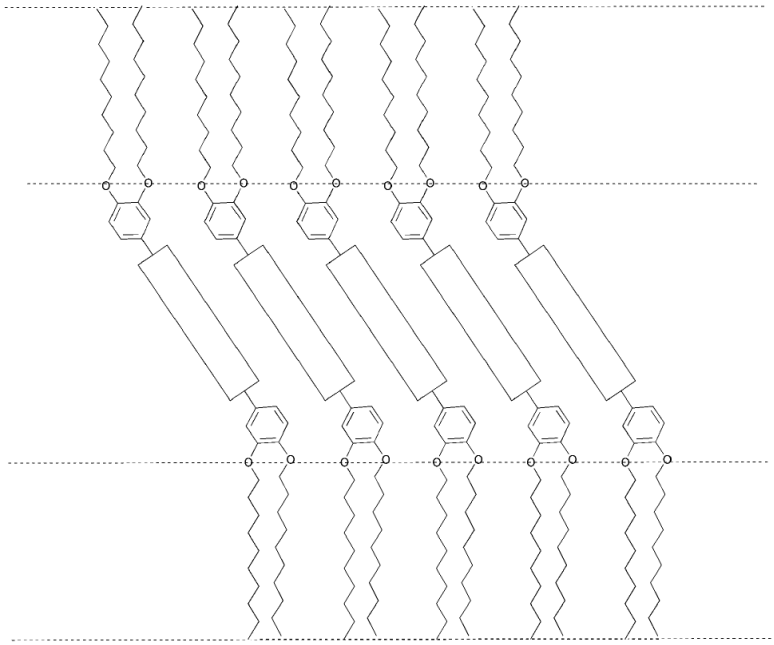

Figure 1.21. Schematic representation of tilting angle typical to a smectic C mesophase of polycatenars.

When the length of the external chains is intermediate, the variety of mesophases displayed is larger, because cubic phase may also be encountered. The logical explanation would be segregation between aromatic rings forming the core and aliphatic chains. The immediate consequence represents the consideration of the polycatenar system as amphiphilic in this case. This is the reason why the analogy between lyotropic and thermotropic mesogens arises into discussion as along with temperature raise, one may be remarked the rectangular/oblique columnar or oblique phase in between the smectic and hexagonal columnar mesophases [14].

With the purpose of explaining the thermotropic/ lyotropic analogy, it is needed that the diagram of a theoretical binary mixture of an amphiphile in water is presented (**Figure 1.22**). In this type of systems the incompatibility of hydrophobic and hydrophilic parts causes the formation of a surface which is a function of both the headgroup size and terminal chain volume. Describing the diagram, I_1 is a simple micellar cubic phase where curvature is significant for that it is reduced further in the H_1 hexagonal and V_1 bicontinuous cubic phases. In the middle of the diagram, there is present a surfactant concentration range when the curvature completely disappears. By keeping increasing surfactant concentration, the water-in-oil phases are formed.

Further on, the order of exhibited phases is reversed: first, a V_2 bicontinuous cubic phase, followed by an H_2 hexagonal and an I_2 micellar cubic phase afterwards. During this evolution, the curvature is increased [2].

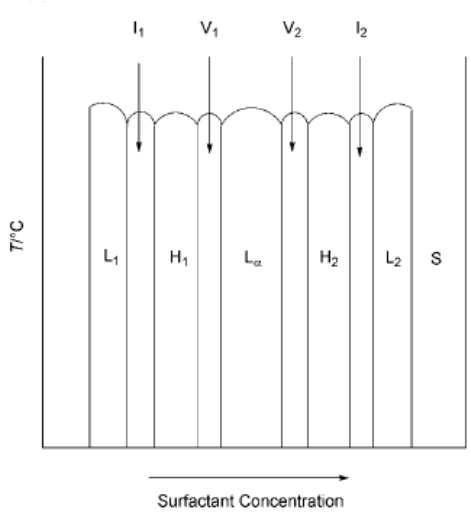

Figure 1.22. Phase diagram of a binary mixture between an amphiphile and its solvent, water. The abbreviations represent: L_1 and L_2 – micellar solutions; I_1 and I_2 – micellar phases; H_1 and H_2 – hexagonal phases; V_1 and V_2 – bicontinuouscubic phases; L_α – lamellar phase; S – solid. The subscripts 1 and 2 denote 'normal' oil-in-water and 'reversed' water-in-oil phase respectively [2].

The order caused in the diagram of mesophases lies within the manner the headgroup and alkyl chains assemble themselves depending on the size of the headgroup compared to the volume of alkyl chains. Sticking with this aspect, a large-sized headgroup will generate a large curvature unlike a very small-sized headgroup which induces large curvature in a reversed way this time (**Figure 1.23**) [2].

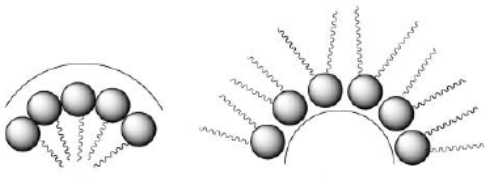

Figure 1.23. Representations (from left to right) of curvatures formed by a large-sized headgroup and a small-sized one, respectively.

Not all the possible lyotropic phase types for amphiphilic systems are shown in **Figure 1.22** but the scope of representation is to have a general idea of the multitude of mesophases. Trying to attain similarities between lyotropic amphiphilic systems and thermotropic mesogens, geometric correlations to the phase diagram from **Figure 1.22** have been explored by Goodby and Tschierske who managed to obtain the phase succession by mixing pairs of carbohydrate compounds. Additionally, they successfully synthesized special molecules with headgroups and chains controlled from their size point of view (**Figure 1.24**). Thus, these amphiphilic molecules phases could reproduce very satisfactorily the lyotropic phase diagram [2].

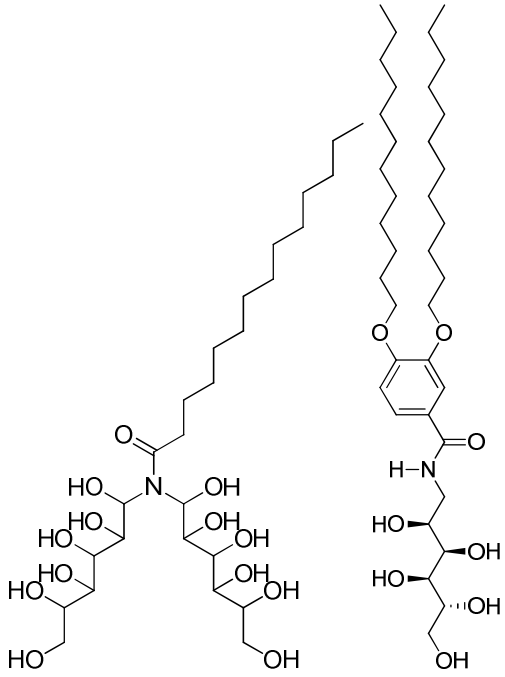

Figure 1.24. Carbohydrate molecules examined (from left to right) by Goodby and Tschierske, respectively.

A former study of a series of tetracatenar 2,2'-bipyridines (**Figure 1.25**) derivatives containing a range of *n* = 1-14 carbon atoms in each of the external chains reveals the evolution from smectic to cubic phase and further on from cubic to columnar phase (**Figure 1.26**) [2], [14]. Therefore, one notices that the transition is influenced by chain length and temperature.

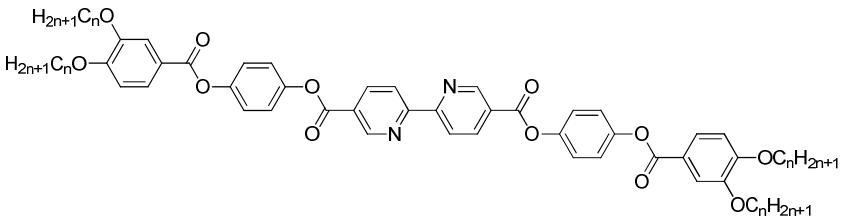

Figure 1.25. Molecular structure of a series of tetracatenar 2,2'-bipyridines on a range of *n* = 1-14.

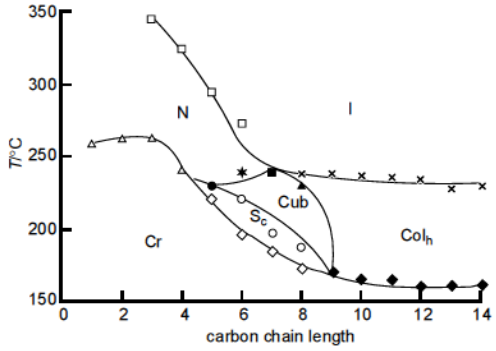

Figure 1.26. Phase diagram corresponding to the tetracatenar 2,2'-bipyridines; the abbreviations are: Cr = crystal, S_c = smectic C, N = nematic, Cub = cubic, Col_h = columnar hexagonal, I = isotropic and the transitions: Δ - crystal to nematic, ◊ - crystal to smectic C, ♦ - crystal to columnar hexagonal, ● - smectic C to nematic, ○ - smectic C to cubic, * - cubic to nematic, ▲- cubic to columnar hexagonal, □ - nematic to isotropic, ■ - cubic to isotropic, × - columnar hexagonal to isotropic.

1.13. The Thermotropic/Lyotropic Analogy

In the case of this similarity, the lyotropic L_α phase (see **Figure 1.22**), when interfaces are planar (hence curvature is absent), is equivalent to the smectic phases of the thermotropic compounds in which areas between the layers or parts of the layers are flat. If one has to find an analogue to the hexagonal 'water-in-oil' lyotropic phase H_2 (see **Figure 1.22**) where a polar core is captured by apolar chains, this would be the columnar hexagonal thermotropic mesophase (here, the polar core of the mesogen is in the centre of a matrix-like coat composed of apolar chains) [2].

The columnar packing of polycatenar systems can be explained using a proposed model of a hexacatenar compound in which the cross-sectional area is formed of several parallelly oriented one next to the other rigid cores [15]. In this arrangement, the terminal aliphatic chains are rather disorganized and confine the rigid cores by forming a liquid matrix-like around. Logically, the clusters of rigid cores thus formed will stack one over another in order to constitute columns (**Figure 1.27**) [2], [13].

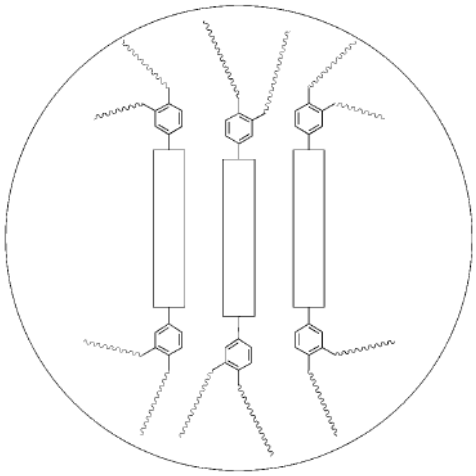

Figure 1.27. Arrangement modelled for the purpose of explaining the organisation in clusters of rod-like tetracatenars in the hexagonal mesophase.

Having a more in-depth look over the features of the columnar hexagonal phase, there are three descriptions available which may show its arrangement. The first one includes types of molecules such as triphenylenes having the centre on a polar core role confined by aliphatic chains. The second model points out most closely the analogy between thermotropic and lyotropic systems, where chains orient themselves outwards (**Figure 1.28**). By analyzing the reason why such carbohydrate mesogens pack in this particular manner, the notable observation represents the bulkiness of terminal chains which is considerable against the headgroups [2].

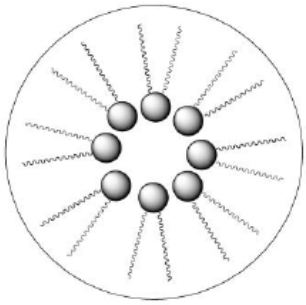

Figure 1.28. Mode of assemblage in a hexagonal thermotropic phase characteristic to carbohydrate molecules [2].

In the third model, an intermediate of the previous two others, there are polycatenars containing polar cores surrounded by apolar chains; the geometric reasons linked to the bulkiness of the chains influence the mode of assembly in a way similar to the carbohydrate molecules' model [2].

Continuing to analyze each of the three cases, the first model refers to discotic molecules that exhibit nematic (not often encountered) or columnar mesophases. Similarly, in the second example which best suits carbohydrate molecules, the variety of mesophases is rather poor. In order to obtain different phase transformations and move around the phase diagram, Goodby reached the conclusion that for the types of molecules synthesized by him (see **Figure 1.24**) every time a structural change needs to be brought to the molecule itself. The third model, unlike the previous two, outlines the possibility of polycatenars to display a diversity of mesophases: smectic, cubic or columnar depending on temperature and chain length.The cubic phases of polycatenars are often exhibited at intermediate temperatures which are between lamellar and columnar phases. Consequently, cubic thermotropic mesophases shall be matched to the lyotropic bicontinuous cubic V_2 phase (see **Figure 1.22**).

Additionally to continue shortly with the thermotropic/ lyotropic analogy, the correspondents of the micellar cubic phases I_1 and I_2 (see **Figure 1.22**) are however met only at particular mesogens.

To describe cubic phases, it is needed to outline that the symmetry is high and therefore the anisotropy lacks. By doing polarizing optical microscopy, no texture is

noticed. Furthermore, the viscosity is high and the kinetics of mesophase formation is generally slow.

Three models describe the cubic phases: the micellar model, the interconnecting rod model, and the infinite periodic minimal surface model. The first one is pliable for micellar cubic lyotropic phases, unlike the two others which approach the bicontinuous lyotropic cubic mesophases and cubic phases of thermotropic compounds.

The rod model displays the rods as being the polar headgroups, while the apolar chains are accommodated in the rest of space thus formed. If one applies this model to thermotropic polycatenars, the rods will represent the central cores which build the net where the chains fill the space. The rods situate at such positions that surfaces dividing the space are minimal. In order this spatial requirement to be respected, the rods constitute the rigid cores and the minimal surfaces are generated by the extended terminal chains (**Figure 1.29**) [16].

In the case of long external chains, the columnar phase is present in the manner of organization of molecules, beside nematic and smectic C phases [2].

To revise the way how polycatenars tend to pack depending on chain lengths (**Figure 1.29**), since the interface is generated between aromatic core and the terminal chains [16], one can specify that:

- in the case of short external chains, the curvature tends to be negligible as the discrepancy between volume of the core and that one of the chains; the consequence is a smectic C phase
- when the number of carbon atoms in each chain increases, the volume of the chains is enhanced enough to cause a dissimilarity in front of the volume of cores; in **Figure 1.29** one notices the undulating layers determined by this mismatch
- if the discrepancy of volumes is high enough, the initial smectic layers will give rise to columns
- at intermediate generated curvatures, which are greater than the one of the smectic layers but smaller compared to the requirements of the columnar phase formation

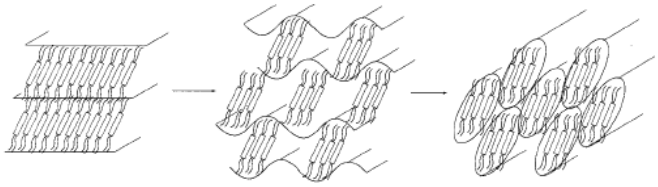

Figure 1.29. Representation of the progression of interface curvature in polycatenar systems (from left to right): the first is a lamellar phase with zero curvature, the middle one shows undulating layers and the third is characteristic to columnar mesophases.

1.14. Smectic-to-Columnar Transition

The transition smectic-to-columnar involves a low enthalpy and the volume changes are negligible. Also, NMR molecular dynamics technique reflected a resemblance among the self-diffusion and reorientational rotations movements in the smectic C and columnar phases [17]. All these arguments build up the belief that the transition cannot undergo a serious change in the local structure.

A model which depicts the smectic-to-columnar transition was proposed to elucidate the mechanism of evolution by explaining that in a smectic C phase, the sublayer composed of rigid cores shows undulation caused by the rejection between aliphatic chains and the rigid cores which needs to be sufficiently efficient when the thickness of the sublayer is maximum. As the temperature is raised, the volume of alkyl chains increases and as a consequence the sublayer undulations will be more pronounced. During the transition, the undulations amplitude reaches the thickness of the sublayer and if temperature continues to be increased, the sublayers will be divided into columns separated by the external chains which form a liquid-like matrix around them.

An observation being made reflects that during the transition from smectic to columnar molecules from adjacent columns are oriented fairly similarly the premise lying in the NMR molecular dynamics study in which smectic C was compared to columnar phase by judging on the contributions on the possible molecular movements to the general proton nuclear magnetic relaxation rate (reorientational

rotations, molecular self-diffusion and collective movements) [17]. Analyzing now the contributions of the collective movements, there is an obvious difference between the structures of each phase: while in the smectic C phase they are layer undulations, in the columnar mesophase, they resemble column deformations. Exploiting the similarity between phases, molecular self-diffusion and reorientational rotations approve this aspect, a local resemblance being confirmed. The mechanism of self-diffusion contribution is influenced by the geometric organization of molecules. During the smectic-to-columnar transition, similar diffusion constants in each case testify the preservation of parallelism between molecules that form adjacent columns and thus, small reminiscences of the sublayers in the smectic C phase will be present in the columnar mesophase. Therefore, it can be argued that molecules of columns in immediate vicinity are almost parallel. In the columnar phase, the hexagonal symmetry is realized by slight transitions of molecular orientations from a cluster to a neighbouring one along the columnar axis, this being possible without disrupting interactions between rigid cores (**Figure 1.30**) [13].

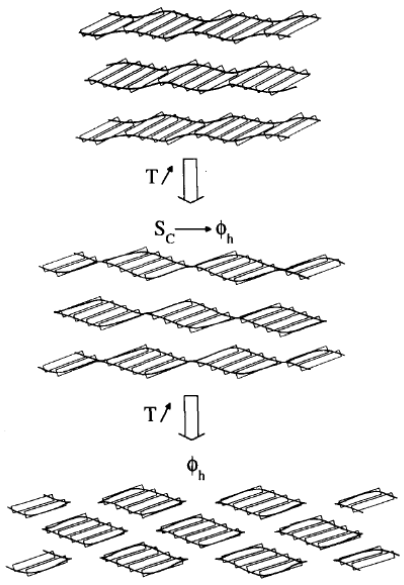

Figure 1.30. Proposed model for a smectic-to-columnar transition.

1.15. Polycatenars with Hydrogenated and Fluorinated Chains

The purpose of introducing fluorine in a molecule may induce the possibility of imprinting liquid crystal properties to the compound thus resulted. One of the industry branches in which liquid crystals are used is electronics, hence the coveted material characteristics: optical and chemical stability, a wide thermal mesomorphic range, a low conductivity and a low melting point. Most of the fluorinated liquid crystals possess low viscosities and conductivities.

Previous papers mention that perfluoroalkyl and perfluoroalkyloxy external chains induce a smectic mesophases due to the increased stiffness and increased polarity of the chain; however, not so many aspects of influence of the perfluoroalkoxy/perfluoroalkyloxy chains on phases have been investigated [18], [19], [20].

Another suggestive example of smectic induction is the single ring compound from **Figure 1.31** [21].

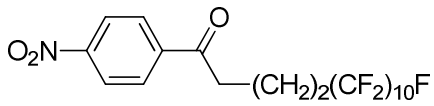

Figure 1.31. Molecule having a lateral fluorinated chain and only one benzene ring.

A pair of isomers from **Figure 1.32** enhanced greatly their smectic behavior if they are compared to a similar alkylated molecule [21]. At the same time, it is noted that if terminal chains are swapped, the smectic phase nature will change in this case (**Table 1.1**).

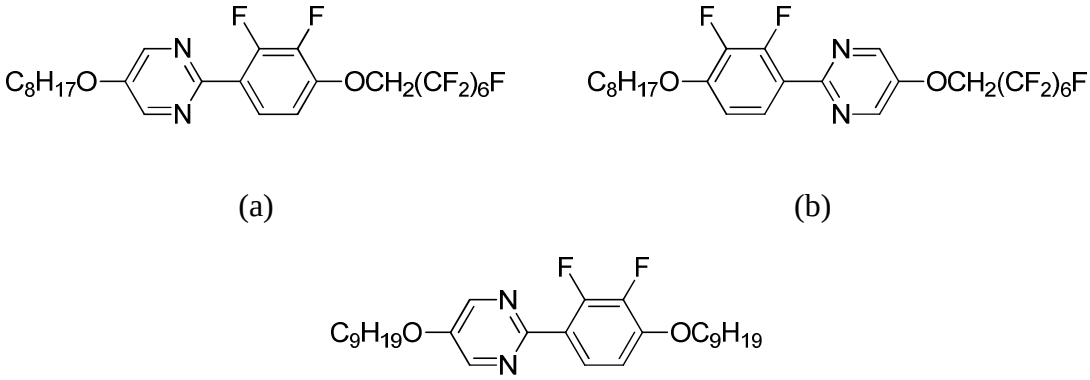

Figure 1.32. Representation of isomeric fluorinated molecules (a and b) and the corresponding alkylated similar compound (c) together with the transition temperatures of mesophases exhibited.

Table 1.1. Types of mesophases shown and temperatures at which transitions occur for each of the compounds from Figure 1.32 [21]; abbreviations are Cr = crystal, SmC = smectic C, SmA = smectic A, I = isotropic.

Mesogen	Transition temperatures (°C)
a	Cr 48 SmC 78 I
b	Cr 65 SmA 138 I
c	Cr 77 SmC 127 I

The notable question arising is that as hydrocarbon and fluorocarbon fragments phase separate, how will the molecules assemble themselves when the fragments are introduced in the same polycatenar system?

Taking into consideration the characteristics of perfluoro chains, one can enumerate [5]:

- the $-CF_2-CF_2-$ will prefer the trans conformation in the chain; furthermore, the fluorinated chain has the shape of a helix and the stiffness of it is greater if compared to a hydrocarbon chain
- there is a strong incompatibility between fluoro chains and aliphatic or aromatic hydrocarbons

Consequently, if one or more fluorinated chains are introduced at the end of polycatenars' terminal rings the flexibility and symmetry of molecule will be facts to be studied [5].

In a previous study in which tricatenars with three benzene rings have been synthesized (**Figure 1.33**), the exhibited mesophases are all smectic (**Table 1.2**) [5].

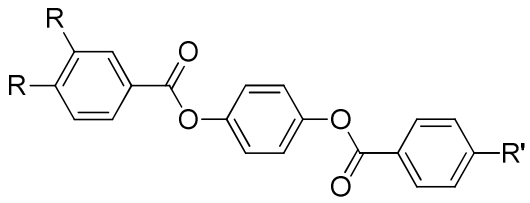

R = −O$(CH_2)_n$H, R' = −$(CF_2)_n$F or –O$(CH_2)_p(CF_2)_q$F

Figure 1.33. Synthesized three-benzene-ring core tricatenar mesogens containing a perfluoro or semi-perfluoro tail where *n*, *p* and *q* have the values comprised in Table 1.2.

In **Table 1.2**, Cr = crystal, S_I = smectic I, $S_{\hat{C}}$ = ribbon (first discovered in 1982 with polar rod-like molecules [22] and in compounds with a low molecular weight and no −CN or $-NO_2$ as functional groups), S_C = smectic C, S_A = smectic A, I = isotropic. Symbol „+" signifies the presence of the particular type of mesophase, whereas „-" stands for the absence of it.

As a general observation, a tilted smectic phase such as S_C and $S_{\hat{C}}$ is exhibited during mesophase transformations in the case of semi-perfluorinated chains but a smectic A phase is completely missing; here the methylenic –$(CH_2)_4$– groups inserted between the fluorinated chain and aromatic ring end impose this difference in liquid crystal behavior [5].

Table 1.2. Temperatures in columns marked by T, corresponding to the phase changes of the Figure 1.33 compounds: a) describes the compounds with *R'* = $-(CF_2)_nF$, while b) belongs to the tricatenars having *R'* = $-O(CH_2)_p(CF_2)_qF$.

n		Cr	T	S_I	T	$S_{\hat{C}}$	T	S_C	T	S_A	T	I
10		+	87	-		+	89.5	-		+	107	+
12		+	98	+	70	+	85	-		+	100	+
14		+	87	-		+	89	-		+	95	+

a)

n	*p*	*q*	Cr	T	S_I	T	$S_{\hat{C}}$	T	S_C	T	S_A	T	I
9	4	6	+	110	-		-		+	138	-		+
11	4	6	+	109	-		+	132	-		-		+
12	4	6	+	103	-		+	130	-		-		+
14	4	6	+	104	-		+	124	-		-		+

b)

Another example showing the effect of association hydrocarbon-hydrocarbon and fluorocarbon-fluorocarbon is encountered in simple types of molecules which demonstrated they show hexagonal phases (**Figure 1.34**) [23].

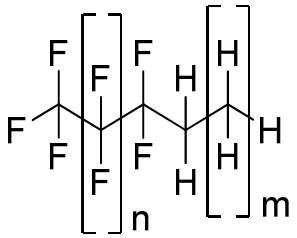

Figure 1.34. Simple type of fluorinated hydrocarbon molecules exhibiting mesomorphism.

In a Tournilhac fluorinated material, smectic A phase appeared to form, as a consequence of the fluorinated chains tending to associate separately from hydrocarbon ones. The molecule possesses a rigid core on which a semifluorinated long chain is attached (**Figure 1.35**) [23].

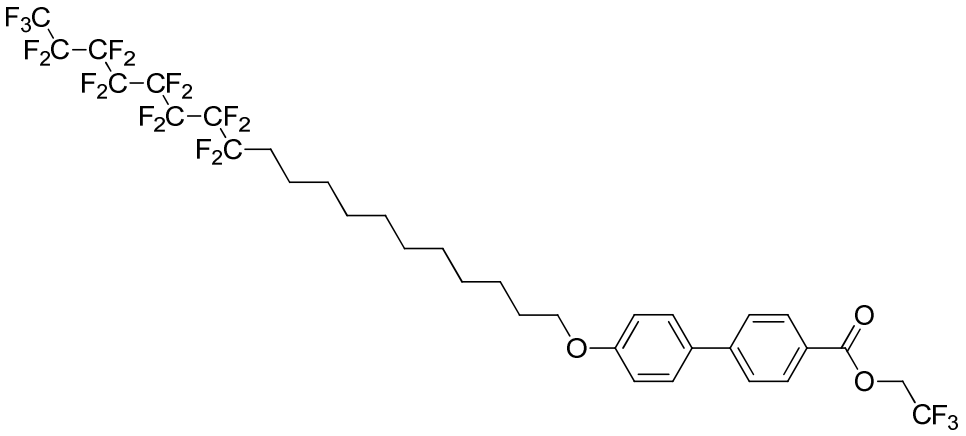

Figure 1.35. Molecule synthesized by Tournilhac.

1.16. Introduction of Fluorinated Chains and Role of Spacers

There have been previously studied several series of materials obtained by replacing the hydrogen atoms with fluorine atoms on an aliphatic chain [24]. The outcome was that the results thus obtained for the new compounds were proved to be different than of the ones containing non-fluorinated chains. In most studied cases, it was noted an increase in the mesophase thermal stability and in the temperature range corresponding to the smectic phase [24]. Nguyen had the idea to make complete replacement of the hydrogen atoms from the alkyl chains, with fluorine atoms on tail of the derivatives of 4-benzoic acid; the immediate result was replacement of nematic properties with smectic phases in comparison with their hydrocarbon analogues (**Figure 1.36** and **Table 1.3**) [19].

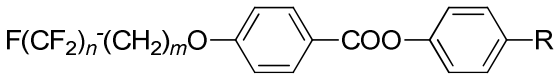

where *R* can be: $-OC_6H_{13}$ or –CN and *n*, *m* have the values comprised in **Table 1.3**

Figure 1.36. General structures of hydrocarbon-tailed mesogens and their corresponding perfluorocarbon-tailed compounds.

Table 1.3. Transition temperatures of compounds from Figure 1.36; abbreviations are: Cr = crystal, S_A = smectic A, I = isotropic, N = nematic, S_C = smectic C.

n	***m***	***R***	**Transition temperatures (°C)**
10	-	$-OC_6H_{13}$	Cr 134 S_A 143 I
-	10	$-OC_6H_{13}$	Cr 47.1 S_A 44.1 N 59 I
6	-	–CN	Cr 101 S_A 123 I
-	6	–CN	Cr 44 N 48.6 I
7	-	–CN	Cr 108 S_A 134 I
-	7	–CN	Cr 44 N 56.5 I
8	-	–CN	Cr 119 S_A 147 I
-	8	–CN	Cr 46 N 55 I
10	-	–CN	Cr 141 S_C 138 S_A 167 I
-	10	–CN	Cr 59 N 61 I

Compounds from **Figure 1.37** show interesting mesomorphism due not only to the presence of a perfluorinated tail but also a spacer consisting of methylene groups. To be more precise, one ethylene spacer enhances the liquid crystalline characteristics of the material, whereas in systems when the fluorinated chain is directly connected to the 4-biphenyl ring group, mesomorphic properties are absent [24].

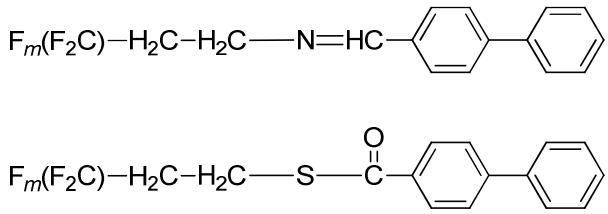

Figure 1.37. Molecules exhibiting mesomorphic properties where *m* = 4,6 or 8.

The important role of the spacer can be explained by varying the nature of spacers inside structures with 4-biphenyl rings as aromatic core. To exemplify, amidic (2),

hemithioacetal (7) or thioether (8) types of spacers will induce a lack in the smectic phase. Ester spacers such as –OCO– (5) give a short range of smectic mesomorphism, while thioesters (6), imines (1), ethers (9) or –COO– (4) esteric type lead to a good range of smectic properties (**Table 1.4**) [24].

Table 1.4. Variation on spacers and the phases observed under the polarizing optical microscope; abbreviations represent: Cr = crystal, S_A = smectic A, I = isotropic.

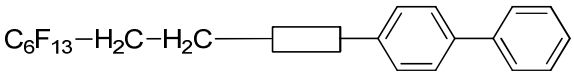

where ▭ represents the spacer

	Spacer	Transition temperatures while heating (°C)
1	−N=CH−	Cr 57 S_A 105 I
2	−NHC(O) −	Cr 175 I
3	−N(CH_3)C(O) −	Cr 87 S_A 90 I
4	−C(O)O−	Cr 80.5 S_A 113.2 I
5	−OC(O) −	Cr 70.5 S_A 72 I
6	−SC(O) −	Cr 51.6 S_A 152 I
7	−SCH_2O−	Cr 71.6 I
8	−SCH_2−	Cr 59.7 I
9	−O−	Cr 81.4 S_A 105.5 I

1.17. Project Aims

The type of molecules proposed to be analyzed from their liquid crystalline properties point of view are polycatenars bearing only fluorocarbonated chains or a mixture of fluorocarbonated and hydrocarbonated chains. The principal aim is to figure out the manner of molecular organization into phases of the polycatenars synthesized bearing in mind the mismatch between fluorocarbon and hydrocarbon chains themselves.

1.18. Characterization of New Materials

^{1}H-NMR,^{13}C-NMR and ^{19}F-NMR will be used as NMR techniques for characterizing the target compounds. Also, elemental analysis and mass spectrometry will confirm the chemical structures. The liquid crystalline properties are investigated by both polarized optical microscopy and differential scanning calorimetry. After the pattern types of liquid crystals are established, a more insight approach will be given by small-angle X-ray diffraction at the Institute of Physics and Chemistry of Materials Strasbourg due to the group having access to a range of experiments such as recording diffraction patterns from uncovered drops this technique being very accurate and giving an in-depth grasp of the liquid crystalline mesophase self-assembly.

Hydrocarbon and fluorocarbon chains phase separately if each of them belongs to different molecules. The next question arising is how will these chains behave if they pertain to the same molecule, hence the interest for molecular arrangement of the fluorinated target materials. Will the fluorinated chains stay close to the others of the same type and will the hydrocarbonated have an analogous preference to associate near hydrocarbon chains? Usually, the mesophase exhibited respecting these conditions is a lamellar phase (generally, smectic A). The compound in **Figure 1.38** demonstrates it packs in a smectic C and a cubic mesophase (see **Table 1.5**) [26].

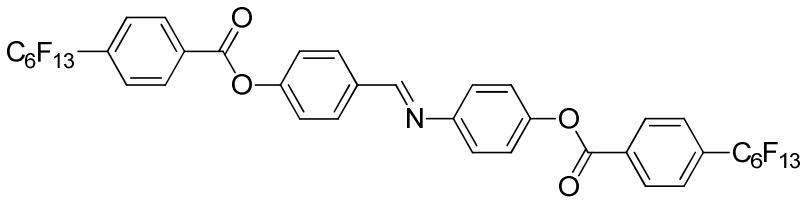

Figure 1.38. Dicatenars with perfluorinated alkyl chains.

Table 1.5. Transitions observed on heating the mesogen from Figure 1.38 together with temperatures and both corresponding enthalpies and entropies; the abbreviations are: Cr = crystal, S_C = smectic C, Cub = cubic, I = isotropic.

Transition type	Temperature (°C)	ΔH (kJ mol^{-1})	ΔS (J K^{-1} mol^{-1})
Cr-S_C	239	48.6	36
S_C-Cub	268	2.4	5
Cub-I	310	5.2	9

Considering the polycatenars bearing solely hydrocarbon chains, the lamellar phase would be a smectic C in which molecules arranged on a tilting angle in layers because of the dissimilarity between the core cross-sectional area and the chains at the interface (see **Figure 1.21**). In the case of fluorocarbon chains which occupy a larger volume than hydrocarbon chains, the mismatch is more pronounced; consequently, the chain substituting the benzene ending ring at the 3 position may be pushed away from the long molecular axis due to its bulkiness (one fluorine atom occupies a larger space than one hydrogen atom).

Now, paying a particular importance on the unsymmetric target molecules, the envisaged possibilities of assemblage are depicted in **Figure 1.39** where clearly the hydrocarbon chains phase together and fluorocarbon likewise. The synclinic model collects all the tetracatenars distributed parallelly in a layer, unlike the anticlinic one when molecules in neighbouring arrays of parallelly disposed tetracatenars form a certain angle between their molecular long axes.

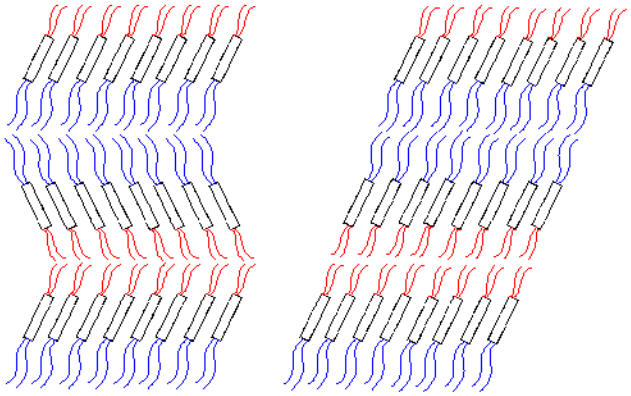

Figure 1.39. Schematical representation of two-dimensional assemblies of unsymmetric tetracatenars bearing only fluoroalkyl chains at one end (blue is the representative color) and only hydrocarbonated chains at the other (colored in red): anti- (left-hand side) and synclinic (right-hand side).

The disadvantage of the above representations will be that the curvature created by dissimilarities introduced by the larger volume of fluorocarbons cannot be literally taken into account.

Alternately, the symmetrical compounds bearing only one fluoroalkyl chain at each end could accommodate molecules in a peculiar way imagining that as spaces will need to be occupied, the representation from **Figure 1.40** shall be in fact three-dimensional.

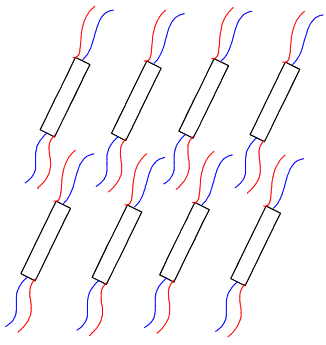

Figure 1.40. Two-dimensional hypothetical arrangement representation of symmetrical tetracatenars possessing only one fluorinated chain at each of the ends (blue symbolizes the fluorinated chains, while red is for hydrocarbonated ones).

Another immediate question arising is would the tricatenar compounds bearing one fluorocarbon chain at one end and two hydrocarbon chains at the other assemble in an orthogonal smectic phase as depicted in **Figure 1.41**?

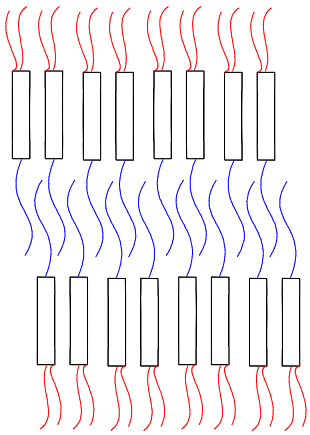

Figure 1.41. Hypothetical assembly of tricatenars (hydrocarbon chains are colored in red and the fluorocarbon ones which are longer are coloured in blue).

References:

1. B. Donnio, D. Guillon, R. Deschenaux and D. W. Bruce, in: *Comprehensive Coordination Chemistry II*; Eds. J. A. McCleverty and T. J. Meyer, Elsevier: Oxford, UK, 2003, **7**, chapter 7.9, 357;

2. D. Fazio, C. Mongin, B. Donnio, Yves Galerne, D. Guillon and D. W. Bruce, *J. Mater. Chem.*, 2001, **11**, 2852;

3. A. I. Smirnova, D. Fazio, E. F. Iglesias, C. G. Hall, D. Guillon, B. Donnio and D. W. Bruce, *Mol. Cryst. Liq. Cryst.*, 2003, **396**, 227;

4. J. Malthête, H. T. Nguyen and C. Destrade, *Liq. Cryst.*, 1993, **13**, 171;

5. H. T. Nguyen, C. Destrade and J. Malthête, *Adv. Mater.*, 1997, **9**, 375;

6. A. M. Levelut, J. Malthête, C. Destrade and H. T. Nguyen, *Liq. Cryst.*, 1987, **2**, 877;

7. H. T. Nguyen, C. Destrade, A. M. Levelut and J. Malthête, *J. de Phys.*, 1986, **47**, 553;

8. C. Destrade, H. T. Nguyen, A. Roubineau and A. M. Levelut, *Mol. Cryst. Liq. Cryst.*, 1988, **159**, 163;

9. H. T. Nguyen, C. Destrade and J. Malthête, *Liq. Cryst.*, 1990, **8**, 797;

10. C. Destrade, H. T. Nguyen, C. Alstermark, G. Lindsten, M. Nilsson and B. Otterholm, *Mol. Cryst. Liq. Cryst.*, 1990, **180B**, 265;

11. J. Malthête, H. T. Nguyen and C. Destrade, *Mol. Cryst. Liq. Cryst.*, 1988, **165**, 317;

12. H. T. Nguyen, C. Destrade and J. Malthête, *Handbook of Liquid Crystals*, H. T. Nguyen, C. Destrade and J. Malthête, *Liq. Cryst.*, 1997, **9**, 375;

13. D. Guillon, B. Heinrich, A. C. Ribeiro, C. Cruz and H. T. Nguyen, *Mol. Cryst. Liq. Cryst.*, 1998, **317**, 51;

14. K. E. Rowe and D. W. Bruce, *J. Mater. Chem.*, 1998, **8**, 331;

15. D. Guillon, A. Skoulios and J. Malthête, *Europhys. Lett.*, 1987, **3**, 67;

16. D. W. Bruce, *Acc. Chem. Res.*, 2000, **33**, 831;

17. C. Cruz, J. L. Figueirinhas, P. J. Sebastiao, A. C. Ribeiro, F. Noack, H. T. Nguyen, B. Heinrich and D. Guillon, *Z. Naturforsch*, 1996, **51a**, 155;

18. E. P. Janulis, J. C. Norack, G. A. Papapolymerou, M. Tristani-Kendra and W. A. Huffman, *Ferroelectrics*, 1988, **85**, 375;

19. H. T. Nguyen, G. Sigaud, M. F. Achard, F. Hardouin, R. J. Twieg and K. Betterton, *Liq. Cryst.*, 1991, **10**, 389;

20. T. Doi, Y. Sakurai, A. Tamatani, S. Takenaka, S. Kusabayashi, Y. Nishihata, H. Teraushi, *J. Mater. Chem.*, 1991, **1**, 169;

21. M. Hird, J. W. Goodby, R. A. Lewis and K. J. Toyne, *Mol. Cryst. Liq. Cryst.*, 2003, **401**, 115;

22. F. Hardouin, H. T. Nguyen, M. F. Achard and A. M. Levelut, *J. Phys. Lett.*, 1982, **43**, 327;

23. M.-A. Guillevic, T. Gelbrich, M. Hursthouse and D. W. Bruce, *Mol. Cryst. Liq. Cryst.*, 2001, **362**, 147;

24. F. Guittard, E. Taffin de Givenchy, S. Geribaldi and A. Cambon, *J. Fluorine Chem.*, 1999, **100**, 85;

25. A. I. Smirnova, N. V. Zharnikova, B. Donnio and D. W. Bruce, *Russ. J. Gen. Chem.*, 2010, **80**, 1331;

26. M.-A. Guillevic and D. W. Bruce, *Liq. Cryst.*, 2000, **27**, 153

CHAPTER 2

RESULTS AND DISCUSSION

Reagents used for synthesis were commercially purchased from Sigma-Aldrich, Fisher Scientific, VWR and solvents for synthesis and purification were HPLC-grade and used as received.

Spectroscopic techniques

Nuclear Magnetic Resonance. Samples were run on JEOL ECX 400 and ECS 400 with a field strength 400 MHz, equipped with an auto-charger. Mest-Rec NMR software was used to process the spectra obtained.

Polarised Optical Microscopy. Mesomorphic studies were performed using an Olympus BX50 Optical Microscope equipped with a Linkam Scientific LTS350 heating stage, Linkam LNP2 cooling pump and a Linkam TMS92 controller.

Differential Scanning Calorimetry. Calorimetry scans were run on a Mettler Toledo DSC822e, equipped with a TSO801R0 Sample Robot and calibrated using pure indium. Samples were run at heating cooling rates of 5 °C min^{-1}.

CHN Elemental Analysis. Analysis was carried out on an Exeter Analytical Inc CE 440 Elemental Analyser and a Sartorius SE2 analytical balance by Dr. Graeme McAllister at the University of York.

Low-angle X-ray Diffraction. Analysis was run at the Institute of Physics and Chemistry of Materials at the University of Strasbourg by Dr. Bertrand Donnio/ Dr. Benoît Heinrich. The XRD patterns were obtained with two different experimental set-ups. In all cases, a linear monochromatic Cu-$K_{\alpha 1}$ beam (λ = 1.5405 Å) was obtained using a sealed-tube generator (900 W) equipped with a bent quartz monochromator. The second set of diffraction patterns was recorded with a curved Inel CPS 120 counter gas-filled detector linked to a data acquisition computer.

2.1. Synthesis

2.1.1. Synthesis of the Symmetric Tetracatenar Mesogen Having all the Four Chains Semiperfluorinated

All the target compounds contain at least one fluorinated chain; therefore, it was necessary to find a manner in which the fluorinated chains containing four methylene groups $-(CH_2)_4-$ as a spacer can be grafted on the external benzene rings of the rigid core. The methylene groups constitute spacers which allow a certain flexibility to the external chains and molecules with semifluorinated chains present an increased mesomorphic stability than the perfluorinated chains. Moreover, the methylene groups optimum number for these characteristics to be present is at least four.

As it will be shown, the subsequent introduction of a fluorinated chain will be made by *O*-alkylation ([1], [2], [3]), and so for this purpose, it was necessary to synthesise the bromides $CF_3(CF_2)_n(CH_2)_4Br$ (n = 7, 9) bearing both the spacer ($-(CH_2)_4-$) and the perfluoro part of the chain ($CF_3(CF_2)_n-$) (**Scheme 2.1**).

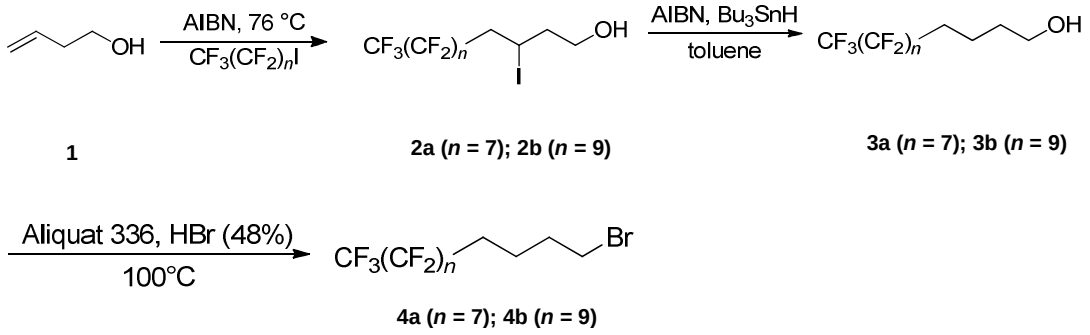

Scheme 2.1. Schematic manner of synthesis of the *O*-alkylating agent $CF_3(CF_2)_n(CH_2)_4Br$, where n = 7, 9.

The series of reactions leading to obtainment of $CF_3(CF_2)_n(CH_2)_4Br$ starts from a radical addition of 1-iodoperfluoroalkane $CF_3(CF_2)_nI$ to 3-buten-1-ol **1** in the presence of the radical initiator AIBN which yields the intermediates **2a** and **2b**. The

alcohols **3a** and **3b** were obtained by reduction of the previously stated intermediate iodinated alcohols in the presence of tributyltin hydride Bu_3SnH and AIBN. The bromination of **3a** and **3b** was realised with an aqueous solution of 48% HBr and Aliquat 336 as a phase transfer reagent. The resulting bromides are thus **4a** and **4b**.

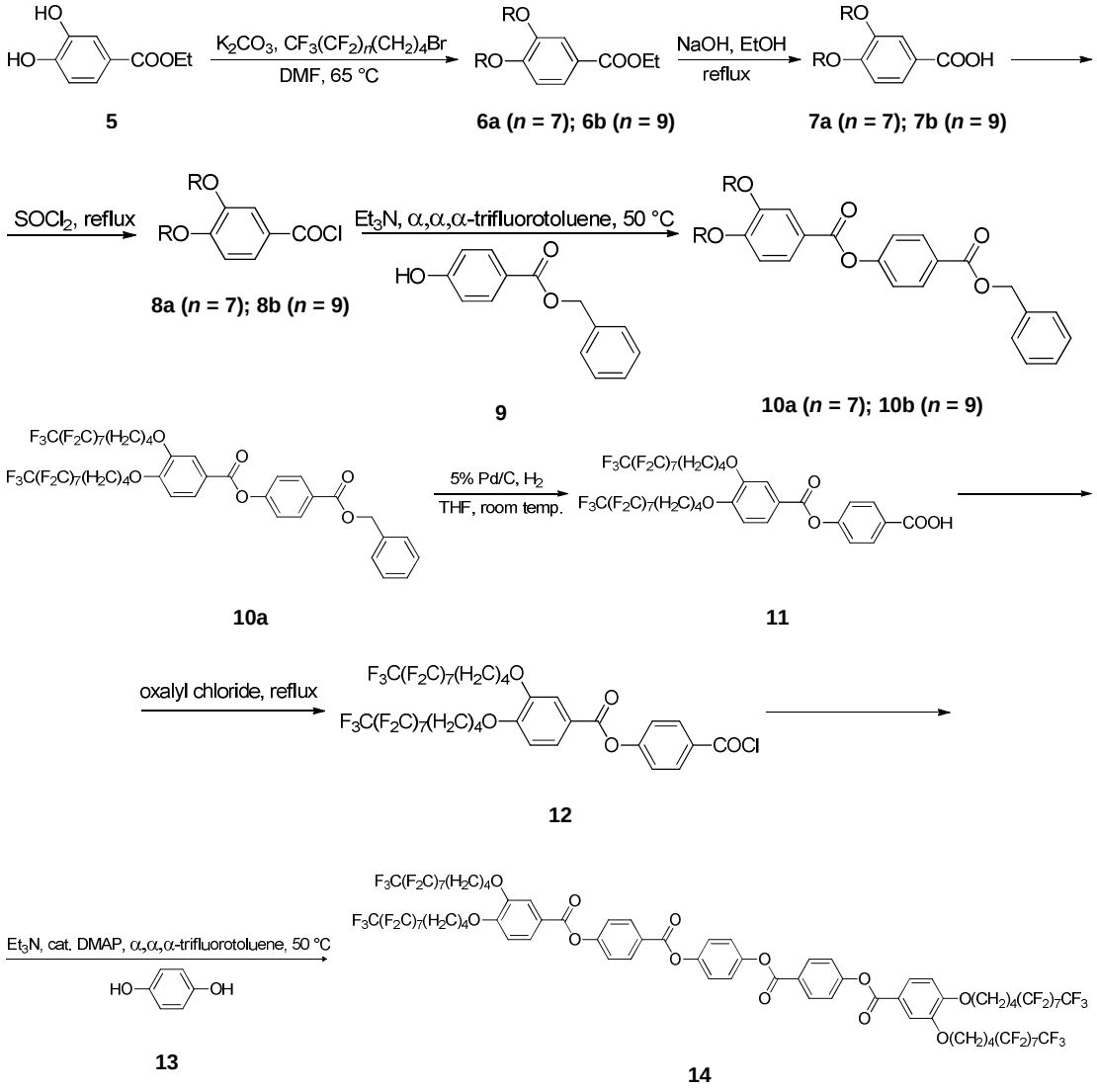

Scheme 2.2. Scheme representing the synthetic approach for the obtainment of tetracatenarmesogens with all terminal chains fluorinated; *R* = $CF_3(CF_2)_7(CH_2)_4$– or $CF_3(CF_2)_9(CH_2)_4$–, letters a and b following numbers of the compounds (6, 7, 8, 10) refer to *n* = 7 and 9, respectively.[†]

Both compounds **6a** and **6b** from **Scheme 2.2** were obtained by a Williamson etherification between ethyl 3,4-dihydroxy benzoic acid **5** and $CF_3(CF_2)_n(CH_2)_4Br$ (**4**) (*n* = 7, 9).

[†]Acknowledgements to research project colleague Mei-Chun Tzeng who synthesized the compounds in **Scheme 2.2**.

The effect of solubility decrease is noticeable when fluoroalkyl chains are introduced in tetracatenar molecules. To be precise, intermediates **7a** and **7b**, which were obtained consequently from hydrolysis **6a** and **6b** in a mixture NaOH/aqueous solution of EtOH, have an extremely low solubility in conventional organic solvents but they are sufficiently soluble in $CDCl_3$ which contains a small amount of CF_3COOH to make possible both NMR and mass spectrometry characterisation. In order to carry on with the reaction series, acids **7a** and **7b** were converted into acid chlorides **8a** and **8b**, respectively, in reflux reactions using thionyl chloride. Thus, the immediate effect was an increase in solubility and reactivity.

The benzyl compounds **10a** and **10b** were then obtained by reaction between the corresponding acid chloride **8a** or **8b** and compound **9**, in the presence of triethylamine (Et_3N) as a base in α,α,α-trifluorotoluene as solvent. Next step constitutes hydrogenolysis of intermediate **10a** at atmospheric pressure and room temperature in the presence of 5% Pd/C, which yielded the two-ring carboxylic acid **11** that was very insoluble. The NMR characterisation of these intermediates was carried using $CDCl_3/CF_3COOH$. The hydrogenolysis for the similar benzyl compound **10b** was not possible due to difficulties met at separation of the resulting carboxylic acid bearing $CF_3(CF_2)_9(CH_2)_4-$ as external chains, from the catalyst 5% Pd/C, as a consequence of the very low solubility of the acid in THF: after filtration of reaction mixture, the carboxylic acid was found in a significant quantity on the sintered funnel mixed together with the catalyst. Attempts of solubilising the carboxylic acid using hot CF_3COOH which was poured over the sintered funnel containing the mixture of acid-catalyst were not successful (the calculated yield after evaporating the solvent mixture THF-CF_3COOH thus resulted was approximately 2%).

Getting back to compound **11**, as found previously, the solution to improve solubility of this acid was to convert it into its corresponding acid chloride **12** in a reflux reaction in the presence of oxalyl chloride. The reason why oxalyl chloride was chosen in detriment of thionyl chloride was because the former would hydrolyse the ester –COO– group connecting the two benzene rings. The final tetracatenar mesogen **14** was synthesised from **12**, respectively, by esterifying it with hydroquinone, **13,** in the presence of Et_3N and a catalytic amount of DMAP using α,α,α-trifluorotoluene as a solvent.

2.1.2. Synthesis of Unsymmetric Tetracatenar Mesogens Having Two Fluoroalkyl Chains at One Side and Two Hydrocarbon Chains at the Other

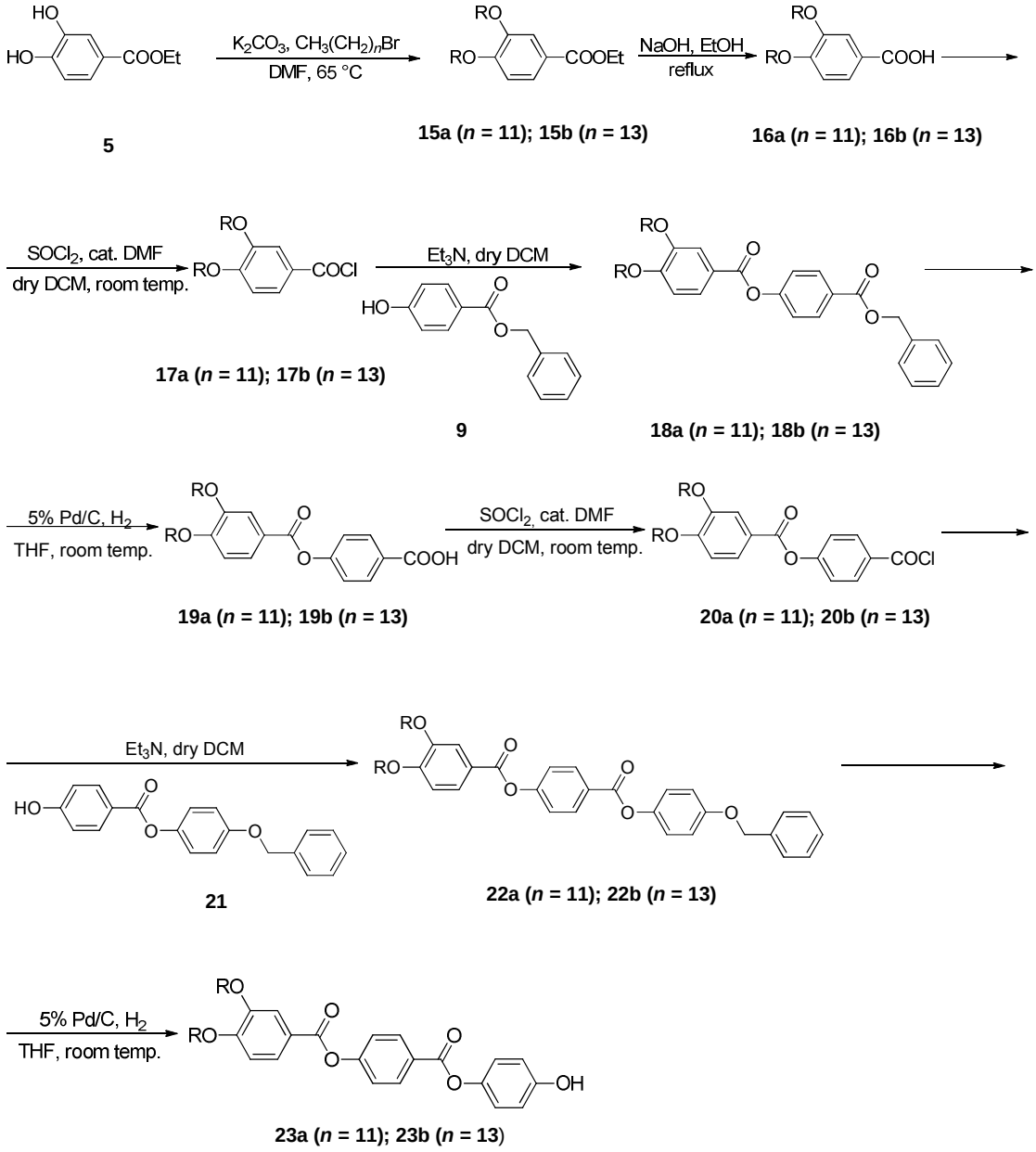

Scheme 2.3. Synthesis of *O*-monosubstituted hydroquinones; *R* = $CH_3(CH_2)_n$–, where *n* = 11, 13, and letters a and b refer to compounds corresponding to the *n* = 11 and 13, respectively.

It is clear that preparation of unsymmetric tetracatenar mesogens will require extra synthetic steps. The approach needed to take into account the fact that both the compounds containing semifluorinated chains were much less soluble than their hydrocarbon analogues and also that solubility decreases as more phenyl rings are added. Consequently, the target compounds were the 3, 4–disubstituted benzoic acids

containing semifluorinated chains and the *O*-monosubstituted hydroquinones, **23a** and **23b**, containing alkyloxy chains.

The preparation of these hydroquinones starts with compound **5**, which is dialkylated with dodecylbromide and tetradecylbromide, respectively, in the presence of K_2CO_3 in dry DMF, reaction carried out at 65 °C. The compounds thus resulted, **15a** and **15b**, are hydrolysed in a 10 N NaOH/EtOH aqueous mixture under reflux. The acids obtained in this manner, **16a** and **16b**, were left in dry DCM, in which it was added $SOCl_2$ and a few drops of catalytic dry DMF, at a temperature of 0-5 °C (ice-water bath used). The acid chlorides resulted from this reaction, **17a** and **17b**, esterified with compound **9**, in presence of Et_3N as a base, yielded the benzyl compounds **18a** and **18b**, which were further hydrogenolysed to compounds **19a** and **19b** using the same conditions as mentioned previously in **Scheme 2.2**. The two-benzene-ring benzoic acids **19a** and **19b** lead to acid chlorides **20a** and **20b** after an analogous procedure to the one for obtaining acid chlorides **17a** and **17b**. The benzyl compounds **22a** and **22b** were delivered after the esterification between acid chlorides **20a** or **20b**, and phenol **21** in dry DMF, at room temperature, in presence of Et_3N. Further hydrogenolysis gave rise to the *O*-monosubstituted hydroquinones **23a** and **23b**.

As presented before, the final compound having two fluorinated chains at one end and two hydrocarbonated chains at the other is delivered after the esterification between **12** and **23a**, in presence of Et_3N using α,α,α-trifluorotoluene as organic solvent– compound **24** (**Scheme 2.4**).

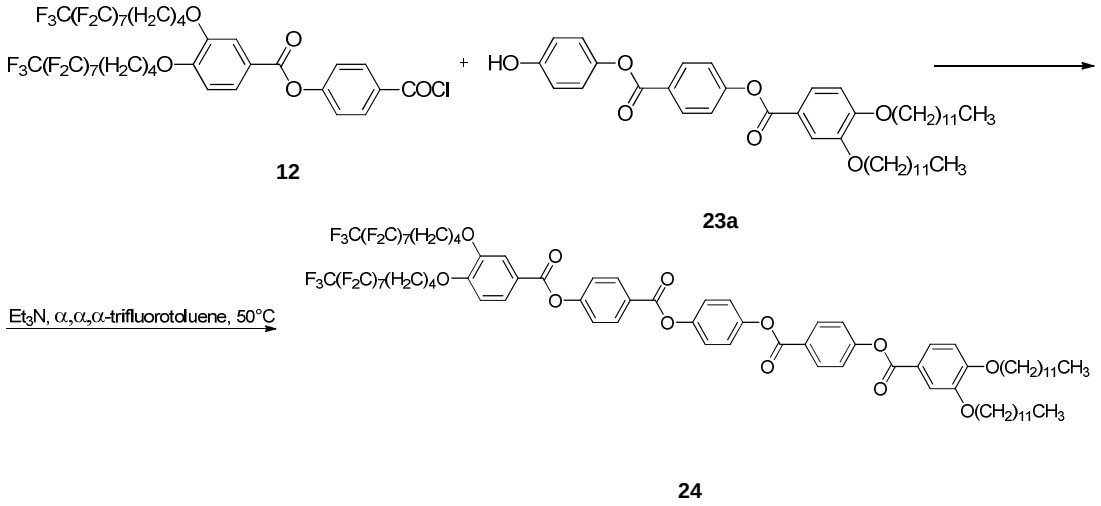

12 **23a** **24**

Scheme 2.4. Synthesis of target compound having two fluoroalkyl chains at one end and two hydrocarbon chains at the other.[†]

2.1.3. Synthesis of Unsymmetric Tetracatenar Mesogens Bearing Mixed Chains at One End and Hydrocarbon Chains at the Other

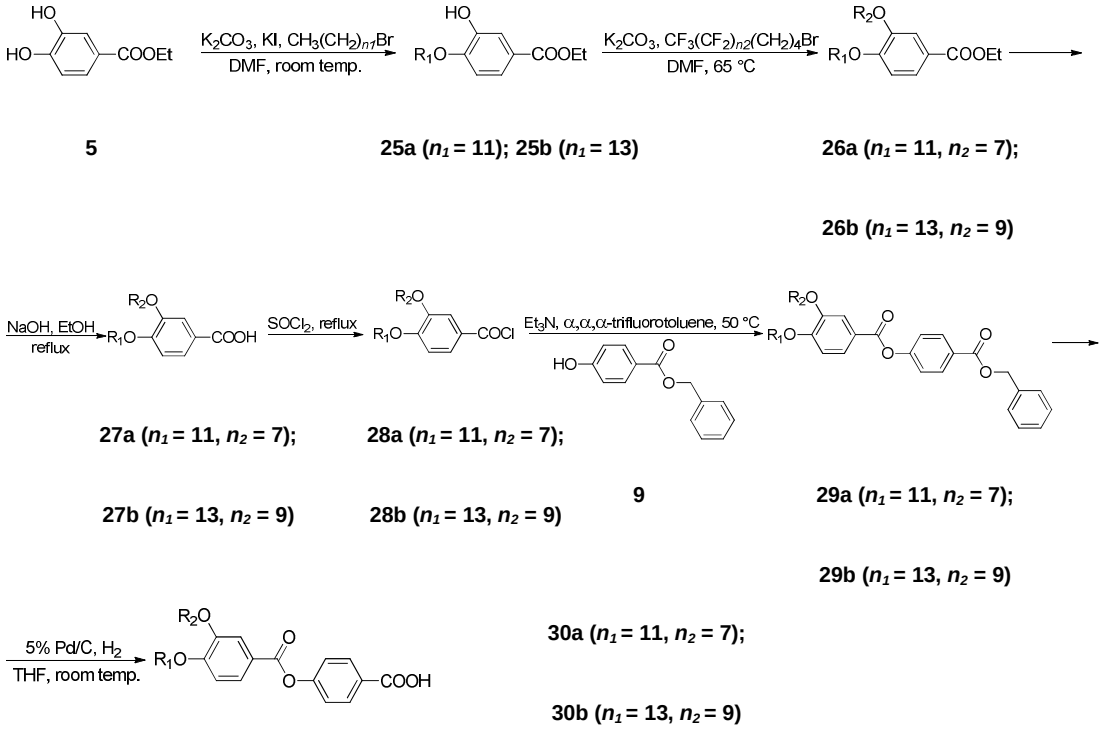

5 **25a (n_1 = 11); 25b (n_1 = 13)** **26a (n_1 = 11, n_2 = 7);** **26b (n_1 = 13, n_2 = 9)**

27a (n_1 = 11, n_2 = 7); **28a (n_1 = 11, n_2 = 7);** **9** **29a (n_1 = 11, n_2 = 7);**

27b (n_1 = 13, n_2 = 9) **28b (n_1 = 13, n_2 = 9)** **29b (n_1 = 13, n_2 = 9)**

30a (n_1 = 11, n_2 = 7);

30b (n_1 = 13, n_2 = 9)

Scheme 2.5. Synthesis of two-benzene-ring benzoic acids possessing a hydrocarbon chain in the 4 and a fluoro chain in the 3 position of the terminal benzene ring; R_1 = $CH_3(CH_2)_{n1}$–, R_2 = $CF_3(CF_2)_{n2}(CH_2)_4$–, where letters a and b refer to n_1 = 11 and n_1 = 13, respectively, for compounds 25, whereas a and b refer to n_1 = 11, n_2 = 7, and n_1 = 13, n_2 = 9, respectively, for compounds 26, 27, 28, 29, 30.

[†]Acknowledged work of Mei-Chun Tzeng for synthesis of compound **24**

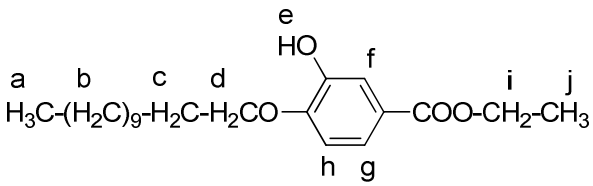

Compound **25a**

The ^{1}H NMR spectrum appears in Figures **2.1** and **2.2.** and is presented below.

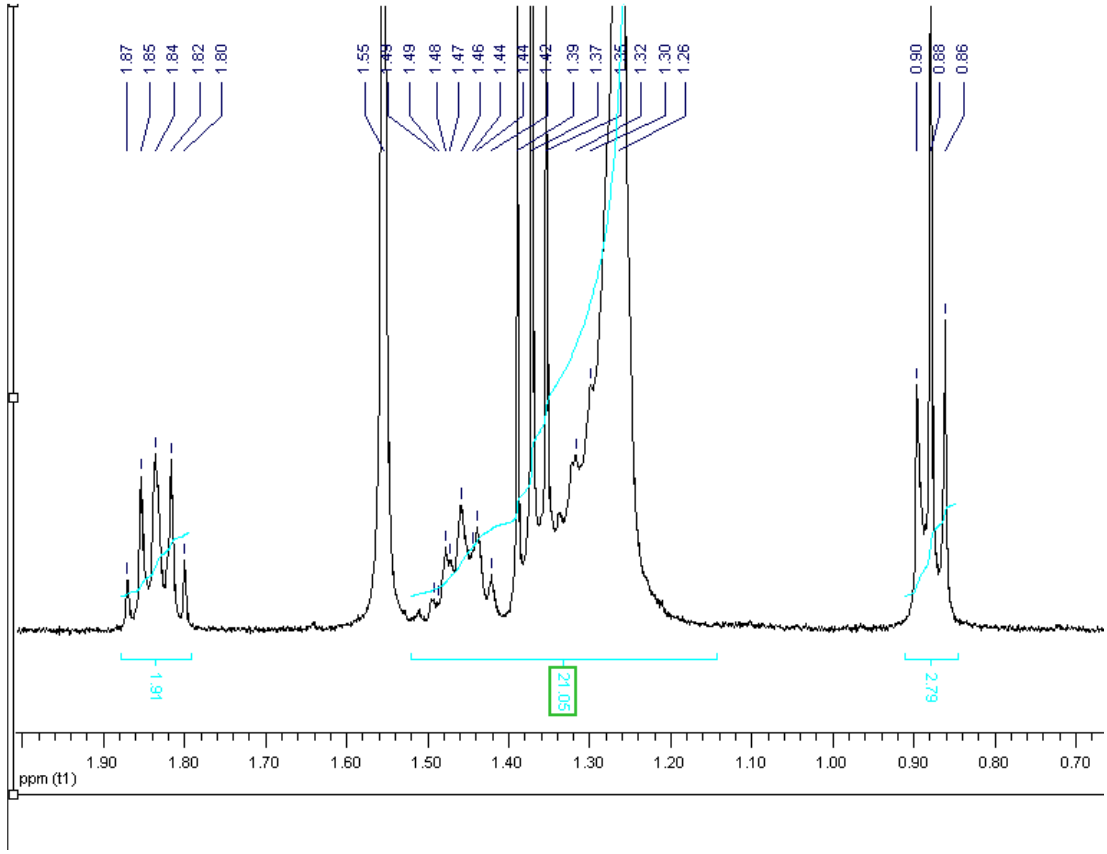

2.1.a.

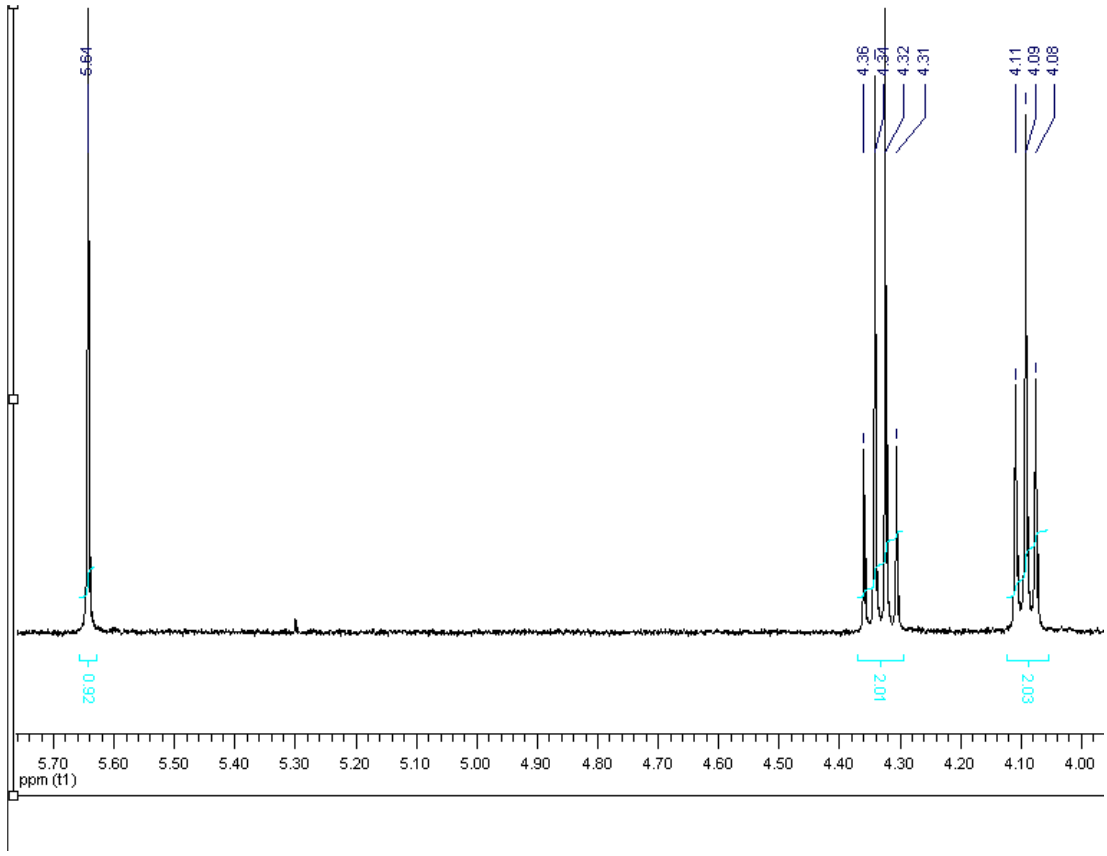

2.1.b.

Figure 2.1.a and 2.1.b. Aliphatic portion of the ^{1}H NMR spectrum of compound 25a.

In the aliphatic part of the ^{1}H NMR spectrum, many proton signals can be distinguished (pertaining to the a, b, c and d protons). Thus, at 0.88 ppm a triplet corresponds to the 3 H_a protons. By integrating the signal area 1.2-1.52 ppm which includes signals from protons H_b and H_j, a value of 21 is obtained.. The residual water peak present in the solvent gives a signal at 1.55 ppm. The next quintet at 1.84 ppm corresponds to the 2 H_c protons of the molecule, while the following triplet at 4.09 ppm is assigned to the 2 H_d protons. Therefore, the closer the methylene groups are to the O bound to the phenyl ring, the more the corresponding signal is shifted.

Further downto 4.33 ppm, a quartet is attributed to the 2 H_i protons. The phenolic H_e proton appears as a sharp singlet at 5.64 ppm confirming the monophenol characteristic of the compound.

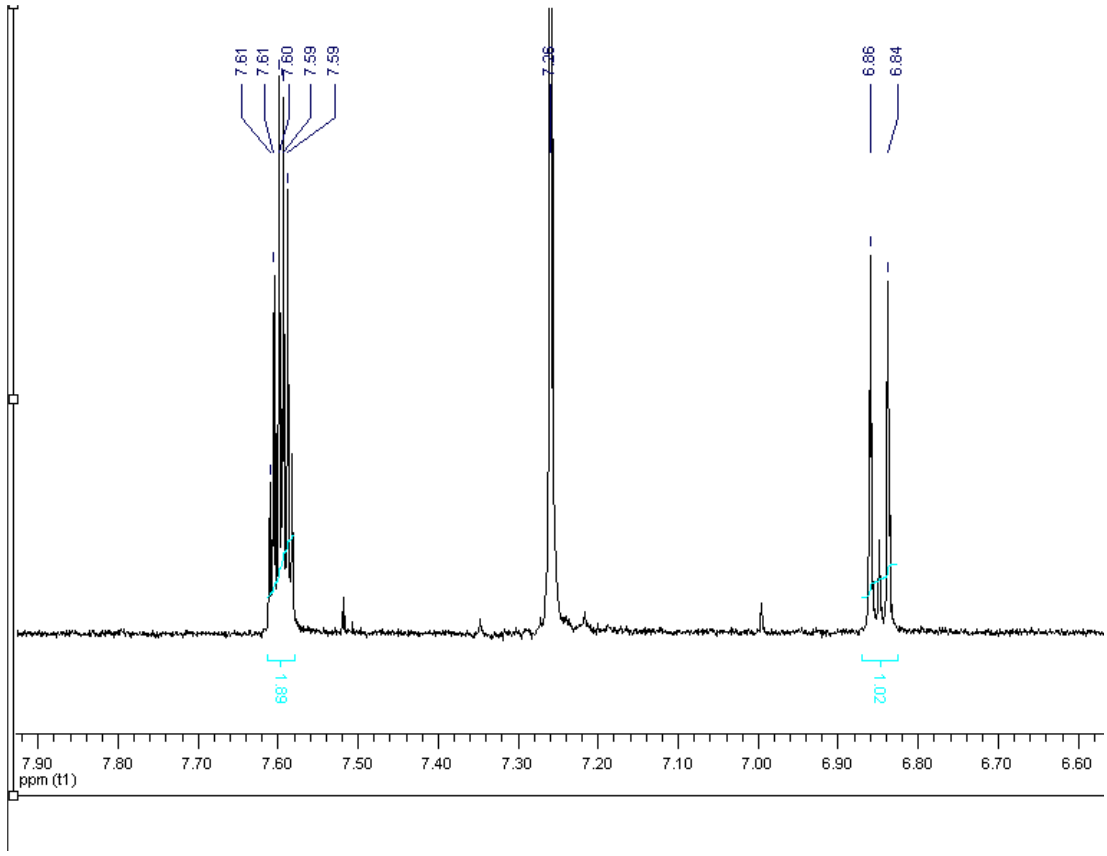

Figure 2.2. Aromatic of the ^{1}H NMR spectrum of compound 25a.

The aromatic ring shows three different signals, one doublet for the H_f at 6.85 ppm and an overlapped signal for the other 2 protons H_g and H_h of the phenyl ring at around 7.60 ppm.

The synthetic route followed for the delivery of the two-benzene-ring benzoic acids with hydrocarbon chains in the 3 position and semiperfluoro chains in the 4 position of the terminal benzene rings starts from ethyl 3, 4- dihydroxybenzoate **5**, which is monoalkylated to the 4 position of the benzene ring leading to compounds **25a** and **25b** using potassium carbonate and potassium iodide in dry DMF, at room temperature. A further alkylation of compounds **25a** and **25b** is carried out introducing a semiperfluoro chain in the 3 position of the benzene ring, using potassium carbonate in dry DMF heating the reaction to 65 °C. Starting from this point, the benzoic acids **30a** and **30b** were synthesized following an analogous route to the one presented in **Scheme 2.2**.

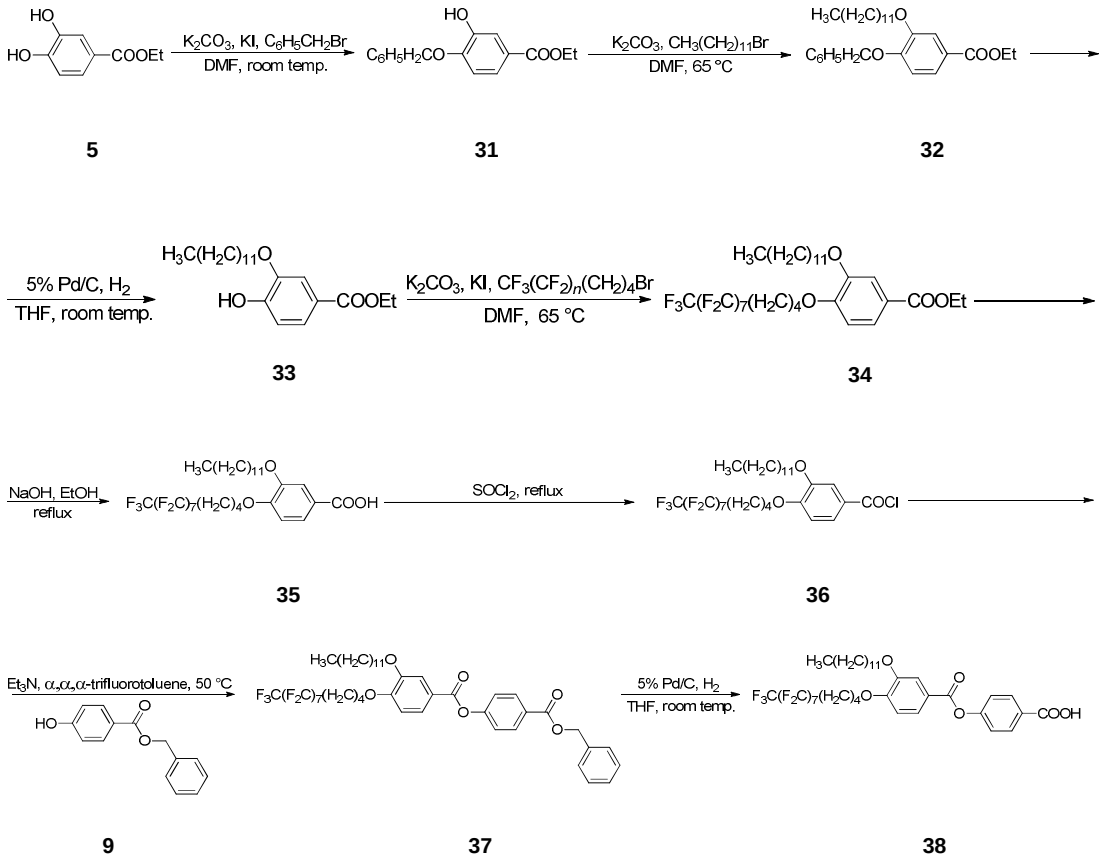

Scheme 2.6. Synthesis of two-benzene-ring benzoic acid with one semiperfluoro chain in the 4 and one hydrocarbon chain in the 3-position of the external benzene ring.

The benzoic acid **35** was delivered following a series of reactions starting from ethyl 3, 4- dihydroxybenzoate **5**, which was 4-benzylated to compound **31** using potassium carbonate and potassium iodide in dry DMF as solvent, reaction set at room temperature. The next step constitutes the introduction of dodecyl chain in the 3 position of the benzene ring using potassium carbonate in dry DMF, the reaction being heated to 65 °C, thus resulting compound **32**. In order that the introduction of the semiperfluoro chain to happen, there is needed that the –OH group in the 4 position of the benzene ring to be de-protected. Therefore, compound **33** is delivered after hydrogenolysis in dry THF, in presence of 5% Pd/C as a catalyst, at room temperature and normal atmospheric pressure. Compound **34** incorporates both a hydrocarbon and a fluoroalkyl chain in its molecule as a result of the alkylation of compound **33** in dry DMF at 65 °C using potassium carbonate as base. From this point onwards, the synthesis of the two-benzene ring benzoic acid **38** follows a similar scheme to the one from **Scheme 2.2**.

Analyzing why the path of protecting the –OH phenol group of the starting material **5** has been chosen, the explanation lies in the fact that semiperfluorobromide $CF_3(CF_2)_7(CH_2)_4Br$ synthesised from $CF_3(CF_2)_7I$, which is an expensive chemical, needed to be used in a good yield reaction; therefore, supposedly there was followed the synthetic route from **Scheme 2.5**, for which the monoalkylation of compound **5** would have used $CF_3(CF_2)_7(CH_2)_4Br$, the 4-fluoroalkylated would have been delivered. In fact, assuming that from this type of monoalkylation in dry DMF at room temperature in the presence of potassium carbonate and potassium iodide, the yield would be lower than the yield of the reaction of semiperfluoro chain introduction from **Scheme 2.6,** due to the fact that side products such as the corresponding dialkylated compound will result. To be more precise, the yield of the monoalkylation reaction from **Scheme 2.5** (after separation and purification of the monoalkylated compound) was 37.6%, while the yield of the semiperfluoro chain introduction from **Scheme 2.6** was 83.6%. Taking into consideration these assumptions, there was searched the way in which as little as possible of the amount of $CF_3(CF_2)_7(CH_2)_4Br$ was lost in the synthetic path.

Getting back now to the synthesis of the tetracatenar mesogens presented in this sub-chapter, the synthetic manner in which these have been made consists in a condensation reaction similar to the one presented before in **Scheme 2.4**.

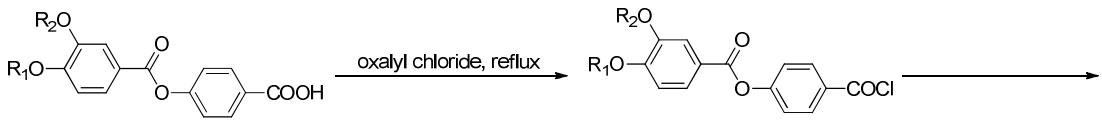

30a (n_1 = 11, n_2 = 7);

30b (n_1 = 13, n_2 = 9)

39a (n_1 = 11, n_2 = 7);

39b (n_1 = 13, n_2 = 9)

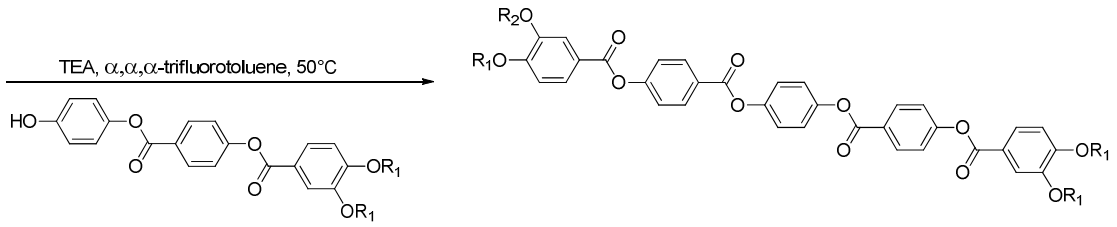

23a (n_1 = 11);

23b (n_1 = 13)

40a (n_1 = 11, n_2 = 7);

40b (n_1 = 13, n_2 = 9)

Scheme 2.7. Synthesis of the unsymmetric tetracatenar mesogens bearing mixed chains at one side and hydrocarbon chains at the other; R_1 = $CH_3(CH_2)_{n1}$–, R_2 = $CF_3(CF_2)_{n2}(CH_2)_4$–, where letters a and b refer to n_1 = 11, n_2 = 7 and n_1 = 13, n_2 = 9, respectively, for compounds 30, 39, 40, while a and b refer to n_1 = 11 and n_1 = 13, respectively, for compounds 23.

Therefore, the acids **30a** and **30b** were converted into the corresponding acid chlorides **39a** and **39b** in a reflux reaction in the presence of oxalyl chloride. The esterification between compounds **39a** and **23a,** or **39b** and **23b**, in the presence of Et_3N using α,α,α-trifluorotoluene as solvent delivered the tetracatenar target compounds **40a** and **40b**.

2.1.4. Synthesis of Symmetric Tetracatenar Mesogen Bearing Mixed Chains at each End

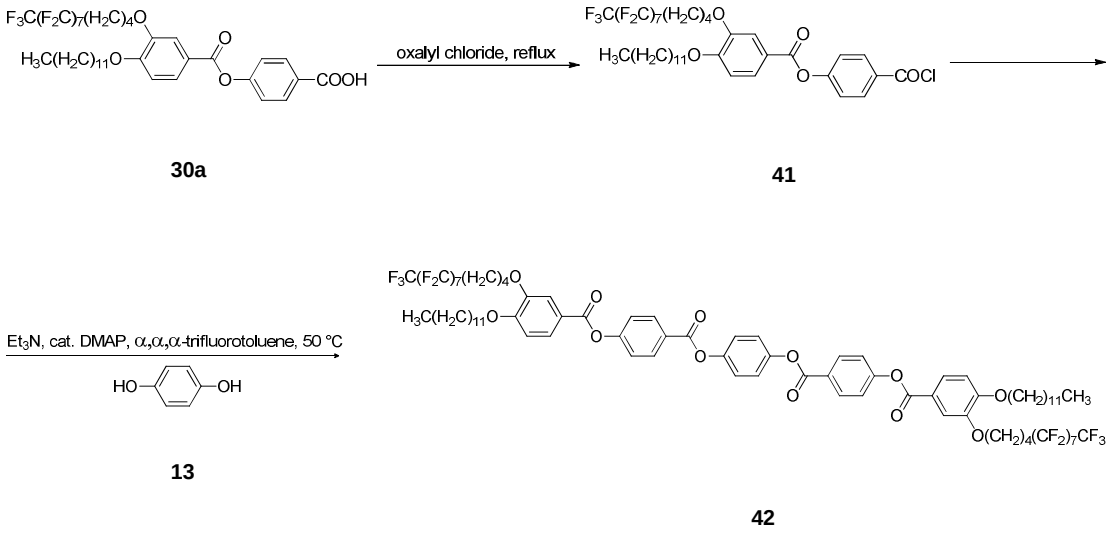

30a **41** **13** **42**

Scheme 2.8. Synthesis of the symmetric tetracatenar mesogen bearing hydrocarbon chains at 3 and fluoro chains at 4 positions of each of the terminal benzene rings.

In **Scheme 2.8**, acid **30a** was converted into its acid chloride, **41**, which was esterified with hydroquinone **13** in a procedure similar to the one in **Scheme 2.2**, delivering the final compound **42**.

2.1.5. Synthesis of Tricatenars Bearing Only One Fluoroalkyl Chain

The tricatenar mesogens that contain one fluoroalkyl chain have at one side the two hydrocarbon chains in the 3 and 4 positions with respect to the terminal benzene ring to which they are attached and at the other the only fluorocarbon in the 4 position with respect to the other terminal benzene ring of the rigid core. The synthetic route is outlined in **Scheme 2.9**.

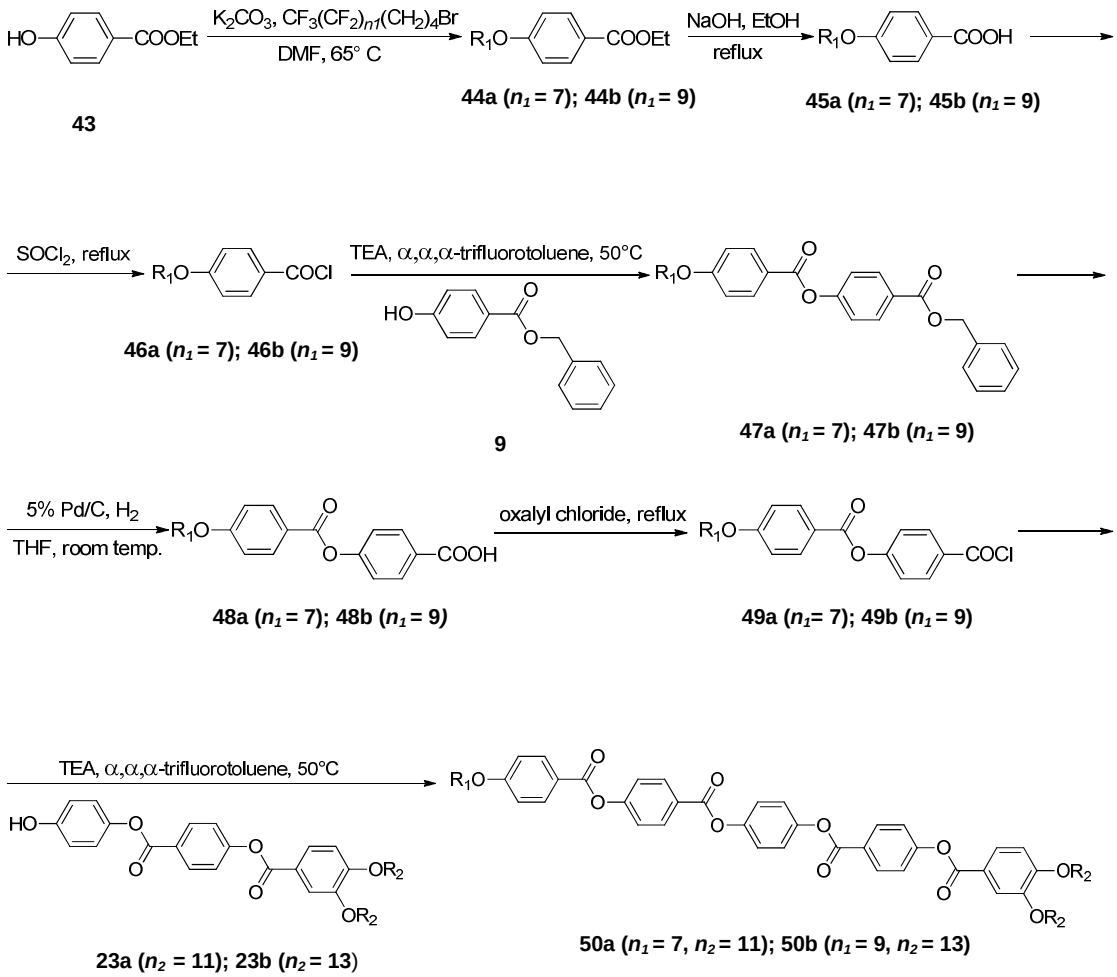

Scheme 2.9. Synthetic route of the tricatenar fluorinated compounds; R_1 = $CF_3(CF_2)_{n1}(CH_2)_4$–, R_2 = $CH_3(CH_2)_{n2}(CH_2)_4$–; compounds 44, 45, 46, 47, 48, 49 followed by a and b represent intermediates with n_1 = 7 and 9, respectively, whereas target molecules 50a and 50b correspond to n_1 = 7, n_2 = 11 and n_1 = 9, n_2 = 13, respectively.[†]

In this synthetic route, the starting material is ethyl 4-hydroxybenzoate **43** which is alkylated using potassium carbonate in dry DMF affording compounds **44a** and **44b**, which were further hydrolysed in a NaOH/EtOH aqueous solution to compounds **45a** and **45b**. These poorly soluble benzoic acids were further converted into acid chlorides **46a** and **46b** using thionyl chloride under reflux to improve their solubility. A further esterification with compound **9** in the presence of Et_3N in α,α,α-trifluorotoluene led to benzyl-protected esters **47a** and **47b**. Subsequent hydrogenolysis of benzyl compounds **47a** and **47b** leads to benzoic acids **48a** and

[†]Acknowledgements to Mei-Chun Tzeng for the synthesis of compounds comprised in **Scheme 2.9**.

48b, which are quite insoluble and needed to be quantitatively transformed into the corresponding acid chlorides, **49a** and **49b**, using oxalyl chloride under overnight reflux. The target compounds, **50a** and **50b** were delivered by esterification between the formerly mentioned acid chlorides, **49a** and **49b**, and the corresponding *O*-monosubstituted hydroquinones, **23a** and **23b** using Et_3N as a base and α,α,α-trifluorotoluene as solvent.

Solubility in conventional organic solvents of one-ring and two-ring benzoic acids bearing fluoroalkyl terminal chains decreases as the number of fluoro chains is increased. At the same time, solubility of polycatenar fragments is lowered when the number of external chains grafted to a terminal benzene ring of the central core is increased. Under these circumstances and paying attention to the target compounds, the tetracatenar mesogen possessing two fluorinated chains at only one side, **24**, is less soluble than the fluorinated tricatenar mesogens, **50a** and **50b**, but more soluble than the tetracatenar molecule with only fluoroalkyl chains, **14**.

2.1.6. Synthesis of Homologuos Tricatenar Mesogens Bearing only Hydrocarbon Chains at each End

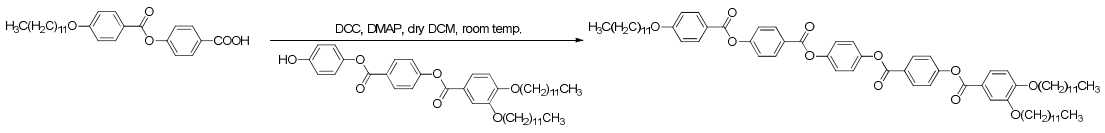

51 **23a** **52**

Scheme 2.10. Synthesis of final all-hydrocarbon tricatenar compound.

The synthesis starts from compound **51**, which was previously obtained by Dr. Richard Date (to which there are addressed acknowledgements) [4]. Owing to the good solubility of this benzoic acid in dry DCM at room temperature, esterification with phenol **23a** in the presence of DCC (*N*,*N*'-dicyclohexylcarbodiimide) and DMAP (*N*,*N*'-dimethyl-4-aminopyridine) led to the tricatenar mesogen **52**.

2.2. Experimental Procedures

Compound 2a:

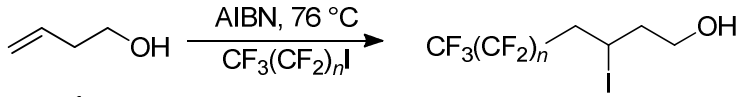

1 **2a (*n* = 7)**

A mixture of the 3-buten-1-ol **1** (0.856 g, 11.73 mmol) and the perfluorooctyliodide $CF_3(CF_2)_7I$ (5.2864 g, 9.682 mmol) was placed in a Schlenk flask and degassed three times successively by the freeze-pump-thaw method. AIBN (0.079 g, 0.482 mmol, 5 mol %) was added into the reaction mixture under a flow of nitrogen. The tube was then sealed under vacuum and the reaction mixture was heated to 76 ^oC for 2 h, more AIBN (0.084 g, 0.512 mmol, 5 mol %) being added under a flow of nitrogen afterwards. The reaction was heated for another 3 h. The flask was cooled down to room temperature and a yellow solid was obtained. The crude compound was crystallised from hexane and the pale yellow solid collected and dried under high vacuum. [1], [2], [3]

Yield: 95.6%. ^1H NMR (400 MHz, $CDCl_3$): δ 4.54 (m, 1H; CHI), 3.84 (m, 2H; CH_2), 2.93 (m, 2H; CH_2), 2.04 (m, 2H; CH_2), 1.43 (t, *J* = 4.9 Hz, 1H; OH).

Compound 2b:

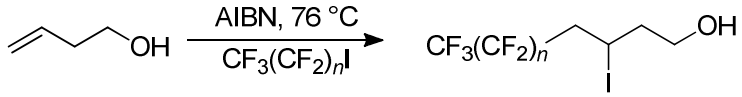

1 **2b (*n* = 9)**

This procedure is analogous to the one above; quantities are perfluorodecyliodide $CF_3(CF_2)_9I$ (6.254 g, 9.682 mmol) and 3-buten-1-ol (0.856 g, 11.73 mmol), AIBN (0.079 g, 0.482 mmol, 5 mol %) for the first addition, and AIBN (0.084 g, 0.512 mmol, 5 mol %) for the second addition.

Yield: 99.0%. ^1H NMR (400 MHz, $CDCl_3$): δ 4.54 (m, 1H; CHI), 3.84 (m, 2H; CH_2), 2.92 (m, 2H; CH_2), 2.03 (m, 2H; CH_2), 1.43 (t, *J* = 4.8 Hz, 1H; OH).

Compound 3a:

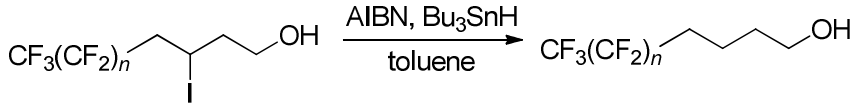

2a (*n* = 7) **3a (*n* = 7)**

Compound **2a** (5.247 g, 8.49 mmol) was dissolved in the anhydrous toluene (50 cm^3, purged with nitrogen for 15 min) in a two-necked round-bottom flask. Tributyltin hydride (4.53 cm^3, 17.168 mmol) and AIBN (0.142 g, 0.868 mmol, 10 mol%) were added afterwards under nitrogen flow at room temperature. The reaction mixture was stirred at 70 ^oC for 4 h and then allowed to cool down. The mixture was concentrated under reduced pressure and the precipitate filtered off. The mixture was washed with cold petroleum ether (5 cm^3) to remove the Bu_3SnH/Bu_3SnI residue and dried under high vacuum.[1], [2], [3]

Yield: 81.6%. ^1H NMR (400 MHz, $CDCl_3$): δ 3.71 (m, 2H; CH_2O), 2.11 (m, 2H; CH_2CF_2), 1.69 (m, overlaped 4H; overlapped 2 CH_2), 1.32 (t, *J* = 5.1 Hz, 1H; OH).

Compound 3b:

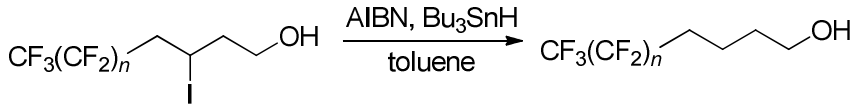

2b (*n* = 9) **3b (*n* = 9)**

This procedure is analogous to the one above. Prepared from **2b** (6.098 g, 8.49 mmol), tributyltin hydride (4.53 cm^3, 17.168 mmol) and AIBN (0.142 g, 0.868 mmol, 10 mol%).

Yield: 87.6%. ^1H NMR (400 MHz, $CDCl_3$): δ 3.70 (t, *J* = 5.9 Hz, 2H; CH_2O), 2.10 (m, 2H; CH_2CF_2), 1.69 (m, 4H; overlapped 2 CH_2).

Compound 4a:

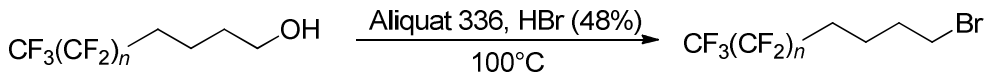

3a (*n* = 7) **4a (*n* = 7)**

A mixture of the alcohol **3a** (0.836 g, 1.7 mmol), Aliquat 336 (0.022 g, 0.054 mmol, 4 mol %) and hydrobromic acid (48% aqueous solution, 0.8 cm^3, 4.7 mmol) was heated to 100 ^oC for 12h. The mixture was diluted with diethyl ether (15 cm^3) and water (10 cm^3) and the upper layer solution was then collected. The solvent was removed under the rotary evaporator and the solid residue was subjected to a pad of silica (hexane:ethyl acetate = 5:1 as eluent). The solvent was evaporated under vacuum leading to the white solid. Crystallization from methanol yielded the bromide as a pale yellow solid. [5], [6], [7]

Yield: 77.0%. ^1H NMR (400 MHz, $CDCl_3$): δ 3.44 (t, *J* = 6.5 Hz, 2H; CH_2Br), 2.11 (m, 2H; CH_2), 1.96 (m, 2H; CH_2), 1.80 (m, 2H; CH_2).

Compound 4b:

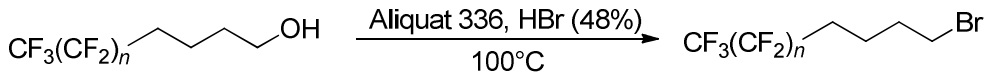

3b (*n* = 9) **4b (*n* = 9)**

This procedure is analogous to the one above. Prepared from **3b** (1 g, 1.7 mmol), Aliquat 336 (0.022 g, 0.054 mmol, 4 mol %) and hydrobromic acid (48% aqueous solution, 0.8 cm^3, 4.7 mmol).

Yield: 73.2 %. ^1H NMR (400 MHz, $CDCl_3$): δ 3.43 (t, *J* = 6.5 Hz, 2H; CH_2Br), 2.10 (m, 2H; CH_2), 1.96 (m, 2H; CH_2), 1.79 (m, 2H; CH_2).

Compound 6a:

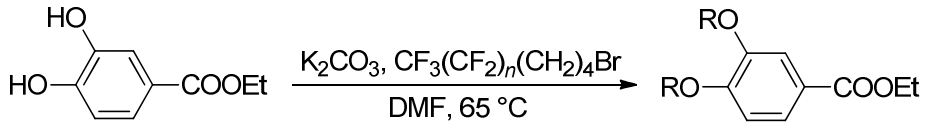

5 **4b (*R* = $CF_3(CF_2)_7(CH_2)_4$)**

Ethyl 3, 4-dihydroxybenzoate **5** (0.446 g, 2.45 mmol) was dissolved in dry DMF (25 cm^3) and potassium carbonate (1.38 g, 10 mmol) was added into the solution and stirred for 15 min. The bromide compound **4a** (2.923 g, 5.27 mmol) was added. The mixture was heated at 65 ^oC for 12 h and cooled down to room temperature. Cold

water (25 cm^3) was poured into the solution. The precipitated white solid was collected after filtration, washed with water (10 cm^3), acetone (5 cm^3) and dried under high vacuum.

Yield: 91.9 %. ^{1}H NMR (400 MHz, $CDCl_3$): δ 7.66 (dd, *J* = 1.9 and 8.4 Hz, 1H; arom. H-6), 7.54 (d, *J* = 2.0 Hz, 1H; arom. H-2), 6.87 (d, *J* = 8.5 Hz, 1H; arom. H-5), 4.08 (t, *J* = 5.6 Hz, 4H; 2 CH_2O), 3.89 (s, 3H; OCH_3), 2.17 (m, 4H; 2 CH_2CF_2), 1.88 (m, 8H; overlapped 4 CH_2).

Compound 6b:

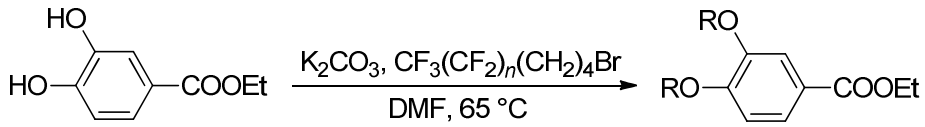

5 **6b (*R* = $CF_3(CF_2)_9(CH_2)_4$)**

This procedure is analogous to the one above. Prepared from ethyl 3,4-dihydroxybenzoate **5** (0.446 g, 2.45 mmol), potassium carbonate (1.38 g, 10 mmol) and bromide **4b** (3.451 g, 5.27 mmol).

Yield: 88.8%. ^{1}H NMR (400 MHz, $CDCl_3$): δ 7.66 (dd, *J* = 2.0 and 8.4 Hz, 1H; arom. H-6), 7.54 (d, *J* = 2.0 Hz, 1H; arom. H-2), 6.87 (d, *J* = 8.5 Hz, 1H; arom. H-5), 4.08 (t, *J* = 5.5 Hz, 4H; OCH_2), 3.89 (s, 3H; OCH_3), 2.18 (m, 4H; CH_2CF_2), 1.88 (m, 8H; overlapped 4 CH_2).

Compound 44a:

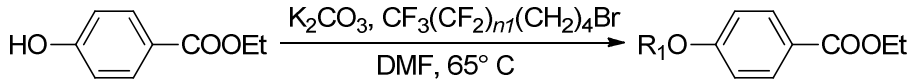

43 **44a (*R* = $CF_3(CF_2)_7(CH_2)_4$)**

The procedure above was repeated starting from compound **43**, ethyl 4-hydroxybenzoate (0.83 g, 5 mmol), potassium carbonate (1.38 g, 10 mmol) and bromide **4a**, $Br(CH_2)_4(CF_2)_7CF_3$ (2.83 g, 5.1 mmol).

Yield: 93.4 %. ^{1}H NMR (400 MHz, $CDCl_3$):δ 8.06 (AA'XX', *J* = 9.0 Hz, 2H; arom. CH), 6.96 (AA'XX', *J* = 9.0 Hz, 2H; arom. CH), 4.10 (t, *J* = 5.9 Hz, 2H; OCH_2), 2.175 (m, 2H, CH_2CF_2), 1.88 (m, 4H; overlapped $2CH_2$)

Compound 44b:

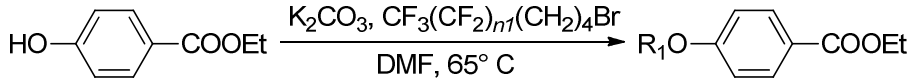

43 **44b (*R* = $CF_3(CF_2)_9(CH_2)_4$)**

The procedure above was repeated starting from compound **43**, ethyl 4-hydroxybenzoate (0.83 g, 5 mmol), potassium carbonate (1.38 g, 10 mmol) and bromide **4b**, $Br(CH_2)_4(CF_2)_9CF_3$(3.34 g, 5.1mmol).

Yield: 90.2%. ^{1}H NMR (400 MHz, $CDCl_3$): δ 8.06 (AA'XX', *J* = 9.0 Hz, 2H; arom. CH), 6.96 (AA'XX', *J* = 9.0 Hz, 2H; arom. CH), 4.10 (t, *J* = 5.9 Hz, 2H; OCH_2), 2.175 (m, 2H, CH_2CF_2), 1.88 (m, 4H; overlapped $2CH_2$).

Compound 7a:

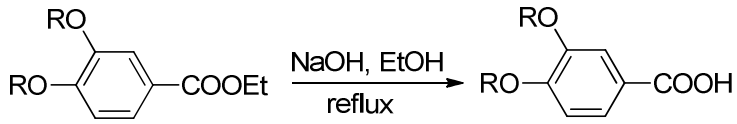

6a (*R* = $CF_3(CF_2)_7(CH_2)_4$) **7a (*R* = $CF_3(CF_2)_7(CH_2)_4$)**

Compound **6a** (2.709 g, 2.4 mmol) was added into a mixture of ethanol (50 cm^3), and NaOH 10 N aqueous solution (3 cm^3). After the suspension was refluxed for 12 h, hydrolysis was completed and the solution was cooled down to room temperature. The reaction mixture was kept in ice bath and brought to an acidic pH = 4 by adding concentrated HCl dropwisely. The resulting white precipitate was collected by suction filter, sequentially washed with water (2 x 5 cm^3) and dried under high vacuum.

Yield: 80.6%. ^{1}H NMR (400 MHz, $CDCl_3$/CF_3COOH): δ 7.81 (dd, *J* = 2.0 and 8.5 Hz, 1H; arom. H-6), 7.62 (d, *J* = 2.0 Hz, 1H; arom. H-2), 6.97 (d, *J* = 8.6 Hz, 1H; arom. H-5), 4.17 (t, *J* = 5.9 Hz, 4H; OCH_2), 2.15 (m, 4H; CH_2CF_2), 1.92 (m, 8H; $2CH_2$), 1.82 (m, 8H; overlapped $2CH_2$).

Compound 7b:

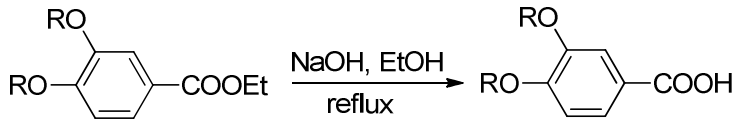

6b (*R* = $CF_3(CF_2)_9(CH_2)_4$) **7b (*R* = $CF_3(CF_2)_9(CH_2)_4$)**

The procedure above was repeated, compound **6b** (3.158 g, 2.4 mmol) being saponified with 3 cm^3 of 10 N NaOH aqueous solution.

Yield: 94 %. ^{1}H NMR (400 MHz, $CDCl_3/CF_3COOH$): δ 7.81 (dd, *J* = 2.0 and 8.5 Hz, 1H; arom. H-6), 7.62 (d, *J* = 2.0 Hz, 1H; arom. H-2), 6.98 (d, *J* = 8.6 Hz, 1H; arom. H-5), 4.18 (t, *J* = 5.9 Hz, 4H; OCH_2), 2.15 (m, 4H; CH_2CF_2), 1.88 (m, 8H; $2CH_2$), 1.82 (m, 8H; overlapped $2CH_2$).

Compound 45a:

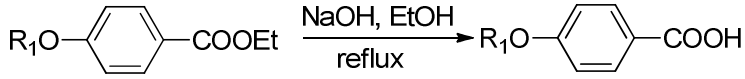

44a (*R* = $CF_3(CF_2)_7(CH_2)_4$) **45a (*R* = $CF_3(CF_2)_7(CH_2)_4$)**

The procedure above was repeated, starting from compound **44a** (1.54 g, 2.4 mmol) which was saponified in 3 cm^3 of 10 N NaOH aqueous solution.

Yield: 95 %. ^{1}H NMR (400 MHz, $CDCl_3$): δ 8.06 (AA'XX', *J* = 9.0 Hz, 2H; arom. CH), 6.96 (AA'XX', *J* = 9.0 Hz, 2H; arom. CH), 4.10 (t, *J* = 5.9 Hz, 2H; OCH_2), 2.175 (m, 2H, CH_2CF_2), 1.88 (m, 4H; overlapped $2CH_2$).

Compound 45b:

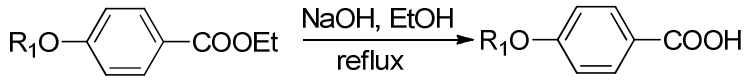

44b (*R* = $CF_3(CF_2)_9(CH_2)_4$) **45b (*R* = $CF_3(CF_2)_9(CH_2)_4$)**

The procedure above was repeated, starting from compound **44b** (1.78 g, 2.4 mmol) which was saponified in 3 cm^3 of 10 N NaOH aqueous solution.

Yield: 93 %. ^{1}H NMR (400 MHz, $CDCl_3$): δ 8.06 (AA'XX', *J* = 9.0 Hz, 2H; arom. CH), 6.96 (AA'XX', *J* = 9.0 Hz, 2H; arom. CH), 4.10 (t, *J* = 5.9 Hz, 2H; OCH_2), 2.175 (m, 2H, CH_2CF_2), 1.88 (m, 4H; overlapped $2CH_2$).

Compound 8a:

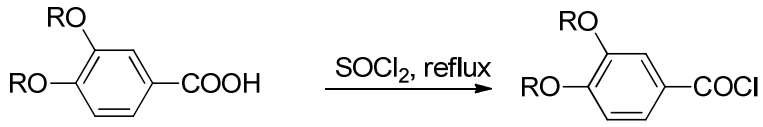

7a (*R* = $CF_3(CF_2)_7(CH_2)_4$) **8a (*R* = $CF_3(CF_2)_7(CH_2)_4$)**

Thionyl chloride (5 cm^3) was added in excess to a flask containing the benzoic acid **7a** (2.204 g, 2.0 mmol). The mixture was stirred at 40 °C under nitrogen atmosphere for one hour and refluxed for 3 h at 80 °C. The unreacted thionyl chloride was evaporated under the rotary evaporator and the solid obtained was dried under high vacuum for several hours without further purification. [8], [9]

Yield: 96.2%. ^{1}H NMR (400 MHz, $CDCl_3$): δ 7.82 (dd, *J* = 1.4 and 8.4 Hz, 1H; arom. H-6), 7.53 (d, *J* = 1.7 Hz, 1H; arom. H-2), 6.91 (d, *J* = 8.6 Hz, 1H; arom. H-5), 4.13 (t, *J* = 5.7 Hz, 4H; OCH_2), 4.08 (t, *J* = 5.7 Hz, 4H; OCH_2), 2.18 (m, 4H; CH_2CF_2), 1.90 (m, 8H; overlapped 4 CH_2).

Compound 8b:

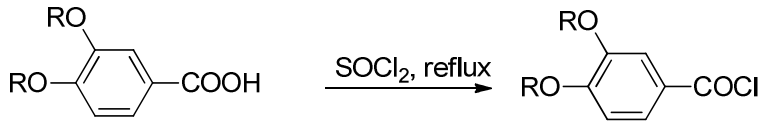

7b (*R* = $CF_3(CF_2)_9(CH_2)_4$) **8b (*R* = $CF_3(CF_2)_9(CH_2)_4$)**

The procedure above was repeated for the benzoic acid **7b** (2.604 g, 2.00 mmol) which was stirred with excess of thionyl chloride (5 cm^3).

Yield: 96.0% ^{1}H NMR (400 MHz, $CDCl_3$): δ 7.82 (dd, *J* = 2.1 and 8.6 Hz, 1H; arom. H-6), 7.53 (d, *J* = 2.2 Hz, 1H; arom. H-2), 6.91 (d, *J* = 8.7 Hz, 1H; arom. H-5), 4.13 (t, *J* = 5.7 Hz, 4H; OCH_2), 4.08 (t, *J* = 5.5 Hz, 4H; OCH_2), 2.18 (m, 4H; CH_2CF_2), 1.90 (m, 8H; overlapped 4 CH_2).

Compound 46a:

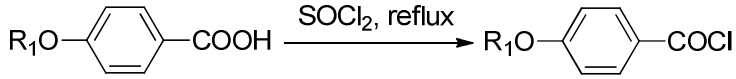

45a (*R* = $CF_3(CF_2)_7(CH_2)_4$) **46a (*R* = $CF_3(CF_2)_7(CH_2)_4$)**

Repeating the procedure above, the acid **45a** (1.22 g, 2.0 mmol) was stirred together with excess of thionyl chloride (5 cm^3).

Yield: 92.2%. ^{1}H NMR (400 MHz, $CDCl_3$/TFA): δ 8.09 (AA'XX', *J* = 9.0 Hz, 2H; arom. CH_2), 6.95 (AA'XX', *J* = 9.0 Hz, 2H; arom. CH_2), 4.10 (t, *J* = 5.9 Hz, 2H; OCH_2), 2.16 (m, 2H; CH_2CF_2), 1.86 (m, 4H; overlapped $2CH_2$).

Compound 46b:

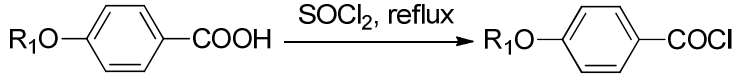

45b (*R* = $CF_3(CF_2)_9(CH_2)_4$) **46b (*R* = $CF_3(CF_2)_9(CH_2)_4$)**

This procedure is analogous to the one above. The acid **45b** (1.424 g, 2.0 mmol) was stirred together with excess of thionyl chloride (5 cm^3).

Yield: 93.2%. ^{1}H NMR (400 MHz, $CDCl_3$/TFA): δ 8.08 (AA'XX', *J* = 9.0 Hz, 2H; arom. CH_2), 6.95 (AA'XX', *J* = 9.0 Hz, 2H; arom. CH_2), 4.10 (t, *J* = 5.9 Hz, 2H; OCH_2), 2.16 (m, 2H; CH_2CF_2), 1.88 (m, 4H; overlapped $2CH_2$).

Compound 10a:

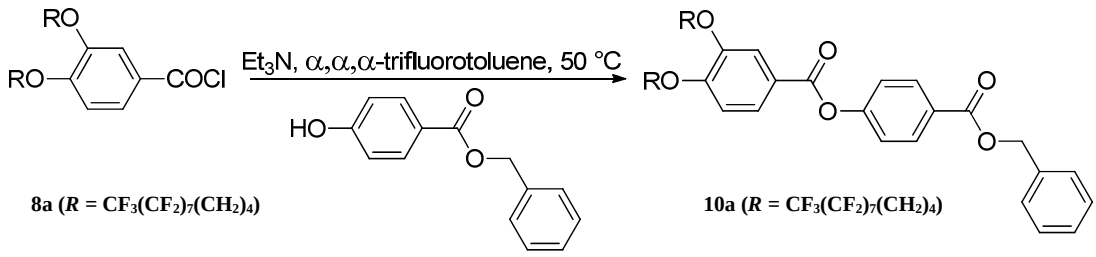

8a (*R* = $CF_3(CF_2)_7(CH_2)_4$) **9** **10a (*R* = $CF_3(CF_2)_7(CH_2)_4$)**

Acid chloride **8a** (2.24 g, 2.0 mmol) and benzyl 4-hydroxybenzoate (compound **9**; 0.490 g, 2.15 mmol) were dissolved in anhydrous α,α,α-trifluorotoluene (25 cm^3) and anhydrous triethylamine (0.5 cm^3, 3.6 mmol) was added afterwards. The mixture was then heated at 50 °C for 12h. The solvent was cooled down to room temperature and evaporated at rotavapor. The crude solid was washed with methanol to remove excess of benzyl 4-hydroxybenzoate, leading to a white solid.

Yield: 89%. ^{1}H NMR (400 MHz, $CDCl_3$): δ 8.15 (AA'XX', *J* = 8.7 Hz, 2H; arom. H), 7.84 (dd, *J* = 2.0 and 8.4 Hz, 1H; arom. H), 7.65 (d, *J* = 2.0 Hz, 1H; arom. H), 7.40 (m, 5H; arom. H), 7.28 (AA'XX', *J* = 8.7 Hz, 2H; arom. H), 6.94 (d, *J* = 8.6 Hz, 1H; arom. H), 5.38 (s, 2H; OCH_2), 4.12 (m, 4H; OCH_2), 2.18 (m, 4H; overlapped 2 CH_2), 1.90 (m, 8H; overlapped 4 CH_2).

Compound 10b:

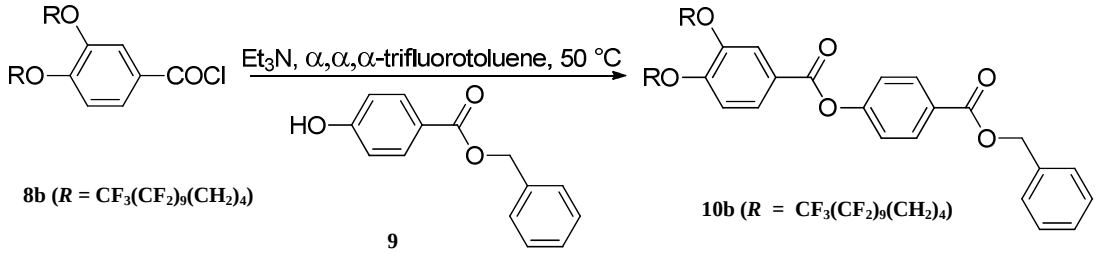

8b (*R* = $CF_3(CF_2)_9(CH_2)_4$) **9** **10b (*R* = $CF_3(CF_2)_9(CH_2)_4$)**

This procedure is analogous to the one above; acid chloride **8b** (2.604 g, 2.0 mmol), benzyl 4-hydroxybenzoate (0.490 g, 2.15 mmol), anhydrous α,α,α-trifluorotoluene (25 cm^3) and anhydrous triethylamine (0.5 cm^3, 4 mmol).

Yield: 94%. ^{1}H NMR (400 MHz, $CDCl_3$): δ 8.15 (AA'XX', *J* = 8.8 Hz, 2H; arom. H), 7.84 (dd, *J* = 2.0 and 8.5 Hz, 1H; arom. H), 7.65 (d, *J* = 2.0 Hz, 1H; arom. H), 7.4 (m, 5H; arom. H), 7.28 (AA'XX', *J* = 8.7 Hz, 2H; arom. H), 6.94 (d, *J* = 8.6 Hz, 1H; arom. H), 5.38 (s, 2H; OCH_2), 4.12 (m, 4H; OCH_2), 2.19 (m, 4H; overlapped 2 CH_2), 1.91 (m, 8H; overlapped 4 CH_2).

Compound 47a:

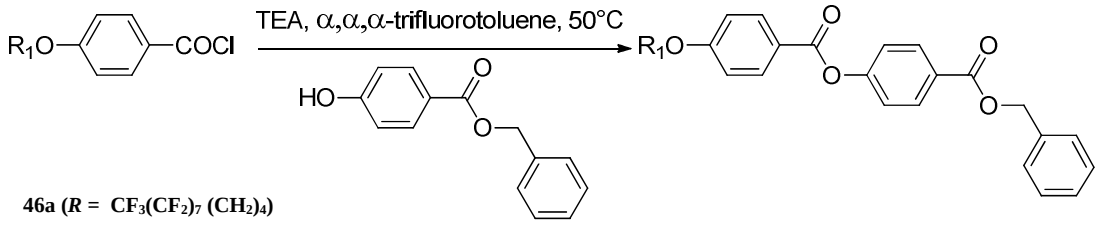

This procedure is analogous to the one above; acid chloride **46a** (1.26 g, 2.0 mmol), benzyl 4-hydroxybenzoate (0.490 g, 2.15 mmol) and anhydrous triethylamine (0.5 cm^3, 4 mmol).

^{1}H NMR (400 MHz, $CDCl_3$): δ 8.16 (AA'XX', *J* = 2.6 Hz, 2H; arom. CH_2), 8.14 (AA'XX', *J* = 2.8 Hz, 2H; arom. CH_2), 7.41 (m, 5H; arom. H), 7.29 (AA'XX', *J* = 8.8 Hz, 2H; arom. CH_2), 6.98 (AA'XX', *J* = 8.9 Hz, 2H; arom. CH_2), 5.38 (s, 2H; OCH_2), 4.10 (t, *J* = 5.8 Hz, 4H; OCH_2), 2.18 (m, 2H; CH_2CF_2), 1.89 (m, 4H; overlapped 2 CH_2).

Compound 47b:

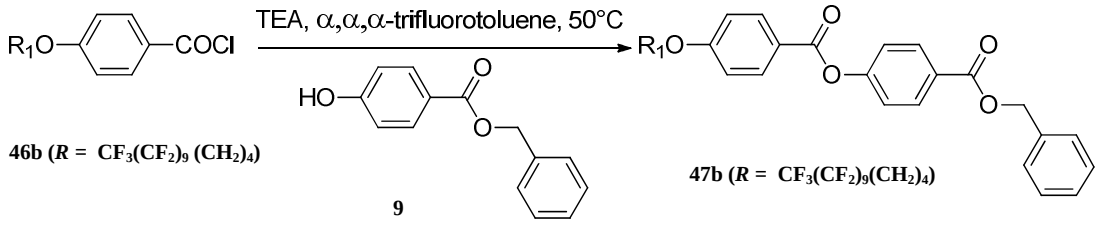

This procedure is analogous to the one above; acid chloride **46b** (1.460 g, 2.0 mmol), benzyl 4-hydroxybenzoate (0.490 g, 2.15 mmol) and anydrous triethylamine (0.5 cm^3, 4 mmol).

Yield: 81%. ^{1}H NMR (400 MHz, $CDCl_3$): δ 8.16 (AA'XX', *J* = 2.5 Hz, 2H; arom. CH_2), 8.14 (AA'XX', *J* = 2.6 Hz, 2H; arom. CH_2), 7.41 (m, 5H; arom. H), 7.28 (AA'XX', *J* = 8.7 Hz, 2H; arom. CH_2), 6.97 (AA'XX', *J* = 8.9 Hz, 2H; arom. CH_2), 5.38 (s, 2H; OCH_2), 4.10 (t, *J* = 5.8 Hz, 4H; OCH_2), 2.18 (m, 2H; CH_2CF_2), 1.89 (m, 4H; overlapped 2 CH_2).

Compound 11:

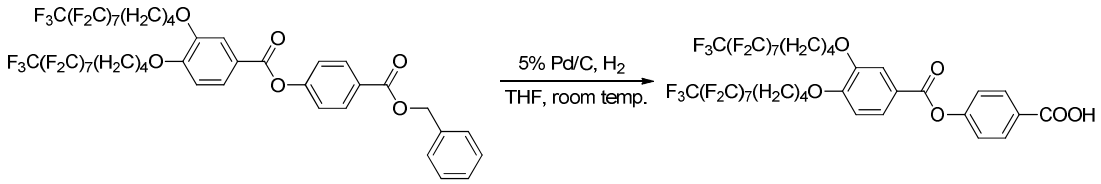

10a **11**

A flask equipped with compound **10a** (2.624 g, 2.0 mmol) suspended in anhydrous THF (100 cm^3) and 5 % palladium on charcoal (0.1 g) as catalyst was connected to a balloon filled with hydrogen at normal atmospheric pressure and room temperature. The reaction was stirred until no hydrogen was taken off (TLC shows completion of the reaction). The solvent was evaporated under reduced pressure. The reaction mixture was filtered on a sintered funnel and the solid washed with a large amount of hot CF_3COOH. The filtrate was removed under the rotary evaporator and the mixture was washed with methanol yielding to a white solid.

Yield: 65.0%. ^{1}H NMR (400 MHz, $CDCl_3$): δ 8.21 (AA'XX', *J* = 8.9 Hz, 2H; arom. H), 7.91 (dd, *J* = 2.0 and 8.5 Hz, 1H; arom. H), 7.71 (d, *J* = 2.0 Hz, 1H; arom. H), 7.34 (AA'XX', *J* = 8.9 Hz, 2H; arom. H), 7.02 (d, *J* = 8.6 Hz, 1H; arom. H), 4.19 (m, 4H; OCH_2), 2.175 (m, 4H; overlapped 2 CH_2), 1.90 (m, 8H; overlapped 4 CH_2).

Compound 48a:

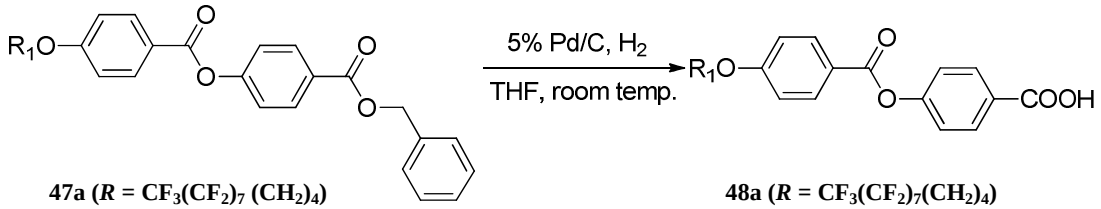

47a (*R* = $CF_3(CF_2)_7(CH_2)_4$) **48a (*R* = $CF_3(CF_2)_7(CH_2)_4$)**

This procedure is analogous to the one above; the compound **47a** (1.64 g, 2.0 mmol) was suspended in anhydrous THF (100 cm^3) and 5% palladium on charcoal (0.1 g) was added as catalyst.

Yield: 82%. ^{1}H NMR (400 MHz, $CDCl_3$/CF_3COOH): δ 8.20 (AA'XX', *J* = 8.8 Hz, 2H; arom. H), 8.17 (AA'XX', *J* = 8.9 Hz, 2H; arom. H), 7.34 (AA'XX', *J* = 8.8 Hz, 2H; arom. H), 7.03 (AA'XX', *J* = 9.0 Hz, 2H; arom. H), 4.14 (t, *J* = 5.9 Hz, 2H; OCH_2), 2.18 (m, 2H ; CH_2CF_2), 1.90 (m, 4H; overlapped 2 CH_2).

Compound 48b:

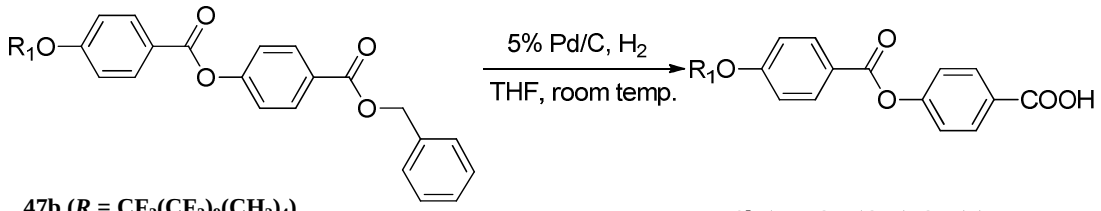

47b (*R* = $CF_3(CF_2)_9(CH_2)_4$) **48b (*R* = $CF_3(CF_2)_9CH_2)_4$)**

This procedure is analogous to the one above; the compound **47b** (1.84 g, 2.0 mmol) was suspended in anhydrous THF and 5% palladium on charcoal (0.1 g) was added as catalyst.

Yield: 60%. ^{1}H NMR (400 MHz, $CDCl_3/CF_3COOH$): δ 8.20 (AA'XX', *J* = 8.8 Hz, 2H; arom. H), 8.17 (AA'XX', *J* = 9.0 Hz, 2H; arom. H), 7.35 (AA'XX', *J* = 8.8 Hz, 2H; arom. H), 7.02 (AA'XX', *J* = 9.0 Hz, 2H; arom. H), 4.13 (t, *J* = 5.9 Hz, 2H; OCH_2), 2.18 (m, 2H ; CH_2CF_2), 1.90 (m, 4H; overlapped 2 CH_2).

Compound 12:

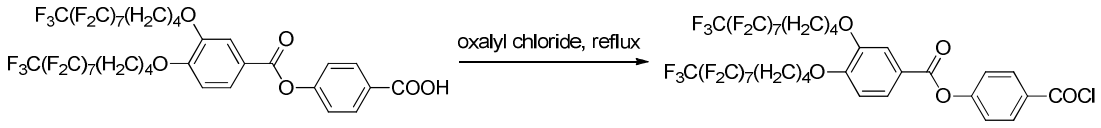

11 **12**

The carboxylic acid **11** (2.44 g, 2.0 mmol) was suspended in excess of oxalyl chloride (5 cm^3) and the mixture was refluxed for 12 h. The solvent was removed and kept under vacuum for a while without further purification.

Yield: 89%. ^{1}H NMR (400 MHz, $CDCl_3$): δ 8.21 (AA'XX', *J* = 8.9 Hz, 2H; arom. H), 7.85 (dd, *J* = 2.0 and 8.5 Hz, 1H; arom. H), 7.64 (d, *J* = 2.0 Hz, 1H; arom. H), 7.38 (AA'XX', *J* = 8.9Hz, 2H; arom. H), 6.95 (d, *J* = 8.8 Hz, 1H; arom. H), 4.14 (m, 4H; OCH_2), 2.19 (m, 4H; overlapped 2 CH_2), 1.91 (m, 8H; overlapped 4 CH_2).

Compound 49a:

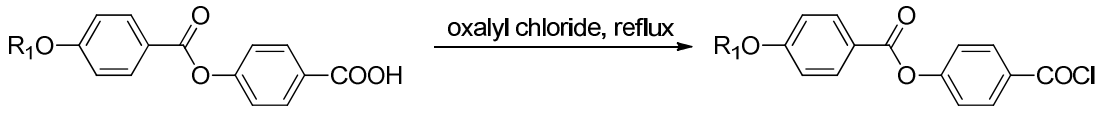

48a (*R* = $CF_3(CF_2)_7(CH_2)_4$) **49a (*R* = $CF_3(CF_2)_7(CH_2)_4$)**

This procedure is analogous to the one above; compound **48a** (1.46 g, 2.0 mmol) was suspended in excess of oxalyl chloride (5 cm^3).

Yield: 85%. ^{1}H NMR (400 MHz, $CDCl_3$): δ 8.21 (AA'XX', *J* = 8.9 Hz, 2H; arom. CH_2), 8.14 (AA'XX', *J* = 9.0 Hz, 2H; arom. CH_2), 7.39 (AA'XX', *J* = 8.9 Hz, 2H; arom. CH_2), 6.99 (AA'XX', *J* = 9.0 Hz, 2H; arom. CH_2), 4.10 (t, *J* = 5.9 Hz, 2H; OCH_2), 2.19 (m, 2H; CH_2CF_2), 1.90 (m, 4H; overlapped $2CH_2$).

Compound 49b:

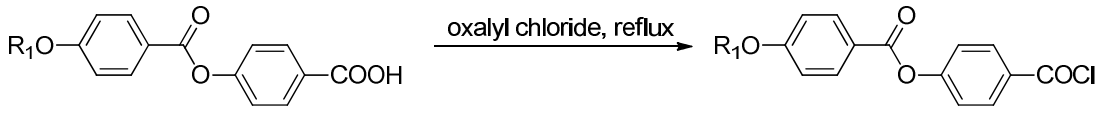

48b (*R* = $CF_3(CF_2)_9(CH_2)_4$) **49b (*R* = $CF_3(CF_2)_9(CH_2)_4$)**

This procedure is analogous to the one above; compound **48b** (1.66 g, 2.0 mmol) and oxalyl chloride (5 cm^3).

Yield: 78.6%. ^{1}H NMR (400 MHz, $CDCl_3$): δ 8.21 (AA'XX', *J* = 8.9 Hz, 2H; arom. CH_2), 8.15 (AA'XX', *J* = 9.0 Hz, 2H; arom. CH_2), 7.39 (AA'XX', *J* = 8.9 Hz, 2H; arom. CH_2), 6.99 (AA'XX', *J* = 9.0 Hz, 2H; arom. CH_2), 4.11 (t, *J* = 5.9 Hz, 2H; OCH_2), 2.18 (m, 2H; CH_2CF_2), 1.89 (m, 4H; overlapped $2CH_2$).

Compound 14:

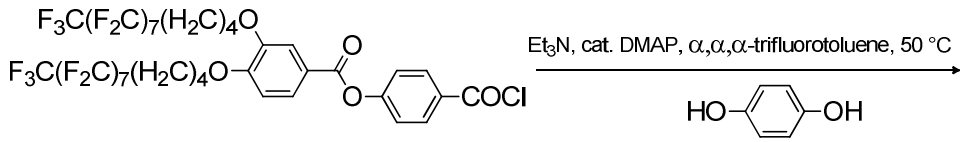

12 **13**

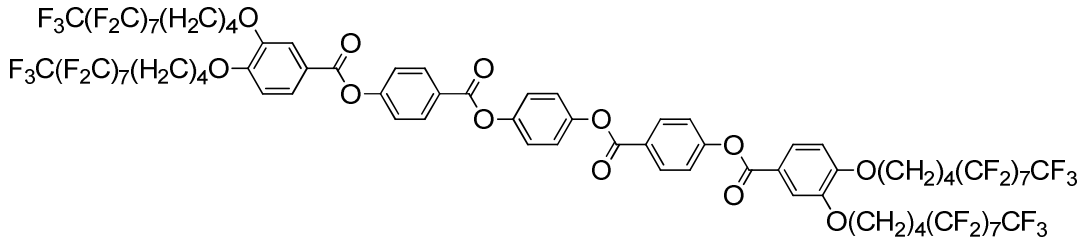

14

The acid chloride **12** (1.364 g, 1.1 mmol) was dissolved in anhydrous α,α,α-trifluorotoluene (10 cm^3) and hydroquinone (0.110 g, 1.0 mmol) was added, followed by triethylamine (0.5 cm^3, 4 mmol) and catalytic DMAP (0.49 g, 0.4 mmol). The mixture was heated at 50 °C for 12 h and the solvent removed under rotary evaporator. The crude solid was washed with methanol yielding white solid. Purification was realized by precipitation from a mixture CF_3COOH/CH_3CN to afford the pure white solid.

Yield: 53%. ^1H NMR (400 MHz, $CDCl_3$): δ 8.32 (AA'XX', *J* = 8.8 Hz, 4H; arom. CH_2), 7.95 (dd, *J* = 2.1 and 8.6 Hz, 2H; arom. CH), 7.75 (d, *J* = 2.0 Hz, 2H; arom. CH), 7.40 (AA'XX', *J* = 8.8 Hz, 4H; arom. CH_2), 7.31 (s, 4H; arom. CH_2), 7.04 (d, *J* = 8.7 Hz, 2H; arom. CH), 4.21 (t, *J* = 6.1 Hz,8H; OCH_2), 2.16 (m, 8H ; CH_2CF_2), 1.90 (m, 16H; overlapped 2 CH_2).

Compound 24:

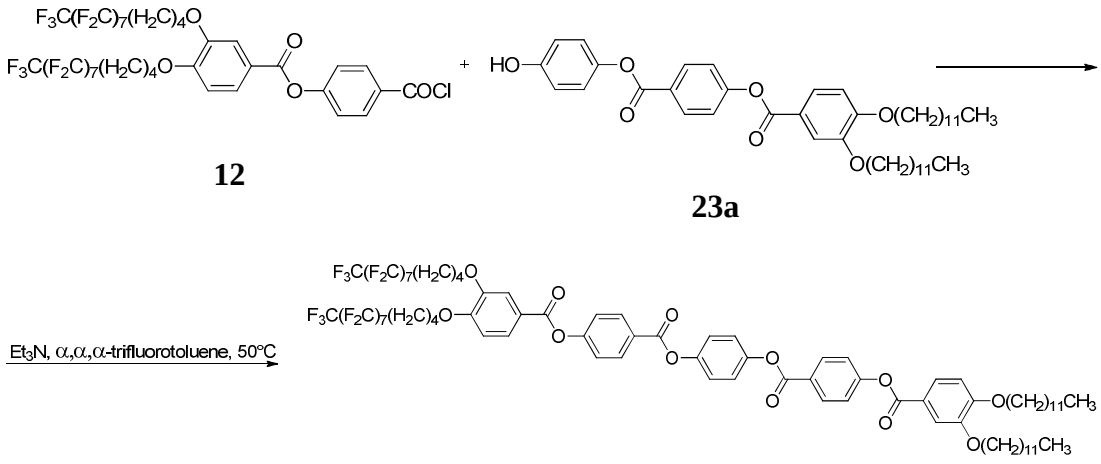

12 **23a**

24

The acid chloride **12** (1.36 g, 1.1 mmol) was dissolved in anhydrous α,α,α-trifluorotoluene (10 cm^3) and *O*-monosubstituted hydroquinone **23a** (0.70 g, 1.0 mmol) was then added, followed by Et_3N (0.5 cm^3, 4 mmol).

^{1}H NMR (400 MHz, $CDCl_3$): δ 8.31 (AA'XX', *J* = 2.0 Hz, 2H; arom. CH_2), 8.29 (AA'XX', *J* = 2.0 Hz, 2H; arom. CH_2), 7.86 (dd, *J* = 1.9 and 8.3 Hz, 1H; arom. CH), 7.84 (dd, *J* = 2.0 and 8.5 Hz, 1H; arom. CH), 7.68 (m, 2H; arom. CH), 7.37 (AA'XX', *J* = 8.7 Hz, 4H; arom. CH_2), 7.31 (s, 4H; arom. CH_2), 6.96 (d, *J* = 4.0 Hz, 1H; arom. CH), 6.94 (d, *J* = 4.0 Hz, 1H; arom. CH), 4.11 (m, 8H; OCH_2), 2.19 (m, 4H; CH_2CF_2), 1.92 (m, 12H; overlapped $4CH_2$ for fluorocarbon chain and 2 $OCH_2CH_2$for hydrocarbon chains), 1.41 (m, 36H; overlapped 18 CH_2), 1.77 (m, 6H; $2CH_3$).

Compound 50a:

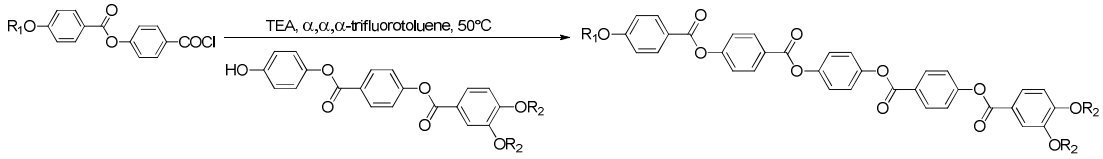

49a (*R*$_1$ = $CF_3(CF_2)_7(CH_2)_4$)

23a (*R*$_2$ = $CH_3(CH_2)_{11}$)

50a

This procedure is analogous to the one above. Acid chloride **49a** (0.83 g, 1.1 mmol) was dissolved in anhydrous α,α,α-trifluorotoluene (10 cm^3) and *O*-monosubstituted hydroquinone **23a** (0.70 g, 1.0 mmol) was then added, followed by Et_3N (0.5 cm^3, 4 mmol).

Yield: 58.2%. ^{1}H NMR (400 MHz, $CDCl_3$): δ 8.29 (AA'XX', *J* = 8.6 Hz, 4H; arom. CH_2), 8.17 (AA'XX', *J* = 8.9 Hz, 2H; arom. CH_2), 7.84 (dd, *J* = 2.0 and 8.4 Hz, 1H; arom. CH), 7.67 (d, *J* = 2.0 Hz, 1H; arom. CH), 7.38 (AA'XX', *J* = 2.5 Hz, 2H; arom. CH_2), 7.37 (AA'XX', *J* = 2.5 Hz, 2H; arom. CH_2), 7.31 (s, 4H; arom. CH_2), 6.99 (AA'XX', *J* = 9.0 Hz, 2H; arom. CH_2), 6.95 (d, *J* = 8.6 Hz, 1H; arom. CH), 4.09 (m, 6H; OCH_2), 2.185 (m, 2H; CH_2CF_2), 1.89 (m, 8H; overlapped $2CH_2$ for fluorocarbon chain and 2 $OCH_2CH_2$for hydrocarbon chains), 1.38 (m, 36H; overlapped $18CH_2$), 0.87 (m, 6H; $2CH_3$).

Compound 50b:

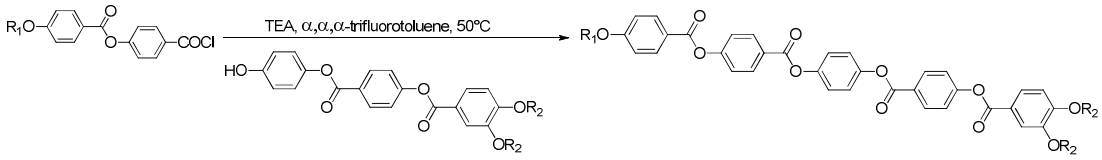

49b (R_1 = $CF_3(CF_2)_9(CH_2)_4$) **23b (R_2 = $(CH_2)_{11}CH_3$)** **50b**

This procedure is analogous to the one above. Acid chloride **49b** (0.94 g, 1.1 mmol) was dissolved in anhydrous α,α,α-trifluorotoluene (10 cm^3) and *O*-monosubstituted hydroquinone **23b** (0.76 g, 1.0 mmol) was then added, followed by Et_3N (0.5 cm^3, 4 mmol).

Yield: 68%. ^{1}H NMR (400 MHz, $CDCl_3$): δ 8.30 (AA'XX', *J* = 8.6 Hz, 4H; arom. CH_2), 8.17 (AA'XX', *J* = 8.9 Hz, 2H; arom. CH_2), 7.84 (dd, *J* = 2.0 and 8.4 Hz, 1H; arom. CH), 7.67 (d, *J* = 2.0 Hz, 1H; arom. CH), 7.39 (AA'XX', *J* = 2.5 Hz, 2H; arom. CH_2), 7.37 (AA'XX', *J* = 2.5 Hz, 2H; arom. CH_2), 7.31 (s, 4H; arom. CH_2), 6.98 (AA'XX', *J* = 9.0 Hz, 2H; arom. CH_2), 6.95 (d, *J* = 8.6 Hz, 1H; arom. CH), 4.09 (m, 6H; OCH_2), 2.19 (m, 2H; CH_2CF_2), 1.89 (m, 8H; overlapped $2CH_2$ for fluorocarbon chain and 2 OCH_2CH_2 for hydrocarbon chains), 1. (m, 4H; overlapped $2CH_2$), 0.88 (m, 6H; $2CH_3$).

Characterization by Elemental Analysis

Compounds showing liquid crystalline mesomorphism were purified and the CHN Elemental Analysis values were inserted in **Table 2.1**. Despite many attempts of purification of compounds **27b**, **11** and **40b**, it was in the end not possible to get results matching the accepted ranges.

Table 2.1. CHN Analysis results for the one-ring, two-ring benzoic acids, benzyl compounds, and target compounds which showed liquid crystal properties

Compound	Experimental Analysis: Found (Required) / %			
	C		H	
45a	36.7	(37.3)	2.1	(2.1)
45b	35.2	(35.4)	1.8	(1.8)
7a	33.5	(33.8)	1.8	(1.83)
7b	32.1	(32.3)	1.5	(1.6)
27a	46.7	(46.7)	4.6	(4.7)
27b	44.0	(45.5)	4.4	(4.5)
48a	42.5	(42.6)	2.3	(2.3)
48b	40.0	(40.4)	2.0	(2.1)
11	38.8	(37.3)	2.6	(2.0)
30a	49.7	(49.8)	4.5	(4.5)
30b	48.5	(48.3)	4.4	(4.3)
38	49.3	(49.8)	4.4	(4.5)
47a	47.9	(48.2)	2.8	(2.8)
10a	41.0	(41.2)	2.3	(2.3)
10b	38.6	(38.9)	2.0	(2.0)
52	74.9	(75.6)	8.3	(8.5)
50a	59.3	(59.3)	5.4	(5.5)
50b	58.2	(58.0)	5.4	(5.5)
14	38.9	(39.1)	2.1	(2.0)
24	51.5	(51.6)	4.4	(4.4)
40a	62.0	(61.5)	6.5	(6.4)
40b	62.5	(60.5)	6.9	(6.4)
42	51.3	(51.6)	4.4	(4.4)

References:

1. L. J. Alvey, R. Meier, T. Soos, P. Bernatis and J. A. Gadysz, *Eur. J. Inorg. Chem*, 2000, **9**, 1975;

2. K. Chiba, K. Kurogi, K. Monde, M. Hashimoto, M. Yoshida, H. Mayama and K. Tsujii, *Colloids and Surfaces – Physicochemical and Engineering Aspects*, 2010, **354**, 234;

3. C. K. Luscombe, S. Proemmel, W. T. S. Huck, A. B. Holmes and H. Fukushima, *J. Org. Chem.*, 2007, **72**, 5505;

4. R. W. Date, E. Fernandez Iglesias, K. E. Rowe, J. M. Elliott and D. W. Bruce, *Dalton Trans.*, 2003, **1916**, 1914;

5. X. H. Cheng, M. K. Das, S. Diele and C. Tschierske, *Langmuir*, 2002, **18**, 6521;

6. V. Percec, M. Glodde, M. Peterca, A. Rapp, I Schnell, H. W. Spiess, T. K. Bera, Y. Miura, V. S. K. Balagurusamy, E. Aqad and P. A.Heiney, *Chem. Eur. J.*, 2006, **12**, 6298;

7. G. Johansson, V. Percec, G. Ungar, J. P. Hou, *Macromolecules*, 1996, **29**, 646;

8. L. Andruzzi, E. Chiellini, G Galli, X. F. Li, S. H. Kang and C. K. Ober, *J. Mater. Chem.*, 2002, **12**, 1684;

9. A. Januszko, K. L. Glab and P. Kaszynsky, *Liq. Cryst.*, 2008, **35**, 549-553.

2.3. Mesomorphism and Thermal Behaviour Studies

The liquid crystal properties of the new compounds and very many intermediates were studied using hot-stage polarised optical microscopy, differential scanning calorimetry and, in some cases, low-angle X-ray diffraction. In the tables, where monotropic transitions are written as heating events, then the temperatures were recorded on re-heating and as such are true thermodynamic temperatures. Where they are written as cooling events then that is how they were recorded with the uncertainty implied by possible supercooling. The properties of individual classes of molecules are first presented and are then discussed subsequently.

2.3.1. Results

2.3.1.1. One-Ring Benzoic Acids

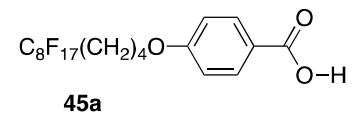

45a

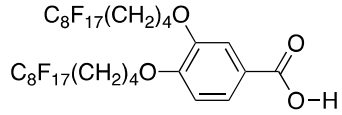

7a

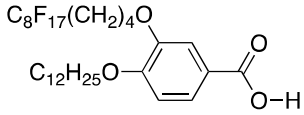

27a

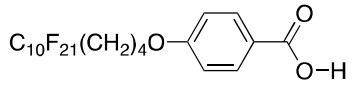

45b

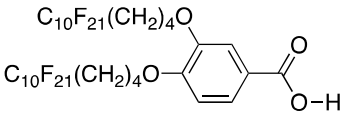

7b

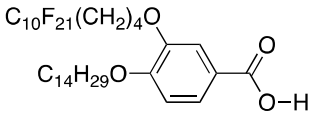

27b

Table 2.2: Thermal behaviour of one-ring benzoic acids

Compound	Transition	*T*/°C	Δ*H*/kJ mol^{-1}
45a	Cr-Sm†	165.0	0.4
	Sm-SmC	178.0	3.4
	SmC-SmA	190.0	-
	SmA-Iso	193.0	2.8
45b	Cr-Sm†	153.1	2.1
	Sm-SmC	197.4	-
	SmC-Iso	203.4	38.5
7a	Cr – Cr_1	46.8	6.12
	Cr_1- Iso	138.2	47.7
	(Col_h-Iso)	(133.8)	(-0.8)
7b	Cr-Iso	167.8	55.1
	(Col_h-Iso)	167.0	(-52.3)
27a	Cr-Iso	113.2	33.3
	(M-Iso)	110.5	-
27b	Cr-Iso	119.8	48.2
	(Col_h-Iso)	(115.0)	-

†Sm represents an undetermined high-order smectic mesophase (*e.g.* SmB, SmE, SmH, SmK) [1]

When considering the mesomorphism of all these acids, it is crucial to realise that these exist as hydrogen-bonded dimers:

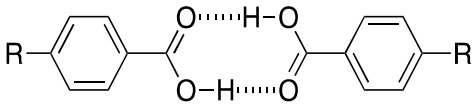

The mesomorphism of the single-chain acids is interesting in several respects. Thus, simple 4-alkyloxybenzoic acids with all-hydrocarbon chains show a nematic and Sm phase up to the dodecyloxy homologue, after which only a SmC phase is seen [2]. However, in **45a**, which has a C_{12} carbon chain, the nematic phase is lost and appears replaced by a SmA phase while the SmC phase is retained, although both phases are at higher temperatures than those found for the hydrocarbon analogue (Cr • 95 • SmC • 129 • N • 137 • Iso). In **45b**, once more a SmC phase is seen but now the nematic phase is absent. Thus it seems that the mesomorphism of **45a** and **45b** somehow parallels that of the all-hydrocarbon analogues although at higher temperatures and with the nematic phase replaced by SmA. The common occurrence of SmA phases in

compounds containing perfluorinated chains is, of course, well known. These data do not agree entirely with those in the literature [3], the main point of difference being that the literature does not report the SmA phase. We are clear about the presence of this phase and would note that SmA phases of compounds bearing perfluorinated chains are very strongly homeotropic, which could account for an oversight on the part of others.

Two-chain acids **7a** and **7b** show a mesomorphism quite different to their hydrocarbon analogues, which are in fact not mesomorphic. Dimers of 3,4-dialkoxybenzoic acids represent, at best, three-ring polycatenar mesogens and so with four terminal chains the lack of mesomorphism is not unexpected. However, compounds **7** show monotropic Col_h (identified by their characteristic optical texture) (**Figure 2.3**) and the induction of mesomorphism is attributed to the rigidity of the perfluorocarbon chains and the increased volume that they occupy.

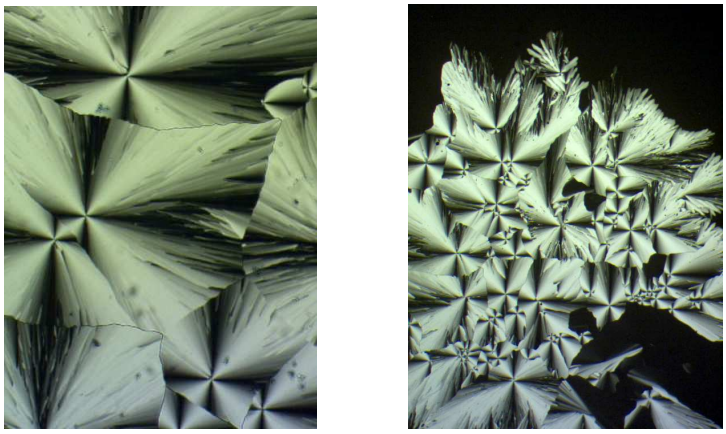

Figure 2.3. Optical photomicrographs representing Col_h mesophase of compound 7a (a) and compound 7b (b), respectively, with cover glass in cooling process.

Compounds **7a** and **27a** differ in structure only by one fluoroalkyl chain which dictates, as it seems, the mesophase behaviour differences. If in compound **7a**, one encounters discotic mesophase due to the large fluoroalkyl chains present in the same molecule, compound **27a** exhibits a fibril-like texture which can be attributed to a discotic or smectic phase (XRD analysis will elucidate the nature of mesophase).

Compounds **7b** and **27b** exhibit the same type of columnar phase on cooling (hexagonal), which suggests that the introduction of only a single perfluoroalkyl chain is necessary to generate this mesophase, fact which was expected since the

analogous benzoic acid with a lower number of carbon atoms in the external chains,**7a**, presents a columnar hexagonal phase on cooling.

Finally, **27a** and **27b** are without precedent, but by analogy with **7a** and **7b** it is perhaps not too surprising that they are mesomorphic. In fact for **27a**, the nature of the mesophase was not at all clear and a fibril-like texture appeared immediately before crystallisation set in (**Figure 2.4).** However matters were clearer for **27b** where a distinctive Col_h texture was seen.

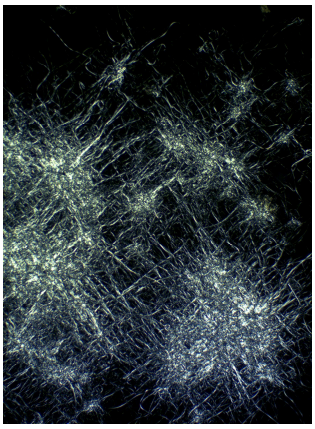

Figure 2.4. Fibril-like texture of compound 27a on cooling, close to the crystallisation temperature.

2.3.1.2. Two-ring Benzoic Acids

Table 2.3. The thermal properties of the two-ring benzoic acids possessing only hydrocarbon chains (data of this table is found in reference [3]).

Compound	Transition	*T*/°C
19a	Cr-Cr_1	105.8
	Cr_1-Iso	143.8
	(N-Iso)	(142.5)
19b	Cr-Cr_1	105.8
	Cr_1-SmC	136.7
	SmC-Iso	139.0

The thermal properties of the two-ring benzoic acids possessing at least one semiperfluorocarbon chain

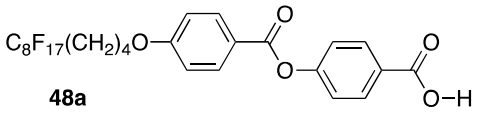

48a

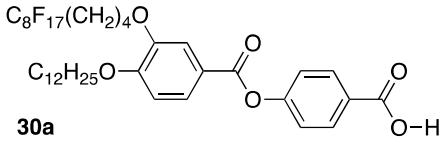

30a

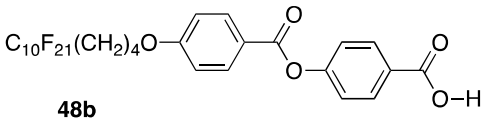

48b

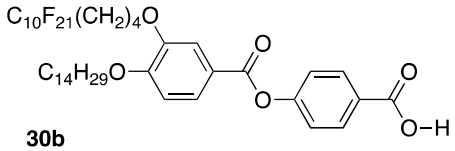

30b

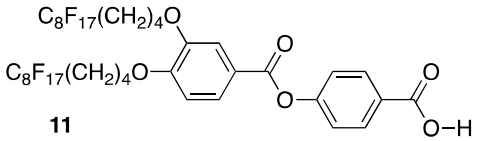

11

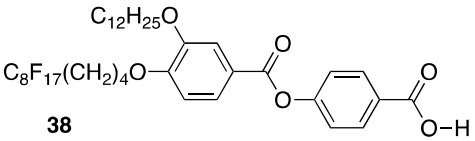

38

Table 2.4. Thermal behaviour of two-ring benzoic acids

Compound	Transition	*T*/°C	Δ*H*/kJ mol^{-1}
48a	Cr-Cr_1	93.3	8.9
	Cr_1-Cr_2	115.2	2.1
	Cr_2-SmC	189.9	17.7
	SmC-dec.	>275	-
48b	Cr-SmC	198.8	21.0
	SmC-dec.	>275	-
11	Cr-Cr_1	46.9	1.5
	Cr_1-Cr_2	58.9	5.3
	Cr_2-Col	180.4	34.2
	Col-Iso	197.9	3.8
30a	Cr-Col	136.9	29.9
	Col-Iso	174.2	5.7
30b	Cr-Col	139.4	53.0
	Col-Iso	181.5	7.4
38	Cr-M	132.2	14.9
	M-Iso	154.6	0.6

The simplest of these compounds, **48a** and **48b**, showed only a SmC phase and at somewhat elevated temperatures so that above 275 °C, the darkening of the sample was clearly due to decomposition and not clearing. Interestingly and in common with the one-ring benzoic acids, a tilted phase is seen whereas in many cases mesogens with perfluorocarbon chains tend to show orthogonal phases such as SmA and SmB. This it seems that formation of the tilted phase is facilitated by the tetramethylene spacer.

By comparing the acid **30a** with the corresponding all-hydrocarbon analogue, **19a** and **30b** with **19b**, the main obvious differences are that the fluorocarbon chains in the third position of external benzene rings favours formation of the discotic phase due to the increase of the molecular cross-sectional area implied by the larger volume of the fluorocarbon chain (fluorine atoms present a bigger volume than hydrogen atoms therefore the total volume of the chain as an addition will be greater for fluorocarbon than the hydrocarbon). Therefore, as a consequence, the organisation of

molecules will be changed: the layers will degenerate in stacks of molecules organised as discs.

Compounds **11** and **30a** show columnar mesophases which denotes that the introduction of only one fluorocarbon chain is necessary to generate them.

Comparing the **48a** tricatenar compound with the corresponding compound **11**, which differentiate themselves only by the additional presence of the fluoroalkyl compound in the 3 position, the first one show a smectic phase but the latter a columnar phase which represents another case in which the cross-sectional molecular area is increased by introduction of an additional fluorocarbon chain in the molecule structure.

The two, related unsymmetric acids **30a** and **30b** both show enantiotropic columnar phases, with the latter showing a slightly higher clearing point. X-ray diffraction studies of **30a** showed a sharp reflection at d = 37.76 Å and, with the identification of the phase as Col_h by microscopy, this gives a lattice parameter a = 43.60 Å. These will latter be compared against all-hydrocarbon analogues.

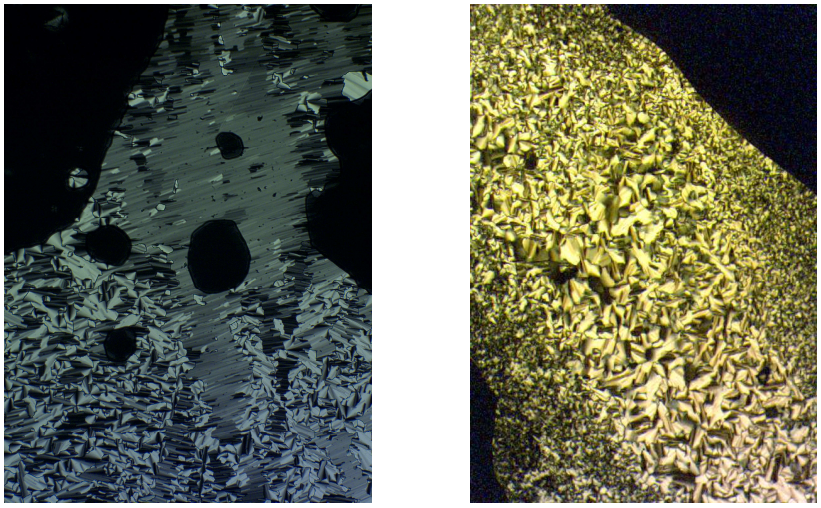

(a) (b)

Figure 2.5. (a) Compound 30b on a cooling process with coverslip on; (b) Compound 11 presenting a columnar phase on heating with coverslip on.

Compound **38** is the chain isomer of **30a** and it is seen that its mesophases are at a lower temperature, which reflects on the relative abilities of lateral hydrocarbon and semiperfluorocarbon chains to destabilise mesophases.

In addition to information obtained from microscopy and differential calorimetry, an XRD investigation will be carried out for compound **30b** in the future to assign the type of the columnar mesophase encountered.

XRD does not elucidate the mesophase types of Compound **38** as it only shows a sharp small-angle reflection and the halo h_F+h_H at 5.15 Å. As a consequence, mesophases that may be attributed are smectic or columnar if birefringent, or cubic if not birefringent.

2.3.1.3. Benzyl Compounds

All-hydrocarbon dialkylated benzyl compounds

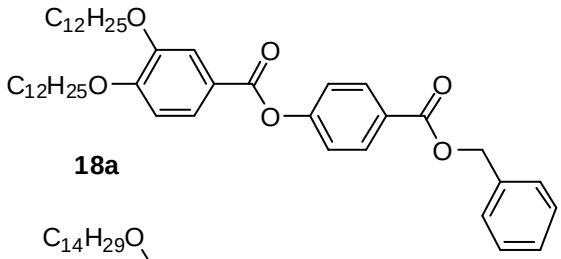

18a

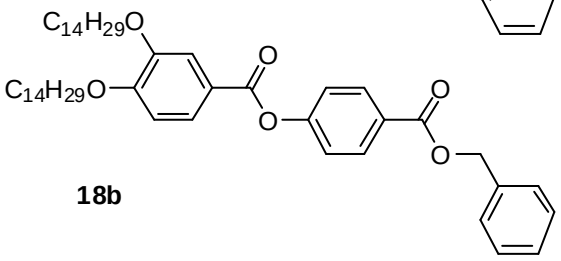

18b

Compound	Transition	*T*/°C	Δ*H*/kJ mol^{-1}
18a	Cr-Iso	111.3	62.25
	(N-Iso)	(108.8)	(-1.58)
	(SmC-N)	(103.9)	(-3.71)
	(Cr-SmC)	(130.3)	(-52.37)
18b	Cr-Iso	83.5	76.22

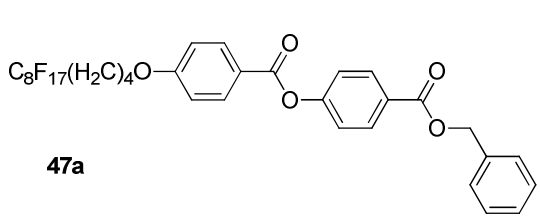

47a

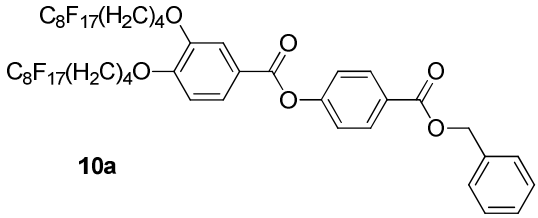

10a

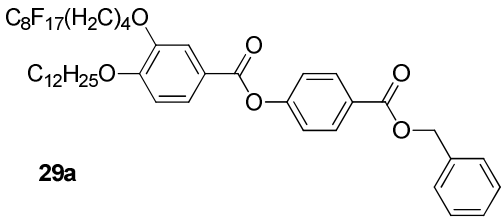

29a

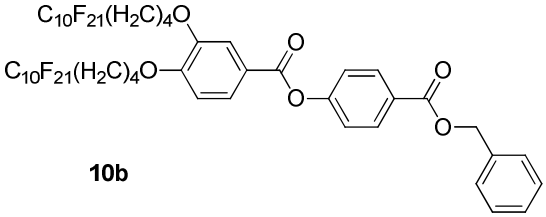

10b

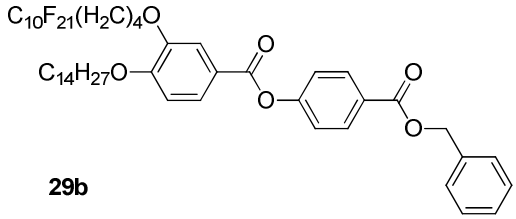

29b

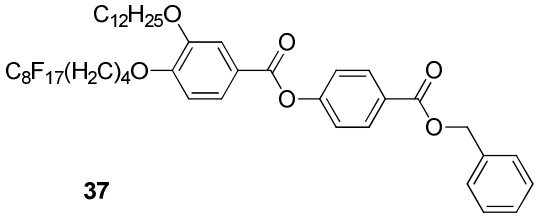

37

Table 2.5. Thermal behaviour of benzyl compounds

Compound	Transition	*T*/°C	Δ*H*/kJ mol^{-1}
47a	Cr-Cr_1	88.6	0.4
	Cr_1-SmA	103.3	32.2
	SmA-Iso	128.3	3.9
	(SmA-Iso)	(130.3)	(-4.2)
10a	Cr-Iso	99.6	42.8
	(SmA-Iso)	104	(-0.5)
	(Cr-SmA)	96.8	(-1.0)
10b	Cr-Col_h	118.5	19.7
	Col_h-Iso	136.4	1.9
	(Cub-Col_h)	(114.6)	(-3.9)
	(Cr-Cub)	(91.4)	(-14.6)

While on cooling, the replacement of hydrocarbon chains with fluorocarbon chains in the case of **18a** and **10a** leads to suppression of nematic phase in favour of SmA phase thing that is expected from fluorocarbon-chained compounds. As it can be seen

from data collected, both of these compounds are monotropic, seeming to exhibit mesophases only on cooling.

Comparing **18b** with **10b**, the difference in thermotropic behaviour is massive. While **18b** does not have liquid crystal properties, **10b** shows an extremely interesting monotropic behaviour: on heating, a columnar hexagonal phase is formed. On cooling, a columnar hexagonal phase precedes a cubic phase. Unusually, the transitions in and out of the cubic phase are rapid and there is noticed a small birefringence.

By comparison, **47a** and **10a** both present smectic phases on cooling; the single difference is that **47a** has an additional smectic phase on heating process. Therefore, this implies that introduction of an additional external fluorinated chain does not affect significantly the liquid crystalline behaviour of these two benzyl derivatives.

What is not expected is that although only a hydrocarbon chain was replaced with a fluoro chain in compounds **29a**, **29b** and **37,** these are not liquid crystals, their melting points being 91.4 °C, 102 °C, 89.5 °C.

Taking into consideration now compounds **29a**, **29b**, **37**, **10a**, **10b** and **47a** as a general conclusion, the presence of the external hydrocarbon chain in the case of **29a**, **29b** and **37** involves the absence of mesomorphism.

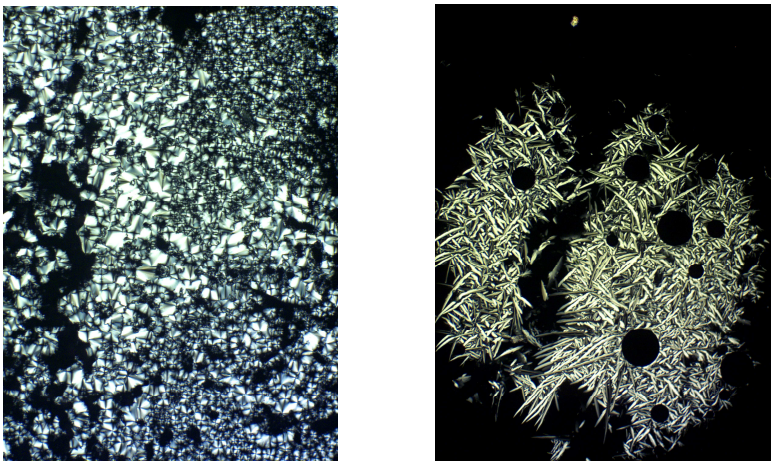

(a) (b)

Figure 2.6. (a) SmA texture of compound 10a on cooling; (b) columnar phase of compound 10b on cooling.

2.3.1.4. The Thermal Properties of the Target Tri- and Tetra-catenar Mesogens

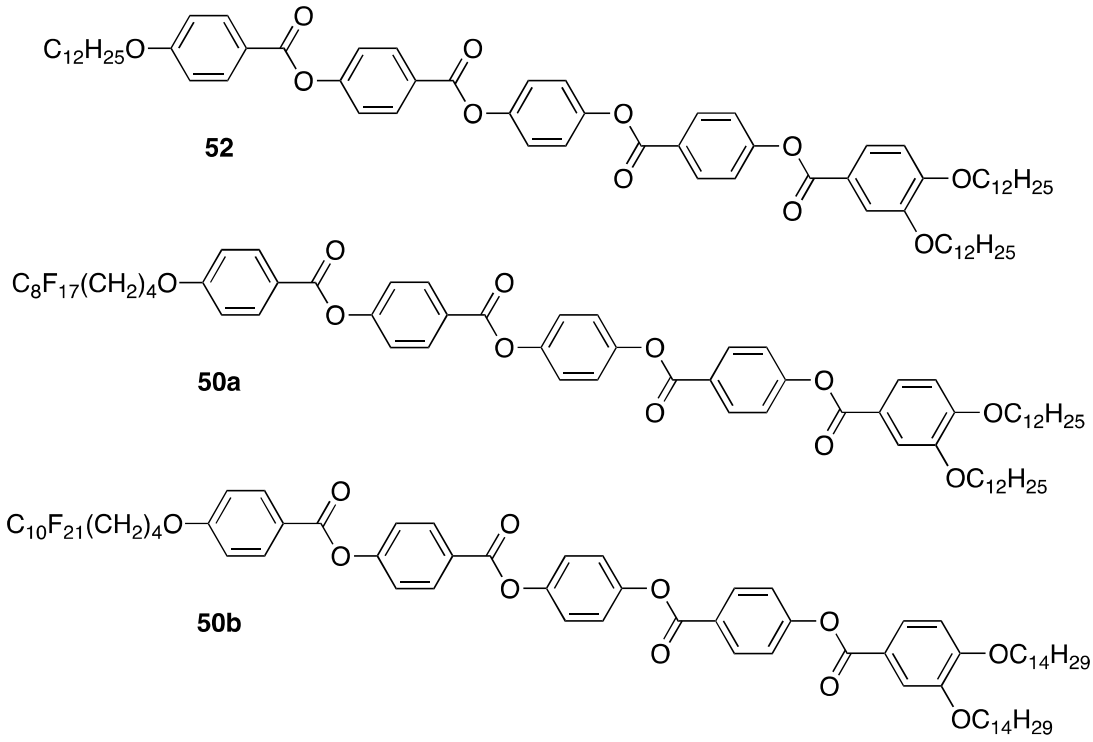

Table 2.6. Thermal behaviour of tricatenar mesogens

Compound	Transition	*T*/°C	Δ*H*/kJ mol^{-1}
52	Cr-SmC	131.8	34.5
	SmC-N	220.0	8.0
	N-Iso	241.5	1.7
	(SmC-Iso)	(236.7)	(-1.7)
	(M-SmC)	(216.3)	(-8.7)
	(Cr-SmC)	(116.3)	(-35.2)
50a	Cr-SmC	131.5	49.9
	SmC-Iso	248.1	9.4
50b	Cr-SmC	137.1	43.8
	SmC-Iso	251.2	10.2

The parent all-hydrocarbon compound, **52**, showed, as expected a SmC and N phase typical of tricatenar mesogens with this substitution pattern [5] and, in addition, a

monotropic phase was found below SmC that had an indistinct texture of a generally mosaic nature.

Both mesogens bearing one semiperfluorocarbon and two hydrocarbon chains (**50a** and **50b**) show a SmC phase over their entire range and so the nematic phase of the parent is suppressed as has been observed commonly in this work when introducing fluorocarbon chains. These compounds were also studied by X-ray methods, which confirmed the lamellar nature of the phase and showed up to six orders of lamellar reflection as found in **Figure 2.8**. In both cases, the wide-angle reflection represents a superposition of the reflections from the hydrocarbon and fluorocarbon chains whose maxima are expected at 4.76 and 5.81 Å, respectively. The determination of the molecular areas suggests that the smectic phase has a bilayer structure, which is governed by the aliphatic chain cross-section area (*i.e.* $2\sigma_H$).

A further feature of the diffraction patterns and one that does not show up well in the data below, is a reflection at nearly 2*d*, *i.e.* at small angles below that found for d_{001}; indicating the presence of a superstructural organisation.

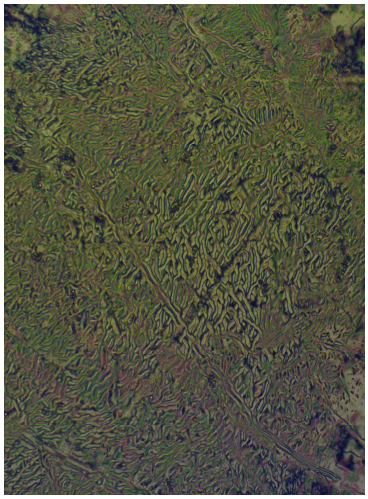

Figure 2.7. Fingerprint-like texture characteristic to a N-SmC transition on cooling process with coverslip, for compound 52.

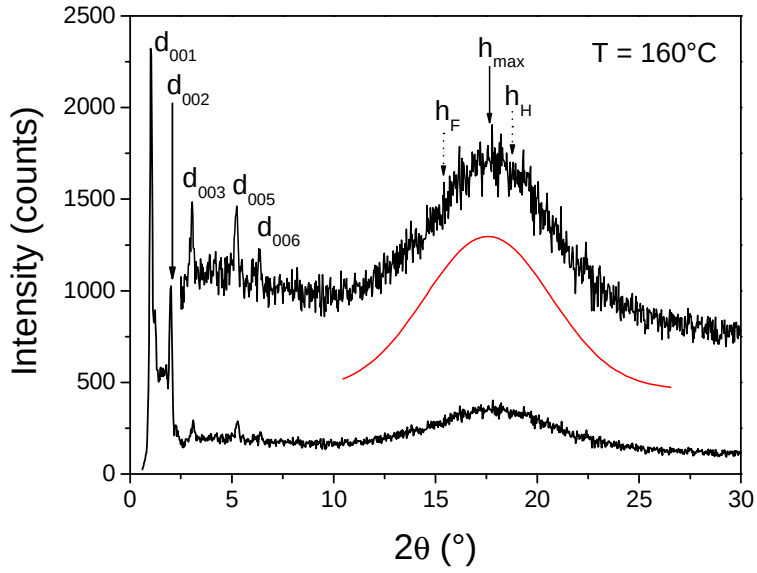

(a)

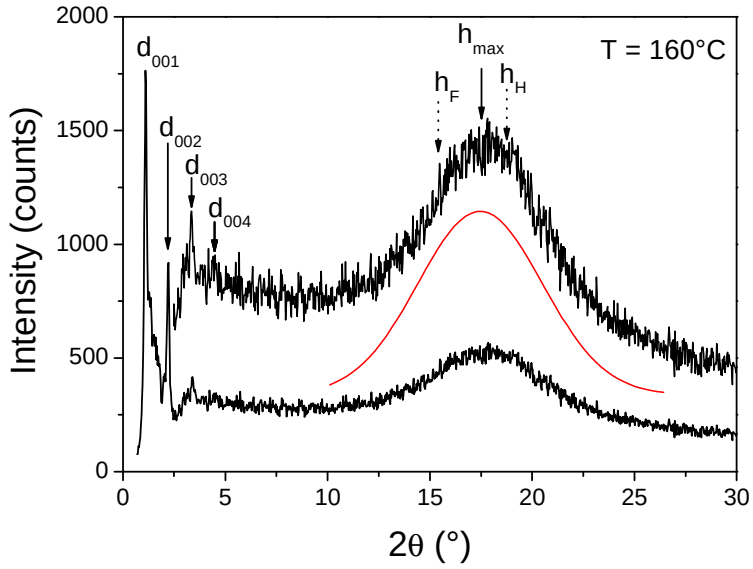

(b)

Figure 2.8. Low-angle X-ray diffraction patterns for (a) compound 50a and (b) compound 50b.

Table 2.7. X-Ray parameters for compounds 50a and 50b

$d_{meas.}$/Å	*hkl*	*I*/a.u.	d_{calc}/Å	Parameters
		50a		
166	sp	S (sh)	-	T = 160°C, Sm
81.9	001	VS (sh)	82.3	d = 82.3 Å
41.38	002	S (br)	41.15	V_{mol} = 2237.6 Å^3 (ρ = 1.17)
27.46	003	M (sh)	27.43	A_{lam} = 54.38 Å^2
16.45	005	M (sh)	16.46	h_H = 4.76 Å, σ_H = 23.81 Å^2
13.7	006	W (sh)	13.72	h_F = 5.81 Å, σ_F = 35.44 Å^2
5.0	-	VS (br)	h_{max} (h_H + h_F)	
		50b		
154	sp	S (sh)	-	T = 160°C, Sm
76.0	001	VS (sh)	76.43	a = 76.43 Å
38.37	002	S (br)	38.21	V_{mol} = 2026.1Å^3 (ρ = 1.16)
25.5	003	M (sh)	25.47	A_{lam} = 53.02 Å^2
19.12	004	M (sh)	19.11	h_H = 4.76 Å, σ_H = 23.81 Å^2
5.0	-	VS (br)	h_{max} (h_H + h_F)	h_F = 5.81 Å, σ_F = 35.44 Å^2

d_{meas} and d_{calc} are the measured and calculated diffraction spacings [d_{calc} is deduced from the following mathematical expressions: $d_{00l} = 1/N_l(\sum d_{00l}.l)$, where N_l is the number of *00l* reflections observed for the lamellar phase; $a = 2\ (\sum d_{hk}.(h^2+k^2+hk)^{½}/N_{hk}\sqrt{3}$, where N_{hk} is the number of *hk* reflections observed for the Col_h phase, $1/d_{hk} = \sqrt{(h^2/a^2+k^2/b^2)}$ for the Col_r]; *I* is the intensity of the sharp reflections (VS: very strong, S: strong, M: medium, W: weak, VW: very weak); sh and br stand for sharp and broad reflection; h_H+h_F, h_F and h_H: maximum of the diffuse scatering due to lateral distances between molten aliphatic tails, rigid core and fluorinated chains, mainly between aliphatic tails (h_H) or mainly between fluorinated chains (h_F); *hkl* are the Miller indexations of the reflections corresponding to the lamellar (00*l*) columnar (*hk*) phases respectively; V_{mol}, molecular volume, ρ, the density in g cm^{-3}; d is the lamellar periodicity, A_{mol} is the molecular area ($A_{mol} = V_{mol}/d$) and A_{lam}, the lamellar cross-section area ($A_{lam} = 2\times A_{mol}$);

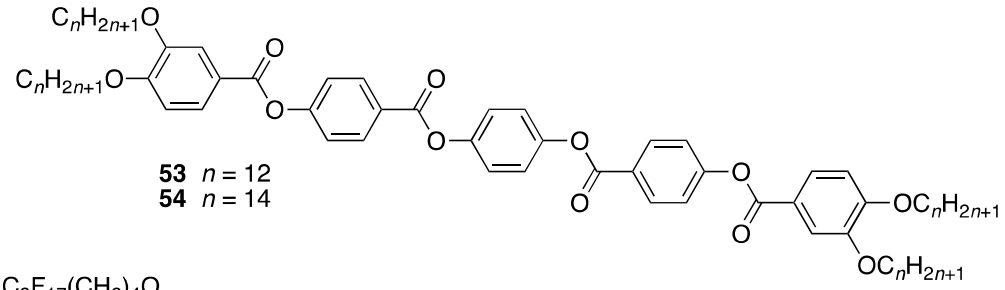

53 $n = 12$
54 $n = 14$

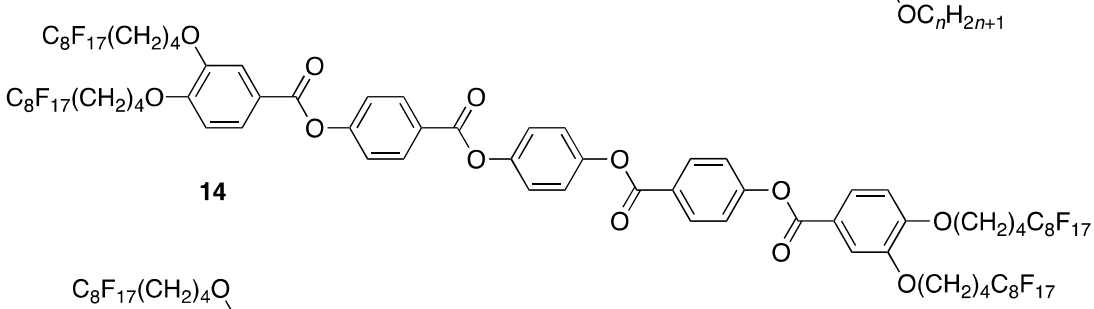

14

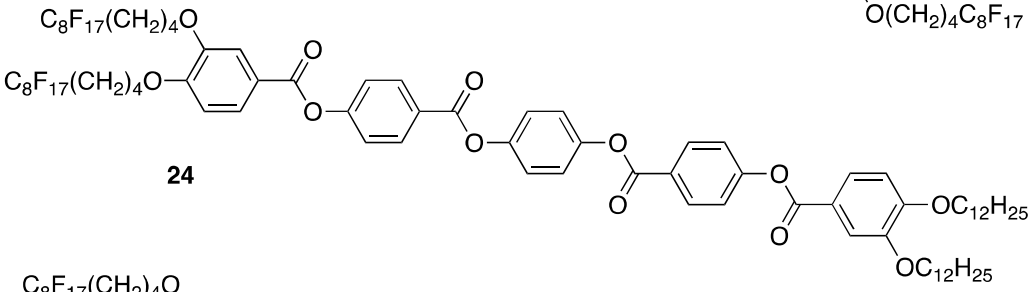

24

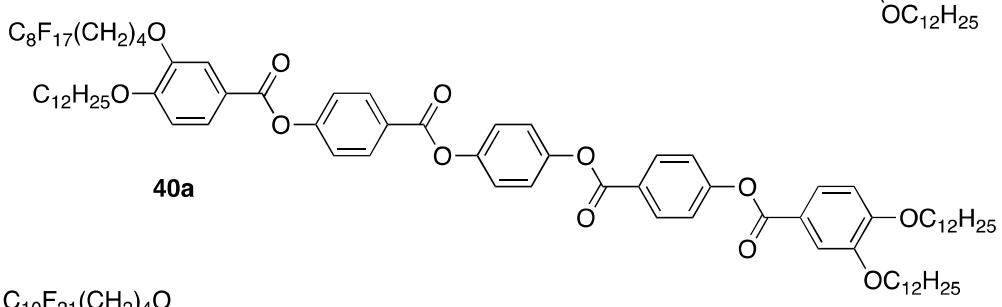

40a

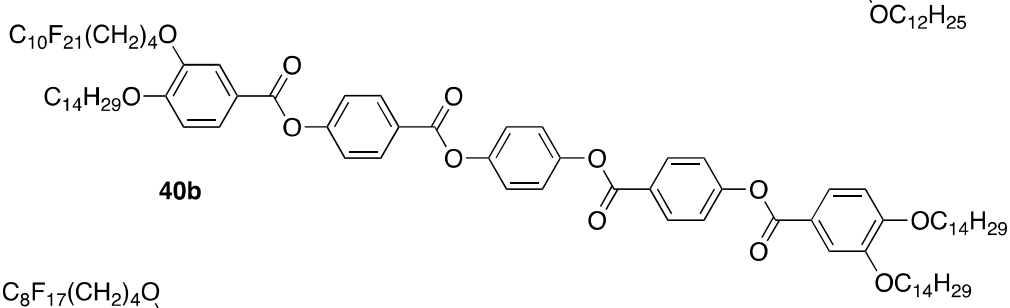

40b

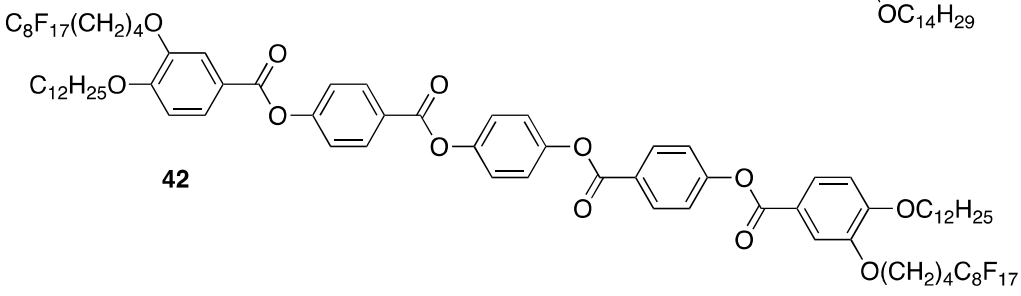

42

Table 2.8. Thermal behaviour of the new tetracatenar mesogens (data for compounds 53 and 54 are from reference [4])

Compound	Transition	*T*/°C	Δ*H*/kJ mol^{-1}
53	Cr-SmC	162.5	73.7
	SmC-N	170.2	4.7
	N-Iso	171.9	0.7
54	Cr-Col_r	154.0	72.2
	Col_r-SmC	162.7	0.6
	SmC-Iso	164.3	8.2
14	Cr-Cr_1	117.9	-12.2
	Cr_1-Col_h	137.4	23.1
	Col_h-Iso	259.5	3.3
24	Cr-Cr_1	112.5	1.9
	Cr_1-SmX	138.6	50.0
	SmX-Col_r	171.1	2.7
	Col_r-Iso	208.2	4.0
40a	Cr-SmC	152.6	53.4
	SmC -Iso	174.1	5.2
40b[†]	Cr-SmC	147.0	-
42[††]	Cr-M_1	94.5	1.8
	M_1-M_2	120.4	10.5
	M_2-M_3	128.3	9.3
	M_3-Iso	169.9	3.5

[†]The tetracatenar compound decomposed at 149 °C.

[††]M_1, M_2, M_3 represent mesophases that could not be certainly identified by polarising optical microscopy; further XRD investigations will be carried out to elucidate the nature of these mesophases.

Compounds **53** and **54** [4] represent the baseline 'parent' materials against which the behaviour of the others can be compared. Compound **53** shows both a SmC and a N phase over a total range of about 10 °C, while compound **54** shows the beginning of the crossover from lamellar to columnar behaviour with the disappearance of the nematic phase and the introduction of a Col_r phase below the SmC. The total mesophase range is again about 10 °C.

Compounds **50a** and **24** differentiate themselves by one external fluorocarbon chain in the third position of the lateral benzene ring. By looking at the mesophases analysis, compound **24** has a columnar phase above 160 °C which denotes another example of discotic formation in case of molecules with longer cross-sectional area due to large volume of external chain substituents.

Comparing **14** and **24**, one can obviously see the different columnar mesophases formed: for **14** it is a hexagonal mesophase, while **24** has a rectangular one. This can be translated by assuming that usually longer symmetrical molecules tend to organize themselves in hexagonal discs (molecule **14**, which possesses only long fluorocabon chains, in exchange for **24**, which presents fluorocarbon chains only at one side and therefore it is shorter in length).

Since compound **14** possesses a columnar hexagonal phase, the tetracatenar mesogen **40a** has only a smectic C phase, which is expected as the number of fluorocarbon long chains is decreased so therefore, the molecules of **40a** tend to form layers rather than discs.

A direct comparison is then possible with compound **14**, which is also a symmetric compound in which all four terminal chains are semiperfluorocarbon, each with a total carbon chain length of twelve. Here, the SmC phase is absent and only a Col_h phase is seen. However, the melting point is appreciably lower than that of compound **53**, yet the clearing point is very much higher so that the Col_h phase shows a range of 120 °C.

X-Ray diffraction studies of this material confirm the hexagonal nature of the phase, showing reflections with relative spacings $1 : \sqrt{3} : \sqrt{4}$; the lattice parameter, a = 53.12 Å. In this case, the diffraction pattern shows low-intensity reflections (**Figure 2.9**) on account of there being very little electronic contrast between the unsaturated rings in

the core of the molecule and the perfluorocarbon fragments at the extremities. The observed *d*-spacing is almost constant across the temperature range.

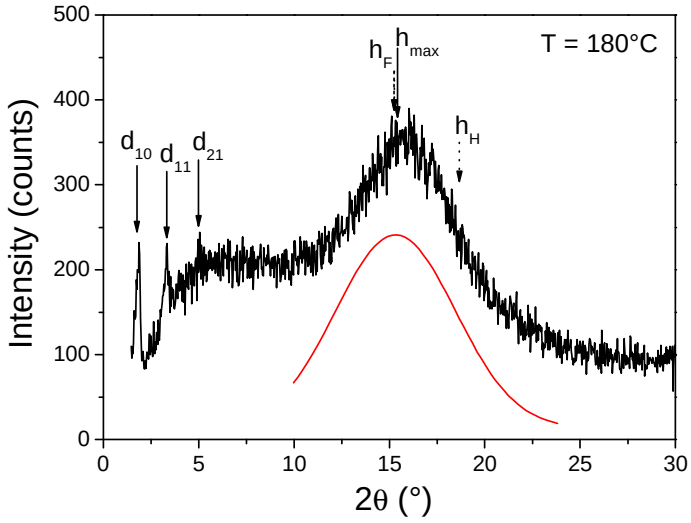

Figure 2.9. X-Ray diffraction pattern for compound 14. The low intensity of the low-angle reflections is observed clearly.

With compound **24**, comparison can now be made with systems that are substituted unsymmetrically. On melting, this compound gives some sort of smectic phase (termed SmX in **Table 2.8**) whose texture does not allow ready identification. However above this phase, microscopy shows clearly the formation of a columnar phase although the texture is not clear enough to allow its symmetry to be determined. Compound **24** melts at almost the same temperature, but its clearing point is midway between that of **14** and **53**.

X-ray diffraction studies of **24** confirm the lamellar nature of the lower-temperature phase and four orders of reflection are seen at small angles, along with a broad halo at wide angles that encompasses the lateral fluorocarbon and hydrocarbon spacings (**Figure 2.10**). For the higher temperature phase, sufficient reflections are present to identify the phase as having a non-centred rectangular symmetry in the *p*2*gg* plane group. The non-centred nature is indicated by the presence of the (12) reflection (this excludes centering on the basis of the extinction rule: $h + k = 2n + 1$). It is likely that this phase arises from a modulation of the underlying lamellar phase to give a superlattice with a = 160.7 Å and b = 92.76 Å ($a/b = \sqrt{3}$ which suggest the rectangular nature of the columnar superlattice).

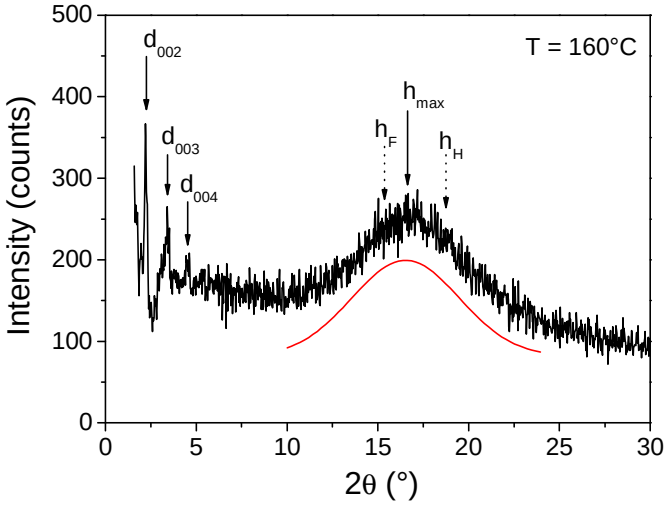

(a)

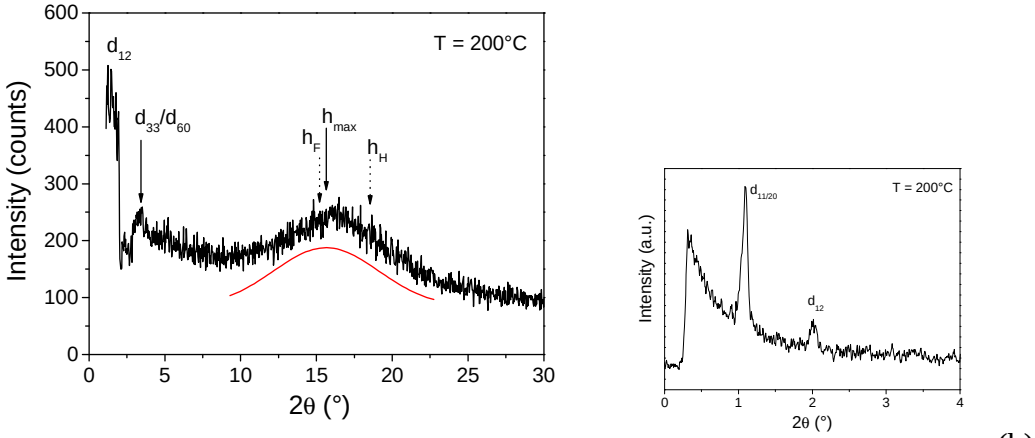

(b)

Figure 2.10. X-Ray diffraction pattern of compound 24 (a) at 160 °C in its lamellar phase and (b) at 200 °C in its Col$_r$ phase (expansion of the low-angle region alongside).

The tetracatenar **40a** presenting one fluoro chain in the 3 and one hydrocarbon chain in the 4 position of one terminal benzene ring, and only hydrocarbon chains at the other terminal ring, seems based on XRD to exhibit a Col$_h$ phase. Only one small-angle reflection is detected on the X-ray pattern, at a distance of 42.33 Å .

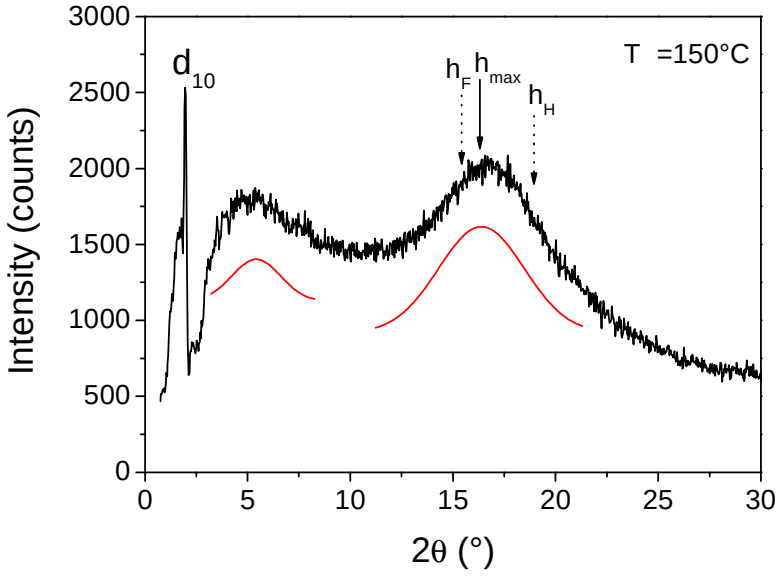

Figure 2.11. X-Ray diffraction pattern for compound 40a at 160 °C.

Table 2.9. X-Ray data for the tetracatenar mesogens (most abbreviations found in the footnotes to Table 2.7)

$d_{meas.}$/Å	*hkl*	I/a.u.	$d_{calc.}$/Å	Parameters
		Compound **24**		
76.0	001	VS (sh)	75.95	T = 160°C, Sm
37.95	002	S (sh)	38.0	d = 75.95 Å
25.3	003	M (sh)	25.3	V_{mol} = 2566.4 Å^3 (ρ = 1.23)
19.0	004	S (sh)	19.0	A_{Lam} = 67.58 Å^2
5.35	–	VS (br)	h_{max} (h_H + h_F)	h_H = 4.73 Å, σ_H = 23.46 Å^2
				h_F = 5.77 Å, σ_F = 34.94 Å^2
80.33	11/20	VS (sh)	80.33	T = 200°C, Col_{rh}
44.4	12	S (br)	44.56	a = 160.66 Å, b = 92.76 Å,
26.75	33/60	M (br)	26.77	S = 1.49×10^4 Å^2
5.66	–		h_{max} (h_H + h_F)	V_{mol} = 2637.24 Å^3 (ρ = 1.20)
				N = 16
				h_H = 4.79 Å, σ_H = 24.1 Å^2
				h_F = 5.85 Å, σ_F = 35.95 Å^2
		Compound **14**		
45.93	10	M (sh)	45.96	T = 180°C, Col_h
26.58	11	M (br)	26.53	a = 53.12 Å
17.35	21	M (sh)	17.37	V_{mol} = 2941.4 Å^3 (ρ = 1.42)
5.7	–	VS (br)	h_{max} (h_H + h_F)	S = 2440 Å^2
				N~ 5
				h_H = 4.76 Å, σ_H = 23.81 Å^2
				h_F = 5.81 Å, σ_F = 35.44 Å^2
		Compound **40a**		
42.33	10	S (sh)	42.33	T = 150°C, Col_h
5.4	-	VS (br)	h_{max} (h_H + h_F)	a = 48.9 Å
				S = 2069.0 Å^2
				V_{mol} = Å^3 (ρ = 1.08)
				h_H = 4.71 Å, σ_H = 23.3 Å^2
				h_F = 5.75 Å, σ_F = 34.69 Å^2

a and b are the lattice parameters of the Col_r ($a \neq b$) and Col_h ($a=b$) phases; for the Col_h, the lattice (column) area is given by S =$2a^2/\sqrt{3}$ and for the Col_r phase, S_r is the rectangular lattice cross-section (S_r=a.b = 2S); N is the number of polycatenar molecules per columnar slice, h_{max} = $N.V_{mol}/S$, σ_F(Å^2)=30.92+0.02514T(°C) and σ_H(Å^2)=20.915+0.01593T(°C), and $h_{H/F}$=0.9763$\sqrt{\sigma_{H/F}}$.

2.3.2. Discussion

The first thing to note is that the series of compounds discussed is not as complete as had been envisaged owing to extreme difficulties in handling many of the compounds, which showed very low solubility in almost every solvent used. This was due to the inclusion of the perfluorocarbon groups and even employing more 'specialised' solvents such as trifluoroacetic acid and trifluoromethyltoluene did not

solve the problem. As liquid crystal properties are so dependent on purity, the compounds discussed are those for which good microanalytical data were obtained. Several other compounds were impure by such analysis.

The aim of the work was to show the influence of the perfluoroalkyl chain in the mesomorphism of polycatenar compounds by preparing a series of unsymmetric materials that contained both hydrocarbon and semiperfluorocarbon chains. Constrained to be in the same molecule, the natural trend of these two fragments to phase separate cannot be realised and so it was of interest to see how they would organise to accommodate their need to be apart. In addition, many of the intermediates prepared along the way showed liquid crystal properties and so where pure compounds were obtained, these were also characterised and where appropriate, conclusions drawn.

2.3.2.1. One-Ring Benzoic Acids

The main point of note here is that the presence of the semiperfluorinated chain acted to raise transition temperatures and to suppress the nematic phase. Furthermore, in compounds where there were two such chains, mesomorphism was induced where it would otherwise have been absent in all-hydrocarbon analogues. This was discussed briefly above.

2.3.2.2 Two-ring Benzoic Acids

It is of a curious matter the fact that acids **48a** and **48b** suffer a decomposition at temperatures above 275 °C, as this is not the case of their analogues with two fluoro terminal chains, nor of the all-hydrocarbon ones. However, while in their analogues with two perfluorocarbon chains melting points are lower, this translates to the fact that the perfluoro chain introduced exclusively in the 4 position tends to de-stabilize the system thus formed.

The lateral hydrocarbon and semiperfluorocarbon chains relative influence that destabilise mesophases is connected to the difference in length of the chains. Since a fluorocarbon chain in the para position will be longer than the other hydrocarbon chain in the meta position, the interidigitation in a spatial self-assembly will have a higher degree than the corresponding one in the case of the chain isomer. Moreover, a hydrocarbon chain in 3-position reduces anisotropy and consequently destabilises the mesophase, therefore the diffence in melting points and clearing points between isomeric analogues.

2.3.2.3. Benzyl compounds

The all-hydrocarbon dodecyloxy benzyl homologue **18a** displays Schlieren texture on cooling and a SmC at a lower temperature, whereas the all-hydrocarbon **18b** does not have liquid crystal properties. The benzyl compound **47a** shows a SmA mesophase likewise the analogue containing two fluoro chains, **10a**. The melting point and clearing point of this monofluoroalkyl mesogen are slightly lower than those corresponding to the difluoroalkyl mesogen, which is obvious due to the fact that the number of fluoro chains increases the transition temperatures.

The behaviour of compound **10b** was of particular interest as below the Col_h phase and monotropically, the bright, birefringent texture of the columnar phase turned rather suddenly dark with an increase in viscosity. Further cooling led to another monotropic phase that was again birefringent; transitions in and out of the dark phase were reversible. The most tempting explanation is that the dark phase possesses cubic symmetry, but it is noted that unlike many cubic phases studied before in the group, the texture was not completely extinct. Also unlike systems studied before, the transitions into and out of the cubic were rather rapid, whereas normally they are very slow and are accompanied by the observation of square edges growing across a mobile, birefringent phase. This prompts two comments. First, it is possible that the small residual birefringence owes its origin to the fact that the transition from columnar to highly organised cubic phase is rapid and so it may be less likely that cubic organisation is perfectly formed in all parts of the sample. Second, it is tempting to speculate that if indeed the phase is cubic (X-ray data were not in hand at

the time of writing), then the rapidity of transition has its origins in the fact that it is mainly driven by the re-organisation of the terminal which, being fluorocarbon in nature, would be expected to show lower viscosity than their hydrocarbon analogues.

The other point of interest relates to why such a compound forms a cubic phase at all. As an isolated example of this type it is difficult to draw many meaningful conclusions but two factors are worth considering. First, with two rather large perfluorodecyl groups at one end and a benzyl group at the other, the mesogen can be considered as somewhat tapered in shape and such motifs, albeit with more significant tapers, have been shown by Percec and co-workers to form well-organised structures of a cubic nature [6]. Second, in line with previous proposals from the group, the presence of terminal fluorocarbon chains creates an amphiphilicity that can contribute to the self-organisation regarded as necessary for the formation of cubic phases [7].

2.3.2.4. Tricatenar Mesogens

Bearing hydrocarbon chains at one end and a semiperfluorocarbon chain at the other, these mesogens were expected to show the first real evidence of the effects of hydrocarbon/fluorocarbon immiscibility on the mesomorphism of single compounds. Thus, as discussed above, the mesomorphism of the all-hydrocarbon compound, **52**, was as expected showing N and SmC phases with a lamellar spacing by X-ray (*ca* 36 Å). However, when considering compounds **50a** and **50b** with a terminal perfluorooctyl and perfluorodecyl chain, respectively, the lamellar period was seen to increase substantially to 75-80 Å, more than double that of **52**. Combined with calculations of molecular area, this points strongly to a bilayer structure, which must have its origins in localised nanophase segregation driven by the mutual incompatibility of the hydrocarbon and fluorocarbon portions of the molecule. Thus, the genuinely speculative **Figure 1.41** (**Chapter 1**) turns out to be almost correct except that the phase is tilted and not orthogonal (**Figure 2.12.b**). Comparing with the organisation possible when chains at both ends are hydrocarbon (**Figure 2.12.a**), it is easy to see exactly why the lamellar periodicity is larger in the amphiphilic material.

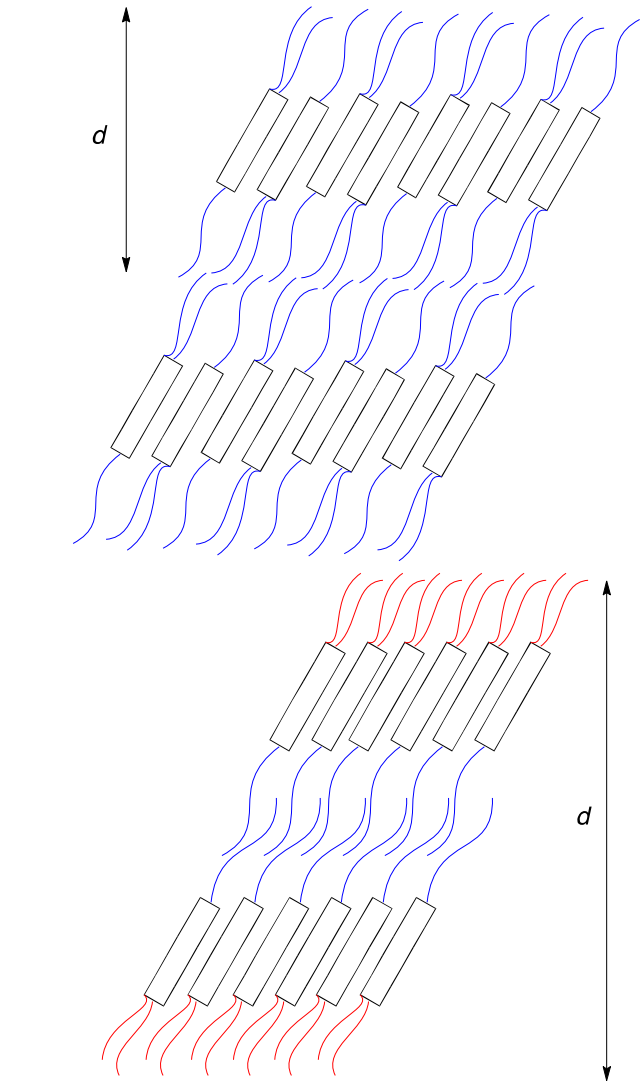

Figure 2.12. Postulated arrangements of (a) compound 52 and (b) compounds 50 in their SmC mesophases showing the origin of the larger lamellar spacing in the latter.

2.3.2.5. Tetracatenar Mesogens

Having established that the tetracatenar mesogen with all fluorocarbon chains (**14**) showed a columnar hexagonal phase and one with a lattice parameter consistent with the single molecule being the basis for aggregation ($a \approx 53$ Å in **Table 2.9**), it was of interest to determine the behaviour of lower-symmetry analogues. Of these, **24** had

two fluorocarbon chains at one end and two hydrocarbon chains at the other. It showed both a lamellar and a columnar phase and the notable feature of both was the very large lattice parameter – almost 76 Å (see **Table 2.9**) for the lamellar phase, while those of the columnar phase were $a \approx 161$ Å and $b \approx 93$ Å (see **Table 2.9**). Once more, this suggests an arrangement (in the *p*2*gg* plane group) in which the arrangement is compartmentalised to accommodate the strongly amphiphilic nature of the molecules (**Figure 2.13**).

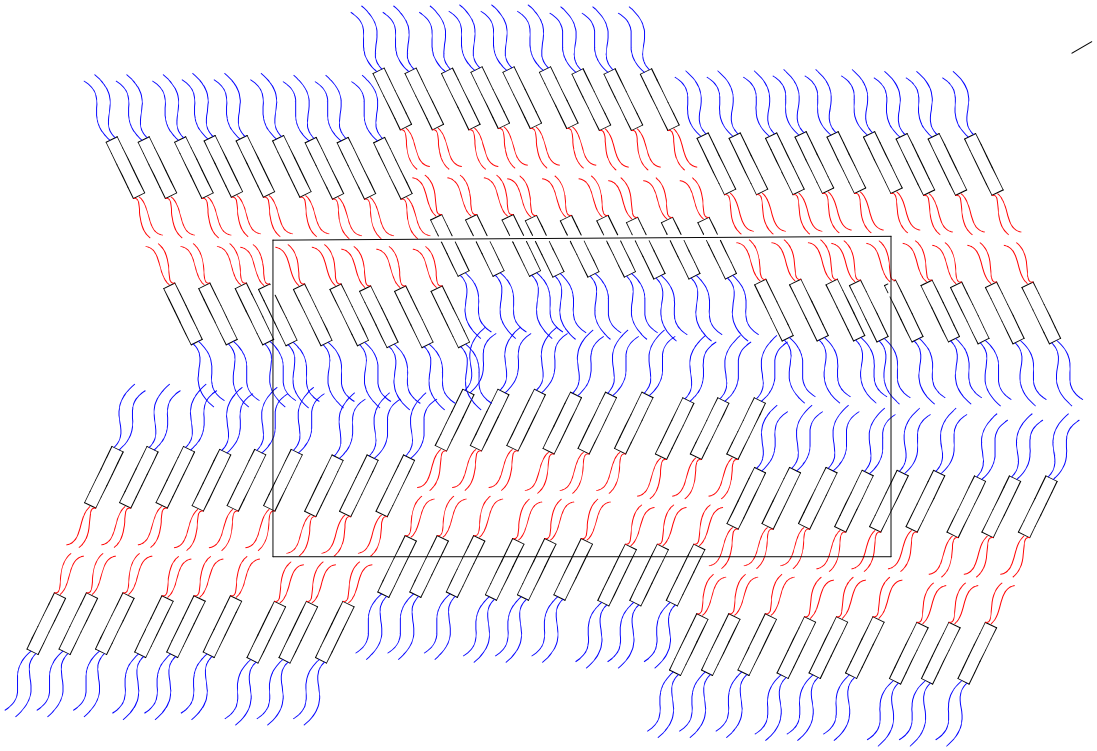

Figure 2.13. Schematic proposal for the arangement of 24 in a *p*2*gg* plane group allowing for the strongly amphiphilic nature of the molecules.

Compound **40a** is then a sort of halfway house between **14** and **24**, possessing three hydrocarbon chains and only one semiperfluorocarbon chain. In this case, the combination of microscopy and X-ray data show a columnar hexagonal phase with a lattice parameter, $a \approx 49$ Å (**Table 2.9**), very similar to that of **14** with all hydrocarbon chains. This implies that a single semiperfluorocarbon chain among three hydrocarbon chains is insufficient to perturb the supramolecular arrangement and so nanophase segregation does not result.

2.3.3. Conclusions

Series of tricatenar and tetracatenar mesogens have been synthesized (containing only hydrocarbon external chains, hydrocarbon and fluorocarbon external chains, or only fluorocarbon external chains – the hydrocarbon chains have the general formula C_nH_{2n+1}– (where n = 12 or 14) and the fluorocarbon chains $C_mF_{2m+1}(CH_2)_4$– (where m = 8 or 10). The low solubility of the carboxylic acids intermediates (benzoic acid derivatives and two-benzene ring carboxylic acids) has been avoided by converting them to the corresponding acid chlorides which are more reactive in their subsequent reactions with phenols (see Schemes **2.2**, **2.3**, **2.4**, **2.5**, **2.6**, **2.7**, **2.8** and **2.9**). Here there needs to be added that the solubility of final compounds decreases with each fluorocarbon chain added; therefore, it is expected that a tricatenar mesogen with only one fluorocarbon chain at the end is more soluble than tetracatenar compounds with two fluorocarbon chains or even all four chains fluorinated, but is also less soluble than the all-hydrocarbon corresponding tricatenar compound.

The general conclusions that can be drawn from the all-hydrocarbon intermediate compounds are that they possess smectic and/or nematic phases while heated or cooled, the columnar phase being totally absent. Now taking into consideration the all-hydrocarbon tricatenar and tetracatenar mesogens, there is only the tetradecyloxy tetracatenar compound which shows a Col_r phase.

Observing the trends in the fluorinated compounds, most of the intermediate mesogens possess also a columnar phase and in terms of the fluorinated tricatenar compounds, the smectic phase is encountered.

Several compounds will need a further investigation for the purpose of establishing the nature of mesophases by XRD, such as compounds **38** and **42**.

As a possible future work, virtual modelling of the way of self-assemblage for the final compounds can be used in comparison to the results obtained from XRD studies in Strasbourg. The aim is to complement the analytical results with the *in silico* simulations and give a better grasp of a relationship between predictions and experiments.

Another key study could be polyphilicity of binary mixtures between final compounds or intermediate compounds of the same nature (one-ring benzoic acid derivatives, benzyl compounds or two-ring benzoic acids) which will provide supplementary information on the way two different types of molecules can assemble by varying the molar ratio between them.

References:

1. G. Johansson, V. Percec, G. Ungar, K. Smith, *Chem. Mater.*, 1997, **9**, 164;

2. F. S. Spring, T. Vickerstaff, B. Jones, D. J. Bell and W. A. Waters, *J. Chem. Soc.*, 1935, 1874;

3. A. Schaz, E. Valaityté and G. Lattermann, *Liq. Cryst.*, 2004, **31**, 1311;

4. A. I. Smirnova, N. V. Zharnikova, B. Donnio and D. W. Bruce, *Russ. J. Gen. Chem.*, 2010, **80**, 1331;

5. J. Malthête, H. T. Nguyen and C. Destrade, *Mol. Cryst., Liq. Cryst.*, 1988, **165**, 317.

6. V. Percec, *Phil. Trans. R. Soc.*, 2006, **364A**, 2709;

7. D. Fazio, C. Mongin, B. Donnio,Y. Galerne, D. Guillon and D. W. Bruce, *J. Mater. Chem.*, 2001, **11**, 2852.

Abbreviations

Δ*G* Gibbs Energy

Δ*H* Enthalpy

Δ*S* Entropy

AIBN 2,2′-Azobis(2-methylpropionitrile)

Col_h Columnar hexagonal

Col_r Columnar rectangular

DCC *N, N'*-Dicyclohexylcarbodiimide

DCM Dichloromethane

DMAP 4-(*N,N'*-Dimethylamino)pyridine

DSC Differential Scanning Calorimetry

Iso Isotropic

N Nematic phase

NMR Nuclear Magnetic Resonance

Sm Undetermined High-Order Smectic Mesophase

SmB Hexatic Smectic B Phase

SmC Smectic C Phase

SmF Hexatic Smectic F Phase

SmI Hexatic Smectic I Phase

THF Tetrahydrofuran

TLC Thin-layer Chromatography

XRD X-ray Diffraction